
Electronic Thesis and Dissertation Repository

5-12-2017 2:00 PM

Design and Validation of Delivery Systems for Galectin-3 for Skin Healing Applications

Karrington A. McLeod
The University of Western Ontario

Supervisor

Dr. Douglas Hamilton
The University of Western Ontario

Dr. Amin Rizkalla
The University of Western Ontario

Graduate Program in Biomedical Engineering

A thesis submitted in partial fulfillment of the requirements for the degree in Master of Engineering Science

© Karrington A. McLeod 2017

Follow this and additional works at: <https://ir.lib.uwo.ca/etd>

 Part of the [Biomaterials Commons](#)

Recommended Citation

McLeod, Karrington A., "Design and Validation of Delivery Systems for Galectin-3 for Skin Healing Applications" (2017). *Electronic Thesis and Dissertation Repository*. 4791.
<https://ir.lib.uwo.ca/etd/4791>

This Dissertation/Thesis is brought to you for free and open access by Scholarship@Western. It has been accepted for inclusion in Electronic Thesis and Dissertation Repository by an authorized administrator of Scholarship@Western. For more information, please contact wlsadmin@uwo.ca.

Abstract

Chronic wounds present a significant burden to patients, causing pain, impairing limb function, and often resulting in the need for amputation. Treatment of chronic dermal wounds is challenging, with current therapies showing limited efficacy in clinical trials. As galectin-3 has been implicated in several wound healing processes, its efficacy as a therapeutic in skin healing was investigated in this study. An electrospun gelatin scaffold loaded with galectin-3 was developed as a delivery system. The influence of human recombinant galectin-3 in skin healing, when delivered topically and using an electrospun scaffold, was then investigated in wild type and diabetic mice. Electrospun gelatin/galectin-3 scaffolds were developed having an overall porosity of approximately 83% and average pore diameter of approximately 1.15 μm . The scaffolds supported the adhesion, deposition of matrix, and proliferation of human dermal fibroblasts *in vitro* providing evidence that they are biocompatible. *In vivo* treatment of wounds with topical galectin-3 and gelatin/galectin-3 scaffolds did not affect wound closure, re-epithelialization or macrophage phenotypes in the wound, casting doubt on its efficacy for these processes. Future work is required to elucidate the exact pathological contexts in which galectin-3 might modulate inflammation in skin healing.

Keywords

Scaffold, Galectin-3, Wound Healing, Chronic Wound, Human Dermal Fibroblast, Re-epithelialization, Inflammation, Electrospinning.

Co-Authorship Statement

This thesis was written by K.A McLeod with input, suggestions, and revisions from Dr. D.W. Hamilton and Dr. A. Rizkalla. Experiments were designed by Dr. D.W. Hamilton and Dr. A. Rizkalla. All experiments were conducted by K.A. McLeod in the laboratories of Dr. A. Rizkalla and D.W. Hamilton with the exception of: D. Zuanazzi (PhD candidate) conducted mass spectrometry and associated sample preparation; T. Kwon (undergraduate student) conducted measurements for epithelial thickness and epithelial tongue lengths on Masson's Trichrome images.

Acknowledgments

I would like to firstly thank my supervisors, Dr. Douglas Hamilton and Dr. Amin Rizkalla for all of their support, mentorship, and guidance over the past few years. Your input in all of my lab work, presentations, and scholarship applications has been instrumental in helping me succeed. I have benefited greatly from your advice and have learned the value of multidisciplinary research while undertaking this project. Thank you for also encouraging my professional development by enabling me to attend multiple conferences and to complete an internship. I am also grateful to my advisory committee members, Dr. Lauren Flynn and Dr. Harvey Goldberg for their insight and contributions to the project.

I would like to thank the Collaborative Training Program in Musculoskeletal Research for providing me with financial support, professional development opportunities, and for the chance to collaborate with other students in the program.

I appreciate all of the help I received from the Siqueira lab in analyzing my scaffold samples. Thank you to David, who helped me learn about protein biochemistry. I am grateful to have also had assistance from members of the Seguin, Beier, Leask, and Dixon labs in learning new laboratory techniques. Thank you also to Ryan and Brandon for being such great lab neighbors and for always being willing to lend a hand.

Thank you to all members of the Hamilton lab, who I have had the pleasure of working with over the past few years. Sarah, Kendal, and Shawna taught me the fundamentals at the beginning of my project and left excellent notes behind that have been a great resource throughout my project. Thank you to JT for showing me how to conduct animal studies. To Georgia and Sarah, thank you for being collaborative, for your positivity, and for always being willing to share a laugh.

Thank you to my family, for always being a phone call away and for your constant support and encouragement throughout my degree. Finally, thank you to Murray, for accompanying me during weekends or late nights at the lab, for making endless delicious meals while I studied, for providing support and encouragement, and for always helping out when you could.

Table of Contents

Abstract	ii
Co-Authorship Statement.....	iii
Acknowledgments.....	iv
Table of Contents	v
List of Tables	ix
List of Figures	x
List of Appendices	xii
List of Abbreviations	xiii
1 Introduction	1
1.1 Skin, Cutaneous Wound Healing and Chronic Wounds.....	1
1.1.1 Skin Anatomy and Physiology.....	1
1.1.2 Cutaneous Wound Healing.....	1
1.1.3 Chronic Dermal Wounds	3
1.1.4 Current Treatments for Chronic Wounds	5
1.2 Pathophysiology of Chronic Wounds.....	7
1.2.1 Impaired Re-epithelialization and Granulation Tissue Formation.....	8
1.2.2 Imbalance of Proteolytic Activity.....	8
1.2.3 Biofilm Formation	9
1.2.4 Advanced Glycation End Products	10
1.2.5 Oxidative Stress	11
1.3 Galectin-3 as a Therapeutic for Chronic Wounds.....	12
1.3.1 Protein Structure	15
1.3.2 Role in Inflammation	18
1.3.3 Role in Angiogenesis	21

1.3.4	Role in Re-epithelialization	21
1.4	Protein Delivery Strategy.....	22
1.4.1	Scaffolds for Protein Delivery	22
1.4.2	Scaffold Design for Tissue Regeneration	23
1.4.3	Scaffold Materials.....	24
1.4.4	Scaffold Fabrication Methods.....	25
1.4.5	The Addition of Bioactive Compounds to Electrospun Scaffolds.....	28
1.5	Hypothesis and Objectives.....	29
1.5.1	Rationale	29
1.5.2	Hypothesis.....	30
1.5.3	Objectives	30
1.6	References.....	31
Chapter 2	43
2	The Influence of a Gelatin/Galectin-3 Scaffold on Normal and Impaired Models of Skin Healing.....	43
2.1	Introduction.....	43
2.2	Materials and Methods.....	46
2.2.1	Electrospinning	46
2.2.2	Assessment of Fiber Morphology.....	51
2.2.3	Mercury Porosimetry	51
2.2.4	Mass Spectrometry.....	51
2.2.5	Scaffold Preparation for Cell Culture and Animal Studies.....	52
2.2.6	Adhesion Assay	52
2.2.7	Proliferation Assay.....	53
2.2.8	Extracellular Matrix Deposition Studies.....	53
2.2.9	Wound Closure Kinetics Study.....	54

2.2.10	Investigation of Re-Epithelialization and Macrophage Polarization	55
2.3	Results.....	57
2.3.1	Influence of Electrospinning Parameters on Fiber Diameter and Scaffold Morphology.....	57
2.3.2	Scaffold Porosity is Sufficient for Cell Growth.....	67
2.3.3	Detection of Galectin-3 in Scaffolds.....	70
2.3.4	Scaffolds Increase the Initial Adhesion of Human Dermal Fibroblasts ...	74
2.3.5	Scaffolds Support the Proliferation of Human Dermal Fibroblasts.....	74
2.3.6	Scaffolds Support the Production of Fibronectin by Human Dermal Fibroblasts.....	74
2.3.7	Gelatin/Galectin-3 Scaffolds Do Not Alter Skin Closure Kinetics in Wild Type and Diabetic Mice.....	83
2.3.8	The Effect of Topical Galectin-3 and Gelatin/Galectin-3 Scaffolds on Re-Epithelialization in Wild-Type and Diabetic Mice.....	94
2.3.9	The Influence of Topical Galectin-3 and Gelatin/Galectin-3 Scaffolds on Macrophage Populations in WT and Diabetic Mice During Healing.....	105
2.4	Discussion.....	114
2.5	Conclusion	121
2.6	References.....	122
Chapter 3	129
3	General Discussion.....	129
3.1	Summary and Final Conclusions	129
3.2	Contributions to the Current State of Knowledge.....	130
3.2.1	Galectin-3 as a Modulator of Re-epithelialization.....	130
3.2.2	Galectin-3 as a Modulator of inflammatory Processes	131
3.2.3	Models of Impaired Healing and Galectin-3	132
3.2.4	The Efficacy of Matricellular Proteins as Therapeutics	133
3.2.5	Galectin-3 Bioactivity.....	134

3.3 Future Directions	135
3.3.1 Improving Scaffold Pore Size.....	135
3.3.2 Establishing Galectin-3 Bioactivity <i>In Vitro</i> and <i>In Vivo</i>	135
3.4 Limitations	137
3.4.1 Animal Model	137
3.4.2 Calculation of Wound Size and Number of Animals Used in Mouse Studies.....	137
3.5 Final Summary.....	138
3.6 References.....	139
Appendices.....	143
Curriculum Vitae	148

List of Tables

Table 1: A summary of parameter combinations used during electrospinning to compare the effects of the flowrate and collector distance on the resulting fiber diameter	47
Table 2: Human recombinant galectin-3 amino acid sequences detected by mass spectrometry.....	71

List of Figures

Figure 1.1 – Upregulation of matricellular proteins during the wound healing response	13
Figure 1.2 – Domains and structures of recombinant human galectin-3	16
Figure 1.3 – Macrophage activation and polarization	19
Figure 2.1 – Schematic representation of the electrospinning process	49
Figure 2.2 – Effect of increasing collector distance and flowrate on mean fiber diameter	59
Figure 2.3 – Effect of increasing concentration on mean fiber diameter.....	61
Figure 2.4 – The effect of increasing concentration on fiber morphology and fiber size distribution	63
Figure 2.5 – Refined scaffold morphology and fiber size distribution	65
Figure 2.6 – Mercury porosimetry pore size distribution plot.	68
Figure 2.7 – Visualization of detected sequences on recombinant human galectin-3	72
Figure 2.8 – Adhesion of human dermal fibroblasts on scaffolds	75
Figure 2.9 – Proliferation of human dermal fibroblasts on scaffolds	77
Figure 2.10 – Visualization of human dermal fibroblast cytoskeleton on scaffolds	79
Figure 2.11 – Deposition of fibronectin by human dermal fibroblasts on scaffolds	81
Figure 2.12 – Representative images of the wound area for evaluation of wound closure kinetics in WT mice	84
Figure 2.13 – Wound closure kinetics <i>in vivo</i> for full thickness wounding in WT mice	86
Figure 2.14 – Representative images of the wound area for evaluation of wound closure kinetics in db/db mice	88

Figure 2.15 – Wound closure kinetics <i>in vivo</i> for full thickness wounding in db/db mice	90
Figure 2.16 – Masson’s Trichrome staining at day 17 following <i>in vivo</i> full thickness wounding in db/db mice.....	92
Figure 2.17 – Wound closure, re-epithelialization and epithelial thickness in WT mice	95
Figure 2.18 – Masson’s Trichrome staining following <i>in vivo</i> full thickness wounding in WT mice.....	97
Figure 2.19 – Wound closure, re-epithelialization and epithelial thickness in db/db mice ..	100
Figure 2.20 – Masson’s Trichrome staining following <i>in vivo</i> full thickness wounding in db/db mice.....	102
Figure 2.21 – Macrophage populations during <i>in vivo</i> full thickness wounding in WT mice	106
Figure 2.22 – Quantification of arginase I-positive macrophages within the wound bed of WT mice at day 7.	109
Figure 2.23 – Macrophage populations during <i>in vivo</i> full thickness wounding in db/db mice	111

List of Appendices

Appendix A: Standard curves for the quantification of cell numbers using the CyQUANT® Cell Proliferation Assay Kit.....	143
Appendix B: No primary antibody negative control for fibronectin immunofluorescence..	145
Appendix C: No primary antibody negative control for arginase I /iNOS immunofluorescence.	146
Appendix D: Copyright permissions	147

List of Abbreviations

AA	Antibiotic-antimicotic
AGE	Advanced glycation end product
ALIX	ALG-2 interacting protein X
ANOVA	Analysis of variance
BMDM	Bone marrow derived macrophage
BSA	Bovine serum albumin
CCN1	Cysteine-rich angiogenic inducer 61
CCN2	Connective tissue growth factor
CRD	Carbohydrate recognition domain
DAPI	4',6-diamidino-2-phenylindole
DFU	Diabetic foot ulcer
DMEM	Dulbecco's modified eagle medium
ECM	Extracellular matrix
EGF	Epidermal growth factor
EGFR	Epidermal growth factor receptor
FBS	Fetal bovine serum
FGF	Fibroblast growth factor
GTA	Glutaraldehyde
ICAM-1	Intracellular adhesion molecule 1

IFN- γ	Interferon gamma
IL	Interleukin
iNOS	Inducible nitric oxide synthase
KGF	Keratinocyte growth factor
LPS	Lipopolysaccharide
MMP	Matrix metalloproteinase
NADPH	Nicotinamide adenine dinucleotide phosphate
Nf- κ B	Nuclear factor kappa-light-chain-enhancer of activated B cells
PBS	Phosphate buffered saline
PCL	Polycaprolactone
PDGF	Platelet derived growth factor
PEO	Poly ethylene oxide
PLACL	Poly(L-lactic acid)-co-poly(ϵ -caprolactone)
RPM	Revolutions per minute
SEM	Scanning electron microscopy
SEM	Standard error of the mean
TGF- α	Transforming growth factor alpha
TGF- β	Transforming growth factor beta
TIMP	Tissue inhibitor of metalloproteinases
TNF- α	Tumor necrosis factor alpha

UV	Ultraviolet
VEGF	Vascular endothelial growth factor
VEGFR	Vascular endothelial growth factor receptor
WT	Wild type

1 Introduction

1.1 Skin, Cutaneous Wound Healing and Chronic Wounds

1.1.1 Skin Anatomy and Physiology

Skin is the largest organ in the human body, playing several important physiological roles including water regulation, thermoregulation as well as acting as a barrier against physical, chemical and biologic stresses (1, 2). Human skin is subdivided into three layers: the epidermis, dermis and the hypodermis. The epidermis is the outermost layer and is responsible for the skin's barrier function. It is a cell dense layer consisting of keratinocytes that synthesize the major structural protein found in the epidermis, keratin. Also present in the epidermis are melanocytes, which produce melanosomes containing melanin, giving skin its pigmentation and providing protection for cell nuclei from ultraviolet light. Langerhans cells are also found in this layer and act as antigen-presenting cells (3). The dermis is the largest layer of the skin and is responsible for protecting the body from mechanical injury (1, 4). The main structural component of dermis is the extracellular matrix (ECM), which consists of proteins including reticulin, elastin, and collagen (types I, III and V) (5). Collagen accounts for the majority of the ECM and is responsible for the elastic and tensile properties of skin (4). The primary cell type of the dermis is the fibroblast which acts to secrete ECM proteins (4). Upon reaction to different stimuli, various leukocyte populations including macrophages can enter the dermis through vascular networks (1). The subcutaneous tissue consists of lipocytes separated by fibrous septa containing blood vessels and collagen, and plays a role in buoyancy and providing energy storage (5).

1.1.2 Cutaneous Wound Healing

Normal cutaneous wound repair involves four overlapping phases of hemostasis, inflammation, proliferation, and remodeling. Upon injury, the inflammatory phase is initiated, with platelets aggregating in the wall of injured blood vessel to form a plug and subsequently a fibrin network. This creates a clot to establish homeostasis (6). Neutrophils are then recruited to debride the wound of foreign particles and bacteria.

Neutrophil populations are removed from the eschar or become engulfed by macrophages. In response to certain chemoattractants, including transforming growth factor beta (TGF- β), monocytes infiltrate the wound and differentiate into macrophages (7). Macrophages are central to development of granulation tissue and are responsible for producing nitric oxide, pro-inflammatory cytokines such as tissue necrosis factor alpha (TNF- α), interleukin 1 beta (IL-1 β), IL-6, and IL-12, and growth factors including fibroblast growth factor (FGF), epidermal growth factor (EGF), TGF- β , and platelet derived growth factor (PDGF) (8, 9).

Within hours of initial injury, epithelial cell proliferation and migration is initiated through the release of EGF, transforming growth factor alpha (TGF- α) and FGF, which begins the re-epithelialization phase (9). The epidermis and the basement membrane separate via dissolution of their hemidesmosomal links and subsequent keratinocyte migration over the dermis separates the eschar from viable tissue (6, 7). Behind the leading edge of migration, the keratinocytes proliferate and mature, eventually restoring the barrier function of the epithelium (6). Macrophages secrete TGF- β that signals fibroblasts to migrate into the granulation tissue and produce new ECM components. These components, including fibronectin, hyaluronic acid, and collagen, serve as a scaffold for cell infiltration of the granulation tissue through cell migration (7). The secretion of vascular endothelial growth factor (VEGF) and PDGF by activated platelets and macrophages initiates angiogenesis (6, 9). This process results in the formation of blood vessels that support the newly formed granulation tissue by providing a nutrient and oxygen supply to sustain cell growth and metabolism (7). TGF- β also stimulates the differentiation of fibroblasts into myofibroblasts, highly contractile cells which contract the wound, pulling the edges together to achieve closure (6, 9).

During the remodeling phase endothelial cells, macrophages, and myofibroblasts undergo apoptosis or exit the wound. The wound consists predominantly of a type III collagen, ECM proteins and is largely acellular. It is subsequently remodeled into a type I collagen matrix by matrix metalloproteinases (MMPs) secreted by fibroblasts, macrophages, and endothelial cells, although the remodeled tissue never fully regains the tensile strength of the original skin (6, 7).

1.1.3 Chronic Dermal Wounds

A dermal wound is classified as chronic if it has failed to progress through the normal sequences of the wound healing process within a twelve week period (10), resulting in the impairment of normal tissue function and anatomy (11). Chronic wounds are characterized by residual inflammation, cellular senescence, lack of cell signaling, and bacterial colonization (11). A variety of factors can contribute to their development, including vascular insufficiency, diabetes, malnutrition, patient age, pressure, infection, and edema (12). These wounds become a significant burden to the patient, as they can be painful, impair limb function, and result in sepsis or the need for amputation (12). Furthermore, they pose a significant burden to the Canadian healthcare system, with the average cost of treatment of a chronic wound being \$10,376 (13). The most common types of chronic wounds, which include venous, arterial, and diabetic foot ulcers (DFUs), are discussed below (11, 14).

Venous ulcers affect around 0.1% of the Canadian population. They are more common in older patients although early onset can begin in patients in their twenties (15). The skin in these patients becomes injured as a result of limb edema and venous hypertension, which can occur due to venous thrombosis, venous valve reflux, or from damage to the venous wall or valves (16, 17). The ulcers develop in the gaiter region of the lower leg, form with an irregular border, and usually contain granulation and fibrinous tissue. Patients typically experience aching of the legs after long periods of standing in addition to leg heaviness and swelling (11).

Up to 10% of patients with lower limb ulcers have arterial insufficiency (18). Arterial ulcers can result from any process that obstructs arterial flow, which includes vasculitis, microthrombotic disease, sickle cell disease, and atherosclerosis. Progressive atherosclerosis is the most common cause for arterial ulcers, where smoking, poorly controlled hypertension and diabetes mellitus can cause high levels of circulating cholesterol and triglycerides, leading to lipid deposition in arterial vessel walls which causes arteries to become stenotic (19). Atherosclerosis causes poor perfusion, impairs skin oxygenation, and causes breakdown of the tissue. The wounds typically develop at

bony prominences or distal points and have dry necrotic wound beds, demarcated borders, and lack granulation tissue (11).

Pressure ulcers affect up to 26% of patients in Canada (20) and are common in patients with impaired mobility or sensory perception, malnutrition, and fecal incontinence (11, 12). They can start to develop in patients after just 2 hours of compression of soft tissues, and commonly occur when there is contact between a surface and bony prominence (19). Several factors can lead to the development of a pressure ulcer including sustained shear forces or forces perpendicular to the point of contact, friction that can lead to blisters or erosions, loss of elastin in aged skin that decreases resistance to pressure, and prolonged exposure to moisture (sweat, urine, fecal) that can result in breakdown of the skin (19). These factors result in localized tissue necrosis that leads to tissue injury (11).

Currently in Canada, 3.5 million individuals live with diabetes (21) and up to 25% of these patients will be affected by a DFU in their lifetime (22). Neuropathy, vascular disease, and previous foot ulceration are major risk factors for the development of a diabetic ulcer (19, 23). Neuropathy can impair a patient's joint mobility and cause an imbalance of pressure distribution on the foot, which can lead to the formation of calluses (19, 23). Additionally, the loss of sensation in the foot can result in repetitive injury that these patients are unable to detect (19, 23). Ischemia resulting from vascular disease impairs oxygenation of the feet leads to dry skin and results in breakdown of the tissue (11). DFUs are commonly located on the plantar surfaces of the feet where they are exposed to repetitive injury, with foot deformities and reduced joint mobility causing callus formation at abnormal pressure points (11). DFUs are a highly problematic outcome of diabetes, as they are the most common cause of non-traumatic lower limb amputations, with 15-20% of DFU patients requiring amputation (10). Furthermore, these amputations are associated with a high incidence of mortality (24). In Canada, the Canadian Diabetes Association reported that 30% of patients with diabetes will die within one year of amputation and 69% of patients with amputations will not survive past 5 years (13). In addition to their comorbidities, DFUs burden the Canadian healthcare system, costing \$150 million annually (13).

1.1.4 Current Treatments for Chronic Wounds

Current management of chronic wounds is based on TIME guidelines which were first described by Schultz et al. (25). The TIME acronym refers to Tissue, Infection, Moisture Balance, and Wound Edge Management (26). In treating chronic wounds, the first step is to remove any necrotic tissue, which can impair healing. This non-viable tissue is removed through debridement that can be conducted using surgery, enzymatic digestion, or using biologic or mechanical methods (27). Bacterial infection of a wound can both delay healing and lead to systemic infections. To address this problem, wounds can be cleaned with water or saline and dilute acetic acid when they are prone to infection. Topical antimicrobial agents, including silver, gel beads for slow-release of cadexomer iodine, and manuka honey are also recommended for treatment of superficial wound infection (27). Moisture retentive dressings can be used to maintain sufficient moisture within the wound while controlling exudate. There are several types of dressings available although their applicability depends on the nature of the wound including level of exudate, depth and area of the injury, healing stage, and skin type (26, 27). Many biologic dressings are also available and are applied with the intent of creating a microenvironment supportive of healing. However, the efficacy of dressings is often specific to the type of chronic wound or underlying disease and there is often limited clinical support for their use (27).

In addition to wound management, many adjunctive therapies exist for the treatment of chronic wounds including use of topical agents, bioengineered dressings, hyperbaric oxygen therapy, and negative pressure wound therapy. Currently, most topical agents available for chronic wound treatment target infection or have anesthetic properties (27). RegranexTM is a topical formulation of PDGFTM and is currently the only growth factor approved by the Food and Drug Administration for the treatment of DFUs (10). Although clinical trials have shown an increase in wound closure with use of RegranexTM relative to placebo controls (27), other studies in animal models have shown it to be less effective for full thickness wounds relative to other drug targets (28). Use of three or more tubes of gel is also associated with an increased risk of cancer-related mortality (10). PROMOGRAN[®] Matrix is another topical dressing agent used to inhibit protease

activity and is approved for use in chronic wounds (27). It has been shown to improve microcirculation in venous ulcers (29); however, a randomized controlled trial failed to demonstrate that PROMOGRAN® Matrix can significantly accelerate healing relative to controls (30).

There are a growing number of bioengineered substitutes being developed for use in chronic wounds (27, 31, 32). The Integra Bilayer Wound Matrix is an acellular matrix consisting of a dermal layer of type I bovine collagen and shark chondroitin-6-sulfate and an epidermal layer of silicone (31). Case reports have described Integra Bilayer Wound Matrix as promoting healing in DFUs when used in combination with other treatment methods (33). A retrospective study reported an 81% healing rate of lower extremity wounds although only 16 patients were included in the study and not all wounds were considered chronic (34). Another acellular dressing is the OASIS® Wound Matrix which is made from porcine intestinal submucosa (27). A multicenter trial of patients with venous ulcers reported that a higher number of patients achieved complete wound closure when OASIS® was used relative to compression bandaging alone, although adverse events, including skin injury and infection, were also reported in two patients (31). Skin substitutes containing cells include Dermagraft® and Apligraf®. Dermagraft® is a polyglactin scaffold implicated for treatment of DFUs. It contains human, neonatal-derived fibroblasts and several growth factors, including TGF- β 1, TGF- β 3, TGF- α , heparin binding epidermal growth factor, PDGF-A, insulin-like growth factor, keratinocyte growth factor (KGF), and VEGF (10). Apligraf® is a matrix intended for use in diabetic and venous ulcers. It contains a stratum corneum of differentiated keratinocytes a dermal layer consisting of type I bovine collagen fibrils (10, 27). There is a stronger body of evidence supporting use of these products for treating chronic wounds, as numerous studies report their efficacy, showing improvements in healing relative to controls (27, 31). However, adverse events have been reported in some studies and multicenter studies for treatment of foot ulcers are still lacking (31, 35).

For treatment of DFUs, hyperbaric oxygen therapy (HBOT) and negative pressure wound therapy can also be conducted in conjunction with other treatments. HBOT entails the delivery of 100% oxygen to the wound, usually for 90 minutes at 1.5-3.0 atmospheres. It

is typically conducted in daily sessions and is intended to increase oxygen saturation of the blood (36). Although there is some evidence to support its efficacy in healing DFUs in patients with concomitant ischemia (36), Health Quality Ontario reported that there was insufficient evidence for its use as adjunct to standard therapy for patients with non-healing DFUs due to inconsistent results in randomized controlled trials (37). Negative pressure wound therapy can also be used for DFU treatment and entails the delivery of sub atmospheric pressures to the wound bed using a vacuum pump in order to promote cell proliferation in the wound bed (38). Although it is effective for post-surgical treatment of acute wounds, its efficacy has not yet been shown for chronic, non-healing wounds (38, 39).

1.2 Pathophysiology of Chronic Wounds

As previously discussed, chronic wounds do not follow the regular wound healing process, resulting in failure to achieve closure (40). Rather, these wounds have decreased levels of growth factors essential for the normal wound healing response including TGF- β and VEGF, preventing essential processes such as re-epithelialization and angiogenesis. Additionally, chronic wounds have increased levels of expression of inflammatory cytokines, such as IL-1, IL-6, and TNF- α , which enhance the immune response and increase local inflammation (41). As a result, there is a continuous, self-perpetuating cycle of inflammation, preventing progression into the proliferative phase of healing and leaving the wound in a non-healing state regardless of wound management and intervention (12, 40). Several underlying factors lead to the continuous state of inflammation, including impaired processes such as re-epithelialization and granulation tissue formation, imbalances in proteolytic activity, bacterial colonization resulting in the development of biofilms, the accumulation of advanced glycation end products (AGEs, in diabetic patients), and the accumulation of oxidative stress in the wounds (12, 41). The independent role each of these factors plays in the perpetuating inflammation is discussed in depth below.

1.2.1 Impaired Re-epithelialization and Granulation Tissue Formation

In chronic wounds, keratinocytes lack the ability to migrate, properly differentiate, and proliferate (41). Keratinocyte migration is impeded due to decreased levels of expression of EGF, FGF and TGF- α and their proliferation is reduced due to lower levels of KGF (9, 42). Nuclear localization of β -catenin and overexpression of c-Myc also impede epithelial cell migration and suppress their terminal differentiation (43). Together, these factors impede re-epithelialization as they prevent keratinocytes at the edge of the wound from migrating to form an epithelial barrier (41, 44).

Chronic wounds also show a significant deficiency in granulation tissue formation. This is thought to be due to the overproduction of anti-angiogenic cytokines along with reduced production of pro-angiogenic cytokines and the sequestering of growth factors (45). Fibroblasts exhibit a phenotypic change in addition to decreased migration and proliferation (41). Their migration and secretion of collagenase is hindered, due to decreased levels of FGF-2 (9). Neovascularization is impaired due to decreased levels of VEGF and FGF-2 (9). Upon treatment with VEGF and FGF-2, diabetic mice have displayed significantly improved angiogenesis and accelerated wound healing (42). Levels of VEGF are decreased due to reduced amounts of TGF- β 1 in the wounds, which acts to upregulate VEGF expression (9). Chronic wounds are also characterized by lower levels of PDGF, further impeding angiogenesis (42). Finally, lowered levels of TGF- β 1 decrease levels of fibronectin, collagen, and protease inhibitors, hindering new ECM formation (9).

1.2.2 Imbalance of Proteolytic Activity

A balance of activity between proteases and their inhibitors is required for the normal wound healing process to occur, as they play a functional role in the maintaining the integrity of the ECM and controlling its degradation to facilitate migration of cells into the wound (42, 46). In chronic wounds, this delicately controlled balance in protease and inhibitor levels is offset, with increased levels of MMPs and decreased levels of tissue inhibitor of metalloproteinases (TIMPs) being well documented in chronic wounds in

both animal models and studies investigating human chronic wound exudate (42, 47). These changes have been attributed to a lack of TGF- β 1 in chronic wounds, which lowers TIMP levels by inhibiting their secretion by fibroblasts (42). Chronic wounds also exhibit a sustained increase in pro-inflammatory cytokines including IL-1 β and TNF- α , which increase production of MMPs, including MMP-1, MMP-2, MMP-3, MMP-9, and MMP-13 while reducing synthesis of TIMPs (9, 46). Moreover, the elevation of certain MMPs can activate other MMPs, triggering further increases in MMP levels (42). Increased MMP activity degrades ECM, inhibits cell migration, and reduces fibroblast proliferation and collagen deposition (12). MMPs have also been shown to degrade growth factors and their target cell receptors, including EGF/epidermal growth factor receptor (EGFR) and PDGF/platelet derived growth factor receptor further impairing the wound healing cascade (9, 46). This enhanced proteolytic activity, taken together with insufficient angiogenesis in chronic wounds, contributes to the inability to form proper granulation tissue (9).

1.2.3 Biofilm Formation

Bacterial colonization of chronic wounds is also known to play a contributing role in delayed healing, although the direct causal relationship in etiology is yet to be established (48). Upon formation of the wound, the resulting loss in barrier function leaves the wound susceptible to infection (23). Bacteria commonly found in wounds include *Staphylococcus aureus*, *Pseudomonas aeruginosa* and β -haemolytic streptococci and counts over 10^5 bacteria per gram of wound tissue are considered detrimental to healing (12). Bacteria secrete a polymeric matrix adherent to the wound, forming a biofilm that is an environment optimal for their survival, as this matrix is resistant to both the innate immune mechanisms and antimicrobial agents (48, 49). Biofilms contribute to inflammation due to their effect on neutrophils and macrophages. Specifically, biofilms inhibit neutrophil chemotaxis and degranulation as well as preventing them from ingesting bacteria, resulting in increased secretion of pro-inflammatory cytokines. They also prevent the phagocytosis of neutrophils by macrophages, causing further dysregulation of inflammation (48). In animal models, biofilms have also been shown to delay re-epithelialization (50).

1.2.4 Advanced Glycation End Products

AGEs are compounds formed through the Maillard reaction, which is a reaction that occurs between the amino groups of proteins and carbonyl groups of reducing sugars (51). AGEs are continuously produced in the body, but accumulate with the presence of hyperglycemia or oxidative stress (52). Higher levels of AGEs in skin have been associated with increased patient age, diabetes, as well as the presence of an ulcer in diabetic patients and there is a large body of evidence implicating their role in the pathogenesis of impaired diabetic wound healing (52, 53). AGEs can crosslink type I collagen which results in its decreased solubility and increased rigidity (52). They can also form on both laminin and type IV collagen, impairing both matrix-matrix interactions and cell-matrix interactions (54). Soluble plasma proteins, including albumin, fibrinogen, immunoglobulin, and low-density lipoprotein can also become glycated, altering their structure and function (51, 54). Glycated albumin plays a role in platelet activation and aggregation and glycated immunoglobulin is associated with inflammation (51).

AGEs can also affect the function of wound healing cell types. In vitro studies have associated AGEs with impaired keratinocyte migration and proliferation (55). They have also been implicated in promoting apoptosis, inhibiting proliferation, and reducing secretion of ECM proteins by fibroblasts, including proteoglycans and hyaluronic acid (52). AGEs can also interact with AGE receptors on macrophages and endothelial cells, which causes oxidative stress and activates nuclear factor kappa-light-chain-enhancer of activated B cells (NF- κ B). NF- κ B increases production of pro-inflammatory cytokines including IL-1 α , IL-6, and TNF- α (51). AGE binding to AGE receptors also increases production of vascular cell adhesion protein 1 and intracellular adhesion molecule 1 (ICAM-1), which contribute to inflammation. The production of TNF- α results in increased production of reactive oxygen species (51). Sustained inflammation and oxidative stress further exacerbate AGE formation by increasing expression of AGE receptors through a positive feedback loop (52).

1.2.5 Oxidative Stress

Wound fluid in patients with non-healing chronic wounds has shown significantly higher levels of oxidative stress relative to wound fluid in patients with healing wounds (17). Oxidative stress occurs when there is excessive generation of reactive oxygen species (ROS) relative to the antioxidant capacity (44). It can cause serious cellular damage by impairing mitochondrial function (56). Elevated levels of ROS are also associated with supporting migration of inflammatory cells into the wound, upregulating ICAM-1, which damages endothelial cells and facilitates recruitment of leukocytes, and impairing keratinocyte migration *in vitro* (47).

Skin has a number of antioxidants including glutathione, ascorbic acid, and vitamin E, which are involved in infection control as well as reducing oxidative stress that is generated from inflammation in acute wounds (47). Chronic wound patients have been shown to have decreased levels of vitamins A and E. Lower limb ulcers have also been found to have decreased levels of selenium, a cofactor to glutathione peroxidase, as well as lower glutathione peroxidase activity (47). Lower levels of antioxidants combined with decreased antioxidant enzyme activity can debilitate antioxidant defense against oxidative stress (47). In patients with venous leg ulcers, iron overload also plays a contributing role to oxidative stress. Patients with venous leg ulcers have been shown to have higher levels of iron with concomitant elevation of MMP-9, suggesting that elevated iron deposits are released through activation of MMPs. Iron overload causes oxidative stress through the production of ROS including superoxide, nitric oxide, hydrogen peroxide, and peroxynitrite (17).

Hyperglycemia resulting from diabetes can result in the over activation of several pathways. One such pathway is the hexosamine pathway, which inhibits the activity of glucose-6-phosphate dehydrogenase and limits the formation of nicotinamide adenine dinucleotide phosphate-oxidase (NADPH). Increased proteinase kinase C activity can also activate NADPH, depleting it (44). NADPH oxidase is required for the formation of reduced glutathione and nitric oxide, which act to neutralize reactive oxygen species; hence its depletion contributes to oxidative stress (44, 57). The polyol pathway, responsible for converting glucose to fructose, can also become over activated, resulting

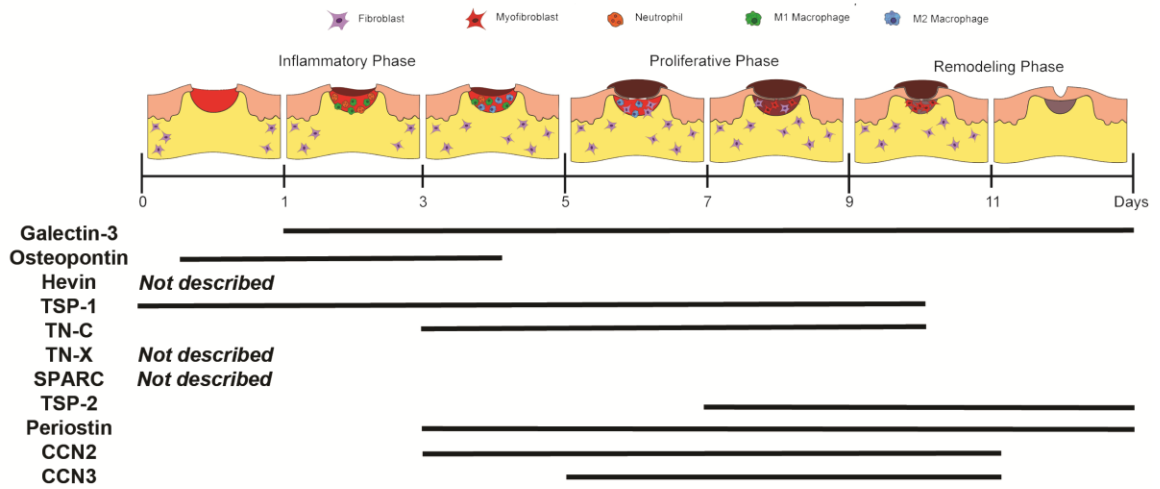
in further depletion of NADPH oxidase. Over production of fructose through this pathway also contributes to the formation of AGEs, which accumulate with hyperglycemia as previously discussed (57). AGE binding to activated AGE receptors leads to the production of cytosolic ROS and the activation of NADPH oxidase, further sources of oxidative stress and cellular dysfunction (51, 58). Finally, the combination of hyperglycemia and presence of free radicals can activate the PARP pathway, further exacerbating oxidative stress (57).

In summary, several factors act in combination to perpetuate the inflammatory response in chronic wounds, which plays an integral role in preventing a wound's progression through the normal wound healing cascade (40). The consequences of remaining in this non-healing inflammatory state are severe, as wounds do not achieve closure, leaving the patient with a high risk of amputation (10), and consequently, at a high risk for mortality following amputation (24). Therefore, due to poor patient outcomes and limited treatment options, it is imperative that new treatment options be pursued. In light of the current knowledge on chronic wound pathology discussed above, new approaches for the treatment of chronic wounds should focus on modulating the inflammatory response, such that the proliferative phase of inflammation can be activated and therefore, the normal wound healing response achieved.

1.3 Galectin-3 as a Therapeutic for Chronic Wounds

Matricellular proteins are non-structural components of the extracellular matrix that become upregulated during wound healing and pathological processes. During the wound healing process, they act spatially and temporally to control specific cell behaviours (Figure 1.1) (59). Galectin-3 is a matricellular protein implicated in several inflammatory and immunomodulatory processes (60), making it an ideal candidate for treatment of chronic wounds. It has shown the ability to influence monocyte and macrophage migration (61), increase clearance of neutrophils (62), and regulate alternative macrophage polarization (63), all processes that can contribute to modulating the inflammatory response. Therefore, it is hypothesized that the use of galectin-3 will be effective in promoting healing in chronic wounds by stimulating the proliferative phase of healing.

Figure 1.1 – Upregulation of matricellular proteins during the wound healing response: Matricellular proteins upregulated during the wound healing response include galectin-3, osteopontin, thrombospondin 1 (TSP-1), tenascin-c (TN-C), thrombospondin 2 (TSP-2), periostin, cysteine-rich angiogenic inducer 61 (CCN1), and connective tissue growth factor (CCN2). Galectin-3 expression peaks at day 1 following wounding in mice and persists throughout the inflammatory process (64). Reprinted with permission from Hamilton D, Walker J, Kim S, Michelsons S, Creber K, Elliott C, et al. Cell-matrix interactions governing skin repair: matricellular proteins as diverse modulators of cell function. *Research and Reports in Biochemistry*. 2015;73 (64). Copyright © 2015, Dove Press Ltd.

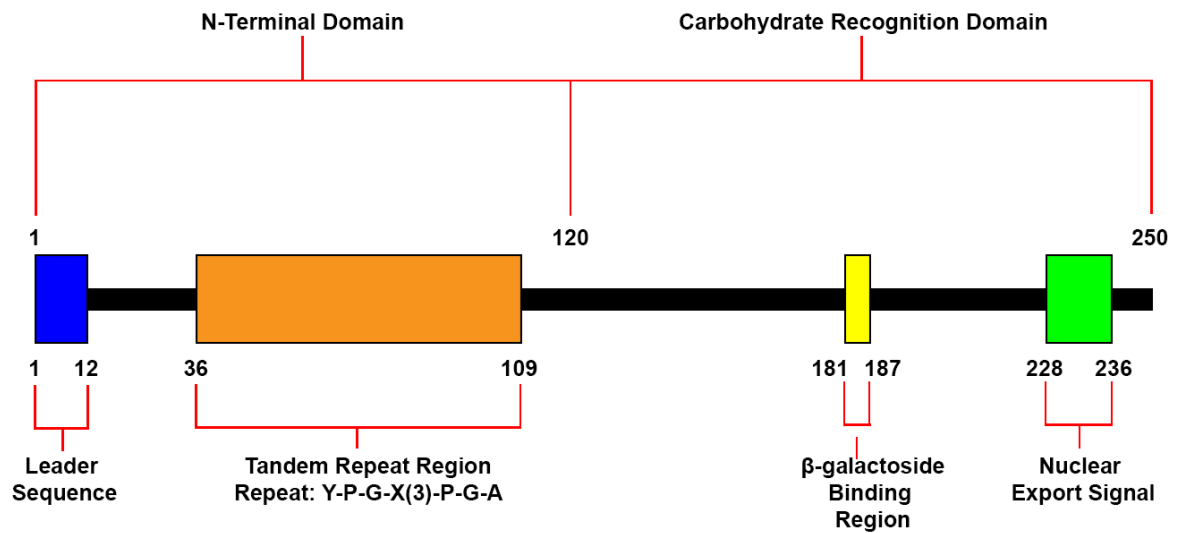


1.3.1 Protein Structure

Galectin-3 is a protein consisting of 250 amino acids, separated into two distinct domains (Figure 1.2) (65). The carbohydrate recognition domain (CRD) of this protein accounts for approximately 130 amino acids and is globular in structure (66). The CRD domain contains S-lectin motifs that provide the protein with the ability to bind β -galactosides, a property shared by all proteins in the Galectin family (67, 68), as well as a nuclear export signal (69).

In addition to its CRD, Galectin-3 contains an amino terminal domain, which spans approximately 120 amino acids and contains a highly conserved tandem repeat rich in proline, glycine and tyrosine (66, 70). The N-terminus contains a 12 amino acid leader sequence that is required for Galectin-3 secretion (66). Within this leader sequence serine⁶ can be phosphorylated, a process which significantly reduces binding to its ligands (laminin and mucin) and may act as an on/off switch for its ability to bind to sugars (71). The N-terminal domain also enables the formation of oligomers and is required for full biological function of the protein, including its role in modulating cell adhesion and inducing intracellular signalling (70, 72). Galectin-3 has been detected within cells, localized in the nucleus and cytoplasm, and has also been described outside of the cell, despite its lack of a known transmembrane domain and sequence (66, 73). It has been found to interact with a variety of wound healing cell types including, keratinocytes, fibroblasts, monocytes and macrophages (61, 74, 75).

Figure 1.2 – Domains and structures of recombinant human galectin-3: Human recombinant galectin-3 is a protein consisting of 250 amino acids. It features a 120 amino acid N-terminal region that contains a leader sequence and a tandem repeat region rich in proline, glycine and arginine. It also comprises of a CRD containing a β -galactoside binding region and a sequence required for nuclear export.

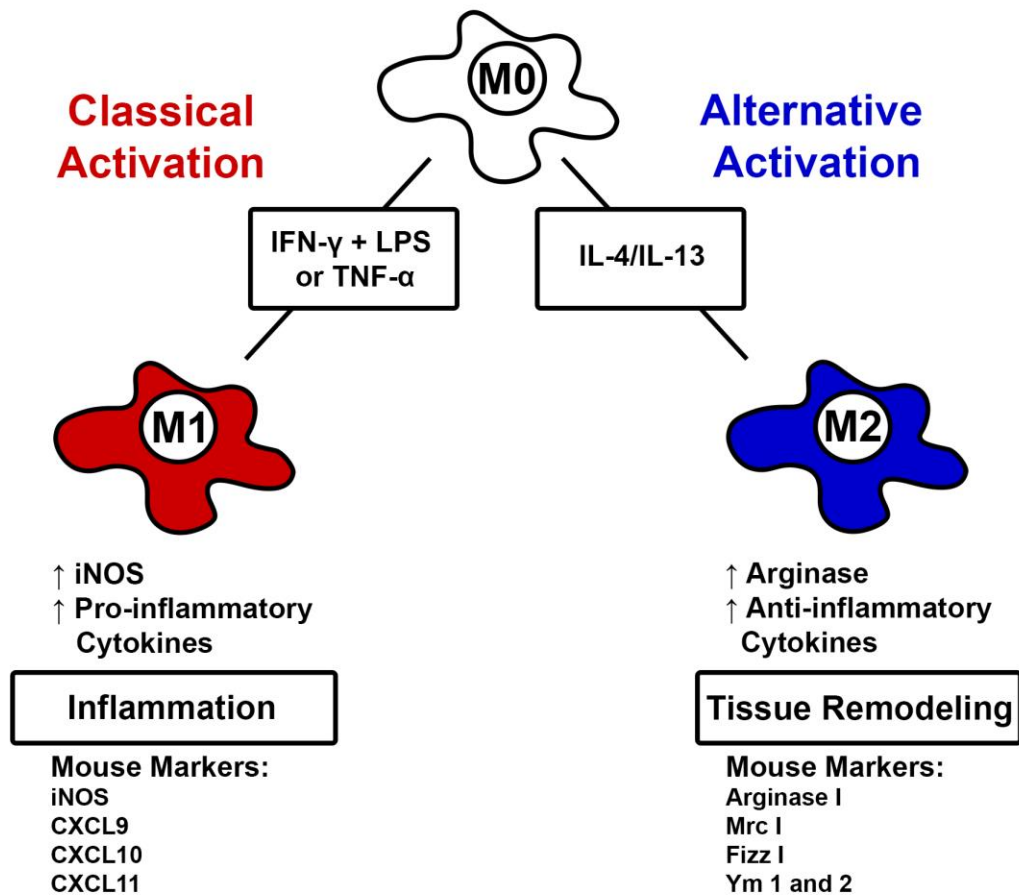


1.3.2 Role in Inflammation

Galectin-3 has been demonstrated to influence a variety of processes associated with inflammation through its interaction with various cell types including neutrophils, monocytes, and macrophages. In the initial stages of inflammation, neutrophils are recruited to the wound to eliminate foreign particles and bacteria. *In vitro* studies have shown that recombinant human galectin-3 can activate neutrophils in a dose-dependent manner, through a process involving its CRD (76). A study investigating NADPH oxidase activity revealed that galectin-3 activated exudate neutrophils, with increased activity corresponding to increased surface-bound protein, while activity was unaltered in peripheral neutrophils (77). In addition to neutrophil activation, galectin-3 has shown to facilitate neutrophil adhesion to laminin *in vitro* and has been implicated in the recruitment of neutrophils in a murine model of cutaneous infection (78, 79).

The inflammatory phase of healing also involves the recruitment of monocytes to the wound, which differentiate into macrophages of varying phenotypes that play distinct roles in inflammatory processes (80). Galectin-3 induces monocyte migration *in vitro*, stimulating chemotaxis at high concentrations and chemokinesis at lower concentrations. A migratory effect from galectin-3 is also observed in macrophages (61). Migration in both monocytes and macrophages is increased in the presence of fibronectin, suggesting that galectin-3 may mediate linkage of these cells to fibronectin (81). One of macrophage's roles in inflammation is to rid the wound of neutrophils, ingesting them and inducing their apoptosis (80). *In vitro* studies suggest that galectin-3 can influence this process as addition of exogenous galectin-3 increases apoptotic neutrophil uptake in macrophages. It has also been postulated that galectin-3 acts as an opsonin, linking the phagocytic macrophages to the neutrophils (62). A study conducted by MacKinnon et al. investigated the effect of galectin-3 on macrophage activation in bone marrow derived macrophages *in vitro* and in resident lung and recruited peritoneal macrophages *in vivo*. Interestingly in all macrophages derived from galectin-3 deficient mice, IL-4/IL-13-induced M2 macrophage polarization was inhibited, suggesting that galectin-3 is involved in the regulation of alternative macrophage activation (63). A summary of macrophage activation and polarization is shown in Figure 1.3.

Figure 1.3 – Macrophage activation and polarization: Monocytes can undergo classical activation in the presence of interferon gamma (IFN- γ) and lipopolysaccharides (LPS) or TNF- α into M1-polarized macrophages, which are associated with inflammation. M1 macrophages produce inducible nitric oxide synthase (iNOS) as well as pro-inflammatory cytokines. In mice, markers of M1 macrophages include iNOS, chemokine ligand 9 (CXCL9), CXCL 10, and CXCL11. Monocytes can undergo alternative activation through stimulation with IL-4 or IL-13 into M2-polarized macrophages. M2 are associated with tissue remodeling and secrete arginase I and anti-inflammatory cytokines. M2 markers in mice include arginase I, Mrc I, Fizz I, Ym1, and Ym 2 (8, 80, 82).



1.3.3 Role in Angiogenesis

Galectin-3 has been shown to induce angiogenesis both *in vitro* and *in vivo*. *In vitro*, the protein stimulated capillary tube formation of human umbilical cord endothelial cells grown on a matrigel, while *in vivo*, a galectin-3-loaded matrigel was able to induce angiogenesis in nude mice. Both of these processes relied on its CRD (83). Markowska et al. later proposed that galectin-3 modulated VEGF and FGF-2-mediated angiogenesis by activating focal adhesion kinase-mediated signalling pathways that modulate endothelial cell migration during this process (84). The protein has also been linked to angiogenesis and the migration of endothelial cells through integrin-linked kinase signalling (85). Galectin-3 was also shown to bind to vascular endothelial growth factor receptor 2 (VEGFR2), promoting its phosphorylation and preventing its internalization, leading to an increased angiogenic response of human umbilical cord endothelial cells to VEGFA *in vitro* (86).

In combination with galectin-1, galectin-3 can activate and prevent the internalization of VEGFR1, another process that enhances angiogenesis (85). Despite these findings, a recent study in mice showed that during wound repair in skin, galectin-3 deficient mice have no difference in vascular density or expression of angiogenic markers relative to wild-type mice (87). These conflicting findings indicate that the role of galectin-3 in angiogenesis likely tissue and context-dependant (64).

1.3.4 Role in Re-epithelialization

The first association of galectin-3 with re-epithelialization came from Kasper and Hughes who noted the surface expression of galectin-3 in Type I and II alveolar epithelial cells in a model of irradiation-induced lung inflammation and repair (88). In a model of corneal wound healing, galectin-3 deficient mice were found to exhibit reduced re-epithelialization rates relative to wild-type counterparts. Interestingly, galectin-3 did not alter proliferation rates of epithelial cells and elevated levels of galectin-3 were detected in the migrating epithelial front following injury, suggesting the protein promotes epithelial cell migration (89). This was supported by later studies showing that galectin-3 promotes cell scattering, lamellipodia formation, and motility in human corneal epithelial

cells (90). Furthermore, studies in mouse corneas showed that galectin-3 knockout mice exhibit impaired re-epithelialization (89). The effect of the addition of exogenous galectin-3 has also been investigated in models of murine corneal healing, where the addition of exogenous galectin-3 increased re-epithelialization in wild type (WT) mice, but not galectin-3 deficient mice (89). The increase in re-epithelialization in WT mice was attributed to the modulation of galectin-7 by exogenous galectin-3, as galectin-7 was found to accelerate re-epithelialization in galectin-3 knockout mice and because mouse embryonic fibroblasts from galectin-3 knockout mice showed reduced levels of galectin-7 (89). Studies of epithelial wounds in monkey corneal explants also demonstrated enhanced re-epithelialization when recombinant human galectin-3 was added exogenously to the media (91).

Consistent with studies in the cornea, studies in skin have revealed that keratinocytes from galectin-3 knockout mice exhibit a migratory defect (75), and that re-epithelialization is delayed in galectin-3 deficient mice (75, 87). However, in skin this defect was attributed to deficient EGFR endocytosis and recycling, which is controlled by cytosolic galectin-3 binding to ALG-2 interacting protein X (ALIX) (75). Additionally, there were no differences between levels of galectin-7 in wound tissue from WT and knockout mice at day 7 post injury, during which re-epithelialization was impaired (87).

Taken together, galectin-3 has been implicated in several processes associated with wound healing, including modulating inflammation and contributing to re-epithelialization. As a result, delivery of this protein during the wound healing process, either topically or via a scaffold, is a potential new therapeutic to enhance repair.

1.4 Protein Delivery Strategy

1.4.1 Scaffolds for Protein Delivery

Although several growth factors and peptides have demonstrated therapeutic potential for chronic wound healing, the effectiveness of applying such treatments topically is limited, due to the peptidase-rich wound microenvironment, which impairs the bioactivity of peptides, and the short half-life of both peptides and growth factors (92, 93). The use of scaffolds for delivery of therapeutic agents aims to overcome this challenge. A scaffold is

a three-dimensional polymeric structure used to treat a defect by acting as an artificial ECM to guide regeneration (94). Their use in the delivery of bioactive molecules offers several advantages, including protecting peptides from rapid biodegradation, providing a large surface area to enable the effective delivery of bioactive molecules, and controlling the release of bioactive molecules so that signals are provided continuously throughout healing (93, 95). Using this method of delivery, the therapeutic agent is able to recruit progenitor cells to the defect and guide cell behavior towards a pro-regenerative response (95). Meanwhile, the scaffold nanotopography is also important in this process, providing a site for cell adhesion and supporting cell proliferation and migration (96-99). Through selection of appropriate therapeutic agents and appropriate scaffold design it is intended that the application of a scaffold to a chronic wound microenvironment will be able to achieve healing by stimulating a pro-regenerative response.

1.4.2 Scaffold Design for Tissue Regeneration

The overall aim in scaffold fabrication is to design an artificial matrix that closely mimics the ECM of the immature granulation tissue (94). Within skin, the dermis consists largely of collagen and contains a meshwork of fibers within the range of 30-130 nm (100). This ECM is responsible for providing mechanical support as well as modulating cell proliferation, migration, differentiation and apoptosis (100). Therefore it is ideal that a scaffold contains fibers with diameters within this range. A high porosity is also needed to support cell ingrowth and to facilitate the diffusion of waste and nutrients (101). Several electrospun scaffolds have been able to obtain porosity values between 60-90%, although 90% porosity has been suggested to be an ideal target (96, 101-103). Scaffolds having pore sizes of approximately 100 μm and porosity in the 90% range have shown the ability to support the infiltration of cells beyond the surface of the scaffold (104). These considerations ensure a high surface area to volume ratio which can accommodate high cell densities (100). Through selection and optimization of scaffold materials, it should also be ensured that the rate of scaffold degradation coincides with the rate of tissue regeneration. Finally, the material itself, along with degradation products, must be biocompatible to ensure it will not elicit an immune response within the host tissue (100).

1.4.3 Scaffold Materials

Scaffolds can be fabricated from a wide range of materials that include natural polymers, synthetic polymers, and polymer composites. Naturally derived polymers commonly used in wound healing include collagen, gelatin, chitosan, and silk fibroin (105). Currently, the majority of artificially made skin substitutes approved for clinical use are collagen-based scaffolds. These scaffolds typically consist of Type I collagen as it is the predominant component of the dermal ECM (105). The use of collagen in scaffolds is advantageous as it can regulate the adhesion, migration, proliferation, differentiation and survival of cells (106). One limitation to collagen scaffold fabrication is that pure collagen is relatively expensive (107). The processing of collagen during scaffold fabrication can also alter its biological and structural properties (108). For example, Zeugolis et al. found that the electrospinning of collagen resulted in its denaturation (109). Alteration of collagen structure can also be caused by many sterilization methods (106). Gelatin is a denatured form of collagen, which can be obtained through both alkaline or acid processing of collagen (106). Use of gelatin for scaffold fabrication is desirable, as it maintains the composition and properties of collagen, while also being commercially available at a low cost (108, 110). Conversion of collagen to gelatin increases exposure of RGD sequences, which may increase cell signaling (111). The use of electrospun gelatin scaffolds has been shown to facilitate the adhesion, migration and proliferation of wound healing cell types, and to increase wound closure in a full thickness wound model in rats (96-99). Overall, natural polymers are strong candidates for wound healing applications as they are biodegradable and biocompatible, supporting cell viability; however, they require crosslinking to control their rate of degradation and mechanical properties (106, 108).

Synthetic polymers include poly-lactic acid (PLA), polycaprolactone (PCL) and polyglycolic acid (PGLA). There are several advantages for the use of synthetic polymers in scaffold fabrication. They are well defined in structure, therefore there is no variation between batches and fine tuning of both their mechanical properties and degradation kinetics can be conducted to suit their application. They can also be supplied in large quantities and are typically less expensive than natural polymers (112). However, cell viability decreases when synthetic polymers are used as these materials have hydrophobic

surfaces, lack the appropriate cell recognition sites and have lower rates of cell adhesion and proliferation (105, 107, 112, 113). To overcome these challenges, researchers are attempting to improve the adhesive properties of these scaffolds by incorporating proteins and amino acids including arginine-glycine-asparagine (RGD) sequences, cysteine, lysine, laminin, and collagen-like proteins (114).

The use of polymer composites aims to overcome the limitations of both natural and synthetic polymers to ultimately create scaffolds with the appropriate biocompatibility as well as physical, mechanical, and chemical properties (107). In this method, a natural polymer, such as collagen, gelatin, or chitosan can be blended with a synthetic polymer such as PCL. This is done at an optimized concentration to improve the mechanical stability using the synthetic component, while also improving the biocompatibility by increasing hydrophilicity and by providing integrin binding sites through the natural component (115, 116). This method also eliminates the need for pre-treatment of the scaffolds to improve functionality (116). Blends of PCL/collagen were found to have more stability relative to collagen-only scaffolds, while also having higher cell proliferation than PCL alone (117). Blends of poly(L-lactic acid)-co-poly(ϵ -caprolactone) (PLACL)/gelatin have also shown significantly higher proliferation of cells relative to PLACL blends after 6 days in culture (115).

1.4.4 Scaffold Fabrication Methods

Several techniques are currently used for the fabrication of scaffolds in skin regeneration. Freeze-drying, or lyophilization, is a process in which water is used to create porous hydrogels (105). The process involves freezing a solution at a temperature between -70°C and -80°C , followed by application of a partial vacuum to lower the pressure so that ice can be removed from the material through sublimation. Unfrozen water is then removed by desorption (118). This method is advantageous due to its use of water rather than organic solvents during the fabrication process (118). The procedure can also be modified to control the pore size and scaffold morphology (105). Decreasing the freezing rate has been associated with increasing the resulting pore sizes in the fabrication of plant-derived collagen sponges (119). In the lyophilization of gelatin, increasing the concentration of gelatin can decrease the pore size, while increasing the freezing temperature creates

larger mean pore sizes. Pore arrangement in parallel sheets can also be achieved by conducting freezing at -196°C in liquid nitrogen (105). Although a simple technique, freeze-drying is expensive and typically requires longer processing times than other fabrication methods. Scaffold porosity is also often irregular and the surface is typically dense, hindering cell migration into the inner areas of the scaffold (120, 121). Surface skin, which is the collapsing of the material's internal pores due to lack of structural integrity, can also occur during the freeze-drying process if the freezing temperature is too high (105).

Gas foaming is a technique in which a foaming agent such as sodium bicarbonate is added to a hydrogel to create an inert gas, typically N_2 or CO_2 . The pores are generated from subsequent removal of the gas phase from the polymer and surfactants are typically added to stabilize the foam that is created during the separation process (122). Using this technique, the pore size and morphology of the scaffold can be modified by adjusting the temperature and pressure during the procedure (105). Several other advantages include the ability of this method to achieve high scaffold porosities and that the technique can be conducted without the use of an organic solvent, enabling the incorporation of bioactive molecules without their degradation (105, 121). However, the use of surfactant in this method has the potential to negatively impact scaffold biocompatibility (122).

Solvent casting/ particle leaching is another scaffold fabrication method in which a porogen, commonly sodium chloride, is added to a polymer solution that is placed into a mould. The porogen is subsequently leached or removed through application of the appropriate solvent (105). The pore sizes can be easily controlled by modifying the particle size of the porogen (105). The mechanical strength of the scaffolds, rate of biodegradation and porosity of the scaffolds can also be easily modified by adjusting the concentration of the porogen (120). One drawback of this process is that longer processing times are required due to the leaching step (121). The width of the scaffold is also limited as it is difficult to remove the salt particles from the center of the material. Thus, as the thickness increases, residual salt particles may remain within the material (105). Another limitation of the salt/leaching method is that the leaching process often requires the use of organic solvents which could negatively impact cell viability (105).

While the aforementioned methods have their merits, electrospinning was the method of choice due to the numerous advantages discussed below. In the electrospinning method, a polymer solution is passed through a needle using an applied force from a syringe pump. An electric potential is applied to the needle through which the polymer solution passes such that as each droplet accumulates at the tip of the needle, it experiences electrostatic repulsion between the surface charges of the droplet and Coulombic force exerted by the applied electric field (100). As charge accumulates on the surface of the droplet, a Taylor cone is formed (100). Once the electrostatic charge exceeds the surface tension of the polymer solution, a polymer jet is expelled and travels towards a grounded mandrel (108). During this process, the solvent becomes evaporated, leaving dried fibers deposited on the mandrel (105).

The use of electrospinning as a technique for creating scaffolds with nanotopographies offers several advantages. Firstly, the electrospinning apparatus requires a minimal amount of specialized equipment and is inexpensive relative to other technologies to set up and operate (107, 108). The simplicity of the technique also makes it ideal for scale-up and large-scale production (108). The technique is versatile, enabling it to be used for many types of polymer and solvent systems. In fact, over 100 types of natural and synthetic polymers have been electrospun with success (123). The properties of the resulting fiber mats can also be tuned for the desired application. For example, the size and shape of the scaffold can be varied through changing the collector substrate, and the thickness of the scaffolds can be adjusted by changing the volume of the polymer solution that is electrospun (100, 108). Parameters can also be modified to produce mats with fibers that are randomly dispersed or aligned in uniaxial arrays (100, 123). Furthermore, the resulting matrices are highly porous, having large surface area to volume ratios, making them ideal for cell attachment and the exchange of nutrients and waste (107, 123). Finally, the fibers can also be used for the encapsulation of ECM proteins, enzymes, and growth factors (123).

1.4.5 The Addition of Bioactive Compounds to Electrospun Scaffolds

A simple approach for loading bioactive molecules into electrospun scaffolds is to use the blend electrospinning method. In this method, the bioactive molecules are simply mixed in the polymer solution prior to electrospinning. The resulting fibers have the bioactive molecules dispersed within them enabling a more controlled release relative to the physical adsorption of the molecules onto the scaffold surface. Using this method, there is typically an initial burst release *in vivo* followed by a sustained release caused by diffusion of the bioactive molecule and degradation of the polymer (95).

Several groups have used blend electrospinning with success, creating scaffolds for the release of ECM proteins, peptides and growth factors while retaining bioactivity. Several growth factors important to the wound healing process, including VEGF, PDGF, FGF have been incorporated into scaffolds and have demonstrated support of the growth and proliferation of cell types including keratinocytes, fibroblasts and endothelial cells (124, 125). Bertonecelj et al. demonstrated that platelet rich plasma, which is known to be abundant in different growth factor types, can be delivered using chitosan/polyethylene oxide scaffolds, stimulating proliferation of keratinocytes and fibroblasts *in vitro* (126). Polyvinyl alcohol scaffolds have also been developed for the delivery of antifungal peptide Cm-p1 (127). Our group has previously shown that type I collagen scaffolds loaded with the matricellular protein periostin are able to recover alpha-smooth muscle actin expression in wounds of periostin knockout mice (128). Another group developed silk fibroin/gelatin scaffolds loaded with astragaloside IV, a natural herb. When tested *in vivo*, the scaffolds were able to accelerate healing and prevented scar formation by stimulating wound closure in partial thickness burn wounds in rats (129). Neurotensin-loaded collagen scaffolds have also been shown to reduce inflammation and improve wound closure in streptozotocin-induced diabetic mice (93). More complex blends of bioactive compounds have also been incorporated into scaffolds. Peh et al. incorporated vitamin C, fat soluble vitamin D3, hydrocortisone, insulin, triiodothyronine, and EGF into poly (lactic-co-glycolic acid)/collagen scaffolds without loss of bioactivity. The

resulting scaffolds were able to induce proliferation of keratinocytes and fibroblasts *in vitro* (130).

1.5 Hypothesis and Objectives

1.5.1 Rationale

The electrospinning method can generate both collagen and gelatin fibers ranging from 50-500 nm, providing a biocompatible matrix of fibers within range of the native tissue collagen fibrils (116, 131-134). The use of gelatin in electrospinning is preferable, as it is similar in structure to collagen, which accounts for 70-80% of the skin's dry weight, while being considerably less expensive (135). Electrospun scaffolds have been successful in supporting cell behaviour such as adhesion, proliferation and scaffold infiltration as well as demonstrating enhanced wound closure kinetics in mouse excisional wound healing models (96-99). In addition to acting as a matrix for cell infiltration, scaffolds can also be used as delivery vehicles for growth factors and ECM proteins in order to stimulate certain cellular behaviours and responses (128, 130, 136, 137). In this work, a nanofibrous gelatin scaffold will be fabricated for the purpose of delivering exogenous galectin-3.

The addition of exogenous galectin-3 in a model of impaired wound healing has not yet been investigated in skin. Previous studies have shown that galectin-3 knock-out mice do not exhibit altered wound closure kinetics (87), although models of both corneal and skin wound healing reveal that galectin-3 deficient mice exhibit delayed re-epithelialization (75, 87, 89). Despite unaltered wound closure kinetics in galectin-3 knockout mice, studies in mouse and monkey corneas reveal that the addition of exogenous galectin-3 enhances wound re-epithelialization in WT mice (89, 91). Whether galectin-3 has a similar effect in WT mice in skin is unknown. Moreover, whether it could represent a therapeutic for reversing impaired wound healing has not yet been tested.

Macrophages play a critical role in regulating the inflammatory phase of wound healing. Classically activated macrophages, defined by their secretion of nitric oxide and pro-inflammatory cytokines, such as TNF- α , IL-6 and IL-12, exhibit pro-inflammatory properties, while alternatively activated macrophages, defined by stimulation by IL-4 and

IL-13 have the ability to control inflammation (8). Galectin-3 has previously been shown to regulate alternative macrophage activation *in vitro*, with galectin-3 deficient cells showing reduced levels of arginase I (63), therefore it will be interesting to determine how delivery of exogenous galectin-3 via a gelatin scaffold will influence macrophage polarization relative to a gelatin scaffold.

1.5.2 Hypothesis

We hypothesize that local delivery of galectin-3 either topically or using a gelatin scaffold will accelerate skin wound closure in WT and db/db mice relative to empty wounds. We secondarily hypothesize that the delivery of galectin-3 either topically or using a gelatin scaffold will increase re-epithelialization and modulate inflammation by stimulating M2 macrophage polarization.

1.5.3 Objectives

The objectives for this thesis were the following:

1. To develop a scaffold for the delivery of exogenous galectin-3
2. To evaluate the biocompatibility of the gelatin/galectin-3 scaffolds *in vitro* using human dermal fibroblasts
3. To evaluate the effect of the gelatin/galectin-3 scaffold on wound healing in murine models
 - a. Assess the influence of the scaffold on wound closure kinetics
 - b. Compare and contrast the efficacy of local delivery of topical galectin-3 versus gelatin/galectin-3 electrospun scaffolds on re-epithelialization and macrophage polarization during skin healing.

1.6 References

1. Kolarsick PAJ, Kolarsick MA, Goodwin C. Anatomy and Physiology of the Skin. *Journal of the Dermatology Nurses' Association*. 2011;3(4):203-13.
2. Madison KC. Barrier Function of the Skin: “La Raison d’Être” of the Epidermis. *Journal of Investigative Dermatology*. 2003;121(2):231-41.
3. Wickett RR, Visscher MO. Structure and function of the epidermal barrier. *American Journal of Infection Control*. 2006;34(10):S98-S110.
4. Montagna W. *The structure and function of skin*: Elsevier; 2012.
5. Haake A, Scott GA, Holbrook KA. Structure and function of the skin: overview of the epidermis and dermis. *The biology of the skin*. 2001;2001:19-45.
6. Gurtner GC, Werner S, Barrandon Y, Longaker MT. Wound repair and regeneration. *Nature*. 2008;453(7193):314-21.
7. Singer AJ, Clark RA. Cutaneous wound healing. *The New England journal of medicine*. 1999;341(10):738-46.
8. Rodero MP, Khosrotehrani K. Skin wound healing modulation by macrophages. *International journal of clinical and experimental pathology*. 2010;3(7):643-53.
9. Barrientos S, Stojadinovic O, Golinko MS, Brem H, Tomic-Canic M. Growth factors and cytokines in wound healing. *Wound repair and regeneration : official publication of the Wound Healing Society [and] the European Tissue Repair Society*. 2008;16(5):585-601.
10. Baltzis D, Eleftheriadou I, Veves A. Pathogenesis and treatment of impaired wound healing in diabetes mellitus: new insights. *Advances in therapy*. 2014;31(8):817-36.
11. Morton LM, Phillips TJ. Wound healing and treating wounds: Differential diagnosis and evaluation of chronic wounds. *Journal of the American Academy of Dermatology*. 2016;74(4):589-605; quiz -6.
12. Zhao R, Liang H, Clarke E, Jackson C, Xue M. Inflammation in Chronic Wounds. *International journal of molecular sciences*. 2016;17(12).
13. Canadian Association of Wound Care. Statistics 2017 [Available from: <http://cawc.net/index.php/public/facts-stats-and-tools/statistics/>].
14. Fonder MA, Lazarus GS, Cowan DA, Aronson-Cook B, Kohli AR, Mamelak AJ. Treating the chronic wound: A practical approach to the care of nonhealing wounds and wound care dressings. *Journal of the American Academy of Dermatology*. 2008;58(2):185-206.

15. Hopman WM, Buchanan M, VanDenKerkhof EG, Harrison MB. Pain and health-related quality of life in people with chronic leg ulcers. *Chronic Dis Inj Can.* 2013;33(3):167-74.
16. Lal BK. Venous ulcers of the lower extremity: Definition, epidemiology, and economic and social burdens. *Semin Vasc Surg.* 2015;28(1):3-5.
17. Raffetto JD. Pathophysiology of wound healing and alterations in venous leg ulcers-review. *Phlebology.* 2016;31(1 Suppl):56-62.
18. Young JR. Differential diagnosis of leg ulcers. *Cardiovasc Clin.* 1983;13(2):171-93.
19. Kirsner RS, Vivas AC. Lower-extremity ulcers: diagnosis and management. *Br J Dermatol.* 2015;173(2):379-90.
20. Woodbury MG, Houghton PE. Prevalence of pressure ulcers in Canadian healthcare settings. *Ostomy Wound Manage.* 2004;50(10):22-4, 6, 8, 30, 2, 4, 6-8.
21. Canadian Diabetes Association. Diabetes in Canada 2016 [Available from: <https://www.diabetes.ca/getmedia/513a0f6c-b1c9-4e56-a77c-6a492bf7350f/diabetes-charter-backgrounder-national-english.pdf.aspx>].
22. Singh N, Armstrong DG, Lipsky BA. Preventing foot ulcers in patients with diabetes. *JAMA.* 2005;293(2):217-28.
23. Alavi A, Sibbald RG, Mayer D, Goodman L, Botros M, Armstrong DG, et al. Diabetic foot ulcers: Part I. Pathophysiology and prevention. *Journal of the American Academy of Dermatology.* 2014;70(1):1 e-18; quiz 9-20.
24. Fortington LV, Geertzen JH, van Netten JJ, Postema K, Rommers GM, Dijkstra PU. Short and long term mortality rates after a lower limb amputation. *European journal of vascular and endovascular surgery : the official journal of the European Society for Vascular Surgery.* 2013;46(1):124-31.
25. Schultz GS, Sibbald RG, Falanga V, Ayello EA, Dowsett C, Harding K, et al. Wound bed preparation: a systematic approach to wound management. *Wound repair and regeneration : official publication of the Wound Healing Society [and] the European Tissue Repair Society.* 2003;11 Suppl 1:S1-28.
26. Skorkowska-Telichowska K, Czemplik M, Kulma A, Szopa J. The local treatment and available dressings designed for chronic wounds. *Journal of the American Academy of Dermatology.* 2013;68(4):e117-26.
27. Powers JG, Higham C, Broussard K, Phillips TJ. Wound healing and treating wounds: Chronic wound care and management. *Journal of the American Academy of Dermatology.* 2016;74(4):607-25; quiz 25-6.

28. Rodgers K, Verco S, Bolton L, Dizerega G. Accelerated healing of diabetic wounds by NorLeu(3)-angiotensin (1-7). *Expert Opin Investig Drugs*. 2011;20(11):1575-81.
29. Wollina U, Schmidt WD, Kronert C, Nelskamp C, Scheibe A, Fassler D. Some effects of a topical collagen-based matrix on the microcirculation and wound healing in patients with chronic venous leg ulcers: preliminary observations. *Int J Low Extrem Wounds*. 2005;4(4):214-24.
30. Veves A. A Randomized, Controlled Trial of Promogran (a Collagen/Oxidized Regenerated Cellulose Dressing) vs Standard Treatment in the Management of Diabetic Foot Ulcers. *Archives of Surgery*. 2002;137(7):822.
31. Greaves NS, Iqbal SA, Baguneid M, Bayat A. The role of skin substitutes in the management of chronic cutaneous wounds. *Wound repair and regeneration : official publication of the Wound Healing Society [and] the European Tissue Repair Society*. 2013;21(2):194-210.
32. Snyder DL, Sullivan N, Schoelles KM. *AHRQ Technology Assessments. Skin Substitutes for Treating Chronic Wounds*. Rockville (MD): Agency for Healthcare Research and Quality (US); 2012.
33. Ramanujam CL, Capobianco CM, Zgonis T. Using a bilayer matrix wound dressing for closure of complicated diabetic foot wounds. *J Wound Care*. 2010;19(2):56-60.
34. Prystowsky JH, Nowygrod R, Marboe CC, Benvenisty AI, Ascherman JA, Todd GJ. Artificial Skin (Integra" Dermal Regeneration Template) for Closure of Lower Extremity Wounds. *Vascular and Endovascular Surgery*. 2000;34(6):557-67.
35. Jeffcoate WJ, Price P, Harding KG, International Working Group on Wound H, Treatments for People with Diabetic Foot U. Wound healing and treatments for people with diabetic foot ulcers. *Diabetes/metabolism research and reviews*. 2004;20 Suppl 1:S78-89.
36. Stoekenbroek RM, Santema TB, Legemate DA, Ubbink DT, van den Brink A, Koelemay MJ. Hyperbaric oxygen for the treatment of diabetic foot ulcers: a systematic review. *European journal of vascular and endovascular surgery : the official journal of the European Society for Vascular Surgery*. 2014;47(6):647-55.
37. Health Quality O. Hyperbaric oxygen therapy for non-healing ulcers in diabetes mellitus: an evidence-based analysis. *Ontario health technology assessment series*. 2005;5(11):1-28.
38. Alavi A, Sibbald RG, Mayer D, Goodman L, Botros M, Armstrong DG, et al. Diabetic foot ulcers: Part II. Management. *Journal of the American Academy of Dermatology*. 2014;70(1):21.e1-.e4.

39. Marston W, Tang J, Kirsner RS, Ennis W. Wound Healing Society 2015 update on guidelines for venous ulcers. *Wound repair and regeneration : official publication of the Wound Healing Society [and] the European Tissue Repair Society*. 2016;24(1):136-44.
40. Velnar T, Bailey T, Smrkolj V. The wound healing process: an overview of the cellular and molecular mechanisms. *The Journal of international medical research*. 2009;37(5):1528-42.
41. Brem H, Tomic-Canic M. Cellular and molecular basis of wound healing in diabetes. *The Journal of clinical investigation*. 2007;117(5):1219-22.
42. Blakytyn R, Jude E. The molecular biology of chronic wounds and delayed healing in diabetes. *Diabetic medicine : a journal of the British Diabetic Association*. 2006;23(6):594-608.
43. Stojadinovic O, Brem H, Vouthounis C, Lee B, Fallon J, Stallcup M, et al. Molecular pathogenesis of chronic wounds: the role of beta-catenin and c-myc in the inhibition of epithelialization and wound healing. *The American journal of pathology*. 2005;167(1):59-69.
44. Gary Sibbald R, Woo KY. The biology of chronic foot ulcers in persons with diabetes. *Diabetes/metabolism research and reviews*. 2008;24 Suppl 1:S25-30.
45. Bodnar RJ. Chemokine Regulation of Angiogenesis During Wound Healing. *Advances in wound care*. 2015;4(11):641-50.
46. Lobmann R, Schultz G, Lehnert H. Proteases and the diabetic foot syndrome: mechanisms and therapeutic implications. *Diabetes care*. 2005;28(2):461-71.
47. Wlaschek M, Scharffetter-Kochanek K. Oxidative stress in chronic venous leg ulcers. *Wound repair and regeneration : official publication of the Wound Healing Society [and] the European Tissue Repair Society*. 2005;13(5):452-61.
48. Schultz GS, Davidson JM, Kirsner RS, Bornstein P, Herman IM. Dynamic reciprocity in the wound microenvironment. *Wound repair and regeneration : official publication of the Wound Healing Society [and] the European Tissue Repair Society*. 2011;19(2):134-48.
49. Demidova-Rice TN, Hamblin MR, Herman IM. Acute and impaired wound healing: pathophysiology and current methods for drug delivery, part 1: normal and chronic wounds: biology, causes, and approaches to care. *Advances in skin & wound care*. 2012;25(7):304-14.
50. Schierle CF, De la Garza M, Mustoe TA, Galiano RD. Staphylococcal biofilms impair wound healing by delaying reepithelialization in a murine cutaneous wound model. *Wound repair and regeneration : official publication of the Wound Healing Society [and] the European Tissue Repair Society*. 2009;17(3):354-9.

51. Singh VP, Bali A, Singh N, Jaggi AS. Advanced glycation end products and diabetic complications. *Korean J Physiol Pharmacol.* 2014;18(1):1-14.
52. Peppas M, Stavroulakis P, Raptis SA. Advanced glycoxidation products and impaired diabetic wound healing. *Wound repair and regeneration : official publication of the Wound Healing Society [and] the European Tissue Repair Society.* 2009;17(4):461-72.
53. Hu H, Han CM, Hu XL, Ye WL, Huang WJ, Smit AJ. Elevated skin autofluorescence is strongly associated with foot ulcers in patients with diabetes: a cross-sectional, observational study of Chinese subjects. *J Zhejiang Univ Sci B.* 2012;13(5):372-7.
54. Brownlee M. Advanced protein glycosylation in diabetes and aging. *Annu Rev Med.* 1995;46:223-34.
55. Zhu P, Yang C, Chen LH, Ren M, Lao GJ, Yan L. Impairment of human keratinocyte mobility and proliferation by advanced glycation end products-modified BSA. *Arch Dermatol Res.* 2011;303(5):339-50.
56. Rolo AP, Palmeira CM. Diabetes and mitochondrial function: role of hyperglycemia and oxidative stress. *Toxicol Appl Pharmacol.* 2006;212(2):167-78.
57. Figueroa-Romero C, Sadidi M, Feldman EL. Mechanisms of disease: the oxidative stress theory of diabetic neuropathy. *Rev Endocr Metab Disord.* 2008;9(4):301-14.
58. Coughlan MT, Thorburn DR, Penfold SA, Laskowski A, Harcourt BE, Sourris KC, et al. RAGE-induced cytosolic ROS promote mitochondrial superoxide generation in diabetes. *Journal of the American Society of Nephrology : JASN.* 2009;20(4):742-52.
59. Midwood KS, Williams LV, Schwarzbauer JE. Tissue repair and the dynamics of the extracellular matrix. *Int J Biochem Cell Biol.* 2004;36(6):1031-7.
60. Rabinovich GA, Rubinstein N, Toscano MA. Role of galectins in inflammatory and immunomodulatory processes. *Biochimica et biophysica acta.* 2002;1572(2-3):274-84.
61. Sano H, Hsu DK, Yu L, Apgar JR, Kuwabara I, Yamanaka T, et al. Human galectin-3 is a novel chemoattractant for monocytes and macrophages. *Journal of immunology.* 2000;165(4):2156-64.
62. Karlsson A, Christenson K, Matlak M, Bjorstad A, Brown KL, Telemo E, et al. Galectin-3 functions as an opsonin and enhances the macrophage clearance of apoptotic neutrophils. *Glycobiology.* 2009;19(1):16-20.

63. MacKinnon AC, Farnworth SL, Hodgkinson PS, Henderson NC, Atkinson KM, Leffler H, et al. Regulation of alternative macrophage activation by galectin-3. *Journal of immunology*. 2008;180(4):2650-8.
64. Hamilton D, Walker J, Kim S, Michelsons S, Creber K, Elliott C, et al. Cell-matrix interactions governing skin repair: matricellular proteins as diverse modulators of cell function. *Research and Reports in Biochemistry*. 2015:73.
65. Robertson MW, Albrandt K, Keller D, Liu FT. Human Ige-Binding Protein - a Soluble Lectin Exhibiting a Highly Conserved Interspecies Sequence and Differential Recognition of Ige Glycoforms. *Biochemistry*. 1990;29(35):8093-100.
66. Domic J, Dabelic S, Flogel M. Galectin-3: an open-ended story. *Biochimica et biophysica acta*. 2006;1760(4):616-35.
67. Barondes SH. Galectins: A family of b-Galactoside-Binding Lectins. *Cell*. 1994;76:597-8.
68. Cherayil BJ, Chaitovitz S, Wong C, Pillai S. Molecular cloning of a human macrophage lectin specific for galactose. *Proceedings of the National Academy of Sciences of the United States of America*. 1990;87(18):7324-8.
69. Nakahara S, Oka N, Wang Y, Hogan V, Inohara H, Raz A. Characterization of the nuclear import pathways of galectin-3. *Cancer research*. 2006;66(20):9995-10006.
70. Seetharaman J, Kanigsberg A, Slaaby R, Leffler H, Barondes SH, Rini JM. X-ray crystal structure of the human galectin-3 carbohydrate recognition domain at 2.1-Å resolution. *The Journal of biological chemistry*. 1998;273(21):13047-52.
71. Mazurek N, Conklin J, Byrd JC, Raz A, Bresalier RS. Phosphorylation of the beta-galactoside-binding protein galectin-3 modulates binding to its ligands. *The Journal of biological chemistry*. 2000;275(46):36311-5.
72. Ahmad N, Gabius HJ, Andre S, Kaltner H, Sabesan S, Roy R, et al. Galectin-3 precipitates as a pentamer with synthetic multivalent carbohydrates and forms heterogeneous cross-linked complexes. *The Journal of biological chemistry*. 2004;279(12):10841-7.
73. Frigeri LG, Liu FT. Surface expression of functional IgE binding protein, an endogenous lectin, on mast cells and macrophages. *Journal of immunology*. 1992;148(3):861-7.
74. Dvorankova B, Szabo P, Lacina L, Gal P, Uhrova J, Zima T, et al. Human galectins induce conversion of dermal fibroblasts into myofibroblasts and production of extracellular matrix: potential application in tissue engineering and wound repair. *Cells, tissues, organs*. 2011;194(6):469-80.

75. Liu W, Hsu DK, Chen HY, Yang RY, Carraway KL, 3rd, Isseroff RR, et al. Galectin-3 regulates intracellular trafficking of EGFR through Alix and promotes keratinocyte migration. *J Invest Dermatol*. 2012;132(12):2828-37.
76. Yamaoka A, Kuwabara I, Frigeri LG, Liu FT. A human lectin, galectin-3 (epsilon bp/Mac-2), stimulates superoxide production by neutrophils. *Journal of immunology*. 1995;154(7):3479-87.
77. Karlsson A, Follin P, Leffler H, Dahlgren C. Galectin-3 activates the NADPH-oxidase in exudated but not peripheral blood neutrophils. *Blood*. 1998;91(9):3430-8.
78. Kuwabara I, Liu FT. Galectin-3 promotes adhesion of human neutrophils to laminin. *Journal of immunology*. 1996;156(10):3939-44.
79. Bhaumik P, St-Pierre G, Milot V, St-Pierre C, Sato S. Galectin-3 facilitates neutrophil recruitment as an innate immune response to a parasitic protozoa cutaneous infection. *Journal of immunology*. 2013;190(2):630-40.
80. Brancato SK, Albina JE. Wound macrophages as key regulators of repair: origin, phenotype, and function. *The American journal of pathology*. 2011;178(1):19-25.
81. Danella Polli C, Alves Toledo K, Franco LH, Sammartino Mariano V, de Oliveira LL, Soares Bernardes E, et al. Monocyte Migration Driven by Galectin-3 Occurs through Distinct Mechanisms Involving Selective Interactions with the Extracellular Matrix. *ISRN Inflamm*. 2013;2013:259256.
82. Martinez FO, Gordon S. The M1 and M2 paradigm of macrophage activation: time for reassessment. *F1000Prime Rep*. 2014;6:13.
83. Nangia-Makker P, Honjo Y, Sarvis R, Akahani S, Hogan V, Pienta KJ, et al. Galectin-3 induces endothelial cell morphogenesis and angiogenesis. *The American journal of pathology*. 2000;156(3):899-909.
84. Markowska AI, Liu FT, Panjwani N. Galectin-3 is an important mediator of VEGF- and bFGF-mediated angiogenic response. *The Journal of experimental medicine*. 2010;207(9):1981-93.
85. Wesley UV, Vemuganti R, Ayvaci ER, Dempsey RJ. Galectin-3 enhances angiogenic and migratory potential of microglial cells via modulation of integrin linked kinase signaling. *Brain research*. 2013;1496:1-9.
86. Markowska AI, Jefferies KC, Panjwani N. Galectin-3 protein modulates cell surface expression and activation of vascular endothelial growth factor receptor 2 in human endothelial cells. *The Journal of biological chemistry*. 2011;286(34):29913-21.
87. Walker JT, Elliott CG, Forbes TL, Hamilton DW. Genetic Deletion of Galectin-3 Does Not Impair Full-Thickness Excisional Skin Healing. *J Invest Dermatol*. 2016.

88. Kasper M, Hughes RC. Immunocytochemical evidence for a modulation of galectin 3 (Mac-2), a carbohydrate binding protein, in pulmonary fibrosis. *The Journal of pathology*. 1996;179(3):309-16.
89. Cao Z, Said N, Amin S, Wu HK, Bruce A, Garate M, et al. Galectins-3 and -7, but not galectin-1, play a role in re-epithelialization of wounds. *The Journal of biological chemistry*. 2002;277(44):42299-305.
90. Saravanan C, Liu FT, Gipson IK, Panjwani N. Galectin-3 promotes lamellipodia formation in epithelial cells by interacting with complex N-glycans on alpha3beta1 integrin. *Journal of cell science*. 2009;122(Pt 20):3684-93.
91. Fujii A, Shearer TR, Azuma M. Galectin-3 enhances extracellular matrix associations and wound healing in monkey corneal epithelium. *Exp Eye Res*. 2015;137:71-8.
92. Choi SM, Ryu HA, Lee KM, Kim HJ, Park IK, Cho WJ, et al. Development of Stabilized Growth Factor-Loaded Hyaluronate- Collagen Dressing (HCD) matrix for impaired wound healing. *Biomater Res*. 2016;20:9.
93. Moura LI, Dias AM, Suesca E, Casadiegos S, Leal EC, Fontanilla MR, et al. Neurotensin-loaded collagen dressings reduce inflammation and improve wound healing in diabetic mice. *Biochimica et biophysica acta*. 2014;1842(1):32-43.
94. Smith LA, Ma PX. Nano-fibrous scaffolds for tissue engineering. *Colloids and surfaces B, Biointerfaces*. 2004;39(3):125-31.
95. Ji W, Sun Y, Yang F, van den Beucken JJ, Fan M, Chen Z, et al. Bioactive electrospun scaffolds delivering growth factors and genes for tissue engineering applications. *Pharmaceutical research*. 2011;28(6):1259-72.
96. Dubsky M, Kubinova S, Sirc J, Voska L, Zajicek R, Zajicova A, et al. Nanofibers prepared by needleless electrospinning technology as scaffolds for wound healing. *Journal of materials science Materials in medicine*. 2012;23(4):931-41.
97. Gomes SR, Rodrigues G, Martins GG, Roberto MA, Mafra M, Henriques CM, et al. In vitro and in vivo evaluation of electrospun nanofibers of PCL, chitosan and gelatin: a comparative study. *Materials science & engineering C, Materials for biological applications*. 2015;46:348-58.
98. Powell HM, Boyce ST. Fiber density of electrospun gelatin scaffolds regulates morphogenesis of dermal-epidermal skin substitutes. *Journal of biomedical materials research Part A*. 2008;84(4):1078-86.
99. Zha Z, Teng W, Markle V, Dai Z, Wu X. Fabrication of gelatin nanofibrous scaffolds using ethanol/phosphate buffer saline as a benign solvent. *Biopolymers*. 2012;97(12):1026-36.

100. Murugan R, Ramakrishna S. Design strategies of tissue engineering scaffolds with controlled fiber orientation. *Tissue engineering*. 2007;13(8):1845-66.
101. Karande TS, Ong JL, Agrawal CM. Diffusion in musculoskeletal tissue engineering scaffolds: design issues related to porosity, permeability, architecture, and nutrient mixing. *Ann Biomed Eng*. 2004;32(12):1728-43.
102. Rho KS, Jeong L, Lee G, Seo BM, Park YJ, Hong SD, et al. Electrospinning of collagen nanofibers: effects on the behavior of normal human keratinocytes and early-stage wound healing. *Biomaterials*. 2006;27(8):1452-61.
103. Li WJ, Laurencin CT, Cateson EJ, Tuan RS, Ko FK. Electrospun nanofibrous structure: a novel scaffold for tissue engineering. *J Biomed Mater Res*. 2002;60(4):613-21.
104. Zhu XL, Cui WG, Li XH, Jin Y. Electrospun fibrous mats with high porosity as potential scaffolds for skin tissue engineering. *Biomacromolecules*. 2008;9(7):1795-801.
105. Nicholas MN, Jeschke MG, Amini-Nik S. Methodologies in creating skin substitutes. *Cell Mol Life Sci*. 2016;73(18):3453-72.
106. Malafaya PB, Silva GA, Reis RL. Natural-origin polymers as carriers and scaffolds for biomolecules and cell delivery in tissue engineering applications. *Adv Drug Deliv Rev*. 2007;59(4-5):207-33.
107. Zhong SP, Zhang YZ, Lim CT. Tissue scaffolds for skin wound healing and dermal reconstruction. *Wiley Interdiscip Rev Nanomed Nanobiotechnol*. 2010;2(5):510-25.
108. Barnes CP, Sell SA, Boland ED, Simpson DG, Bowlin GL. Nanofiber technology: designing the next generation of tissue engineering scaffolds. *Adv Drug Deliv Rev*. 2007;59(14):1413-33.
109. Zeugolis DI, Khew ST, Yew ES, Ekaputra AK, Tong YW, Yung LY, et al. Electro-spinning of pure collagen nano-fibres - just an expensive way to make gelatin? *Biomaterials*. 2008;29(15):2293-305.
110. Hassiba AJ, El Zowalaty ME, Nasrallah GK, Webster TJ, Luyt AS, Abdullah AM, et al. Review of recent research on biomedical applications of electrospun polymer nanofibers for improved wound healing. *Nanomedicine (Lond)*. 2016;11(6):715-37.
111. Brett D. A Review of Collagen and Collagen-based Wound Dressings. *Wounds*. 2008;20(12):347-56.
112. Garg T, Rath G, Goyal AK. Biomaterials-based nanofiber scaffold: targeted and controlled carrier for cell and drug delivery. *Journal of drug targeting*. 2015;23(3):202-21.

113. Asti A, Gioglio L. Natural and synthetic biodegradable polymers: different scaffolds for cell expansion and tissue formation. *Int J Artif Organs*. 2014;37(3):187-205.
114. Rossi F, van Griensven M. Polymer functionalization as a powerful tool to improve scaffold performances. *Tissue engineering Part A*. 2014;20(15-16):2043-51.
115. Chandrasekaran AR, Venugopal J, Sundarajan S, Ramakrishna S. Fabrication of a nanofibrous scaffold with improved bioactivity for culture of human dermal fibroblasts for skin regeneration. *Biomed Mater*. 2011;6(1):015001.
116. Kim HN, Jiao A, Hwang NS, Kim MS, Kang do H, Kim DH, et al. Nanotopography-guided tissue engineering and regenerative medicine. *Adv Drug Deliv Rev*. 2013;65(4):536-58.
117. Gautam S, Dinda AK, Mishra NC. Fabrication and characterization of PCL/gelatin composite nanofibrous scaffold for tissue engineering applications by electrospinning method. *Materials science & engineering C, Materials for biological applications*. 2013;33(3):1228-35.
118. Lu T, Li Y, Chen T. Techniques for fabrication and construction of three-dimensional scaffolds for tissue engineering. *Int J Nanomedicine*. 2013;8:337-50.
119. Willard JJ, Drexler JW, Das A, Roy S, Shilo S, Shoseyov O, et al. Plant-derived human collagen scaffolds for skin tissue engineering. *Tissue engineering Part A*. 2013;19(13-14):1507-18.
120. Lee SB, Kim YH, Chong MS, Hong SH, Lee YM. Study of gelatin-containing artificial skin V: fabrication of gelatin scaffolds using a salt-leaching method. *Biomaterials*. 2005;26(14):1961-8.
121. Garg T, Goyal AK. Biomaterial-based scaffolds--current status and future directions. *Expert Opin Drug Deliv*. 2014;11(5):767-89.
122. Dehghani F, Annabi N. Engineering porous scaffolds using gas-based techniques. *Curr Opin Biotechnol*. 2011;22(5):661-6.
123. Xie J, Li X, Xia Y. Putting Electrospun Nanofibers to Work for Biomedical Research. *Macromolecular rapid communications*. 2008;29(22):1775-92.
124. Said SS, Pickering JG, Mequanint K. Controlled delivery of fibroblast growth factor-9 from biodegradable poly(ester amide) fibers for building functional neovasculature. *Pharmaceutical research*. 2014;31(12):3335-47.
125. Han F, Jia X, Dai D, Yang X, Zhao J, Zhao Y, et al. Performance of a multilayered small-diameter vascular scaffold dual-loaded with VEGF and PDGF. *Biomaterials*. 2013;34(30):7302-13.

126. Bertonecelj V, Pelipenko J, Kristl J, Jeras M, Cukjati M, Kocbek P. Development and bioevaluation of nanofibers with blood-derived growth factors for dermal wound healing. *European journal of pharmaceutics and biopharmaceutics : official journal of Arbeitsgemeinschaft fur Pharmazeutische Verfahrenstechnik eV*. 2014;88(1):64-74.
127. Viana JF, Carrijo J, Freitas CG, Paul A, Alcaraz J, Lacorte CC, et al. Antifungal nanofibers made by controlled release of sea animal derived peptide. *Nanoscale*. 2015;7(14):6238-46.
128. Elliott CG, Wang J, Guo X, Xu SW, Eastwood M, Guan J, et al. Periostin modulates myofibroblast differentiation during full-thickness cutaneous wound repair. *Journal of cell science*. 2012;125(Pt 1):121-32.
129. Shan YH, Peng LH, Liu X, Chen X, Xiong J, Gao JQ. Silk fibroin/gelatin electrospun nanofibrous dressing functionalized with astragaloside IV induces healing and anti-scar effects on burn wound. *International journal of pharmaceutics*. 2015;479(2):291-301.
130. Peh P, Lim NS, Blocki A, Chee SM, Park HC, Liao S, et al. Simultaneous Delivery of Highly Diverse Bioactive Compounds from Blend Electrospun Fibers for Skin Wound Healing. *Bioconjugate chemistry*. 2015;26(7):1348-58.
131. Li M, Mondrinos MJ, Gandhi MR, Ko FK, Weiss AS, Lelkes PI. Electrospun protein fibers as matrices for tissue engineering. *Biomaterials*. 2005;26(30):5999-6008.
132. Yang L, Fitie CF, van der Werf KO, Bennink ML, Dijkstra PJ, Feijen J. Mechanical properties of single electrospun collagen type I fibers. *Biomaterials*. 2008;29(8):955-62.
133. Matthews JA, Wnek GE, Simpson DG, Bowlin GL. Electrospinning of Collagen Nanofibers. *Biomacromolecules*. 2002;3(2):232-8.
134. Song JH, Kim HE, Kim HW. Production of electrospun gelatin nanofiber by water-based co-solvent approach. *Journal of materials science Materials in medicine*. 2008;19(1):95-102.
135. Riekkki R, Parikka M, Jukkola A, Salo T, Risteli J, Oikarinen A. Increased expression of collagen types I and III in human skin as a consequence of radiotherapy. *Arch Dermatol Res*. 2002;294(4):178-84.
136. Guo X, Elliott CG, Li Z, Xu Y, Hamilton DW, Guan J. Creating 3D angiogenic growth factor gradients in fibrous constructs to guide fast angiogenesis. *Biomacromolecules*. 2012;13(10):3262-71.

137. Montero RB, Vazquez-Padron RI, Pham SM, D'Ippolito G, Andreopoulos FM. Electrospun Gelatin Constructs with Tunable Fiber Orientation Promote Directed Angiogenesis. Open Journal of Regenerative Medicine. 2014;03(01):1-12.

Chapter 2

2 The Influence of a Gelatin/Galectin-3 Scaffold on Normal and Impaired Models of Skin Healing

2.1 Introduction

Normal skin healing involves a series of four overlapping phases: hemostasis, inflammation, proliferation and remodeling (1). During healing, these processes occur in a spatiotemporal manner to remove bacteria and damaged cells, restore the epithelial barrier, as well as to synthesize and remodel the extracellular matrix at the site of injury, restoring tissue function (2). Chronic wounds result when wounds fail to complete this process and achieve healing, usually within twelve weeks of initial injury, resulting in impaired tissue function and anatomy (3). The most common types of chronic wounds are venous ulcers, arterial ulcers, pressure ulcers, and diabetic ulcers (3, 4). A variety of factors can lead to their development, including vascular insufficiency, diabetes, malnutrition, patient age, pressure, infection, and edema (5). These wounds become a significant burden to the patient, as they can be painful, impair limb function, and result in sepsis or the need for amputation (5). In addition, the burden to the Canadian healthcare system is large, with the average cost of chronic wound treatment being \$10,376 (6).

Conventional treatment strategies involve removal of necrotic tissue, cleaning of the wound, and use of antimicrobial agents to treat infection. Dressings can be applied to retain moisture and promote healing, although their efficacy depends on specific wound characteristics including the amount of exudate, depth and area of the wound, stage of healing, and skin type of the patient (7, 8). Many adjunctive therapies are also available for the treatment of chronic wounds including topical formulations, bioengineered skin substitutes, hyperbaric oxygen therapy, and negative pressure wound therapy (8-12). However, support for their use in this application is limited, as many treatments lack multi-center studies that apply to broader patient populations and to non-healing chronic wounds (11, 12). Therefore, new treatment strategies aimed at promoting healing in chronic wounds are needed.

When considering the development of new therapeutics for chronic skin wounds, it is extremely important to factor in the underlying pathophysiology. Chronic wounds are stalled in a deleterious pro-inflammatory state, with increased expression of inflammatory cytokines such as interleukin-1 (IL-1), IL-6, and tissue necrosis factor alpha (TNF- α), coupled with decreased levels of pro-regenerative cytokines including transforming growth factor beta (TGF- β) and vascular endothelial growth factor (VEGF) (13). Several molecular processes are known to exacerbate the inflammatory processes and prevent progression into the proliferative phase of healing. The decreased levels of growth factors, including keratinocyte growth factor, fibroblast growth factor 2 (FGF-2), and VEGF, impede keratinocyte migration and granulation tissue formation (14, 15). Additionally, there is an imbalance of proteolytic activity that leads to excessive degradation of the extracellular matrix, inhibiting cell migration and proliferation (5, 15, 16). In diabetic patients, advanced glycation end products (AGEs) also accumulate due to hyperglycemia (17) and can cause oxidative stress through interaction with AGE receptors on macrophages and endothelial cells, triggering the release of pro-inflammatory cytokines (18). Considering the pathophysiology of chronic wounds, therapeutic agents that can regulate inflammatory processes present an ideal treatment strategy.

Galectin-3 is a protein implicated in the regulation of several processes required in wound healing, particularly inflammation. Galectin-3 consists of a 120-amino acid N-terminal domain and a 130-amino acid carbohydrate recognition domain (CRD) providing the capability to bind β -galactosides (19-21). *In vitro*, it has been shown to increase migration of monocytes and macrophages (22). Additionally, galectin-3 has been shown to link phagocytic macrophages to neutrophils as well as increase their neutrophil uptake (23). This protein has also been associated with regulating alternative macrophage activation, a process important in resolving inflammation (24). Studies in galectin-3 knockout mice have shown that re-epithelialization is impaired in both the cornea and in skin, suggesting an important role for galectin-3 in re-epithelialization (25-27). In skin, impaired re-epithelialization is attributed to deficient epidermal growth factor receptor (EGFR) endocytosis and recycling, a process controlled by cytosolic galectin-3 binding to ALG-2 interacting protein X (ALIX) (27). In the cornea, the addition of exogenous

galectin-3 led to increased re-epithelialization, credited to its upregulation of galectin-7 which is decreased in mouse embryonic fibroblasts (25); however in skin, differences in expression of galectin-7 in wound tissue are not observed concomitantly with impaired re-epithelialization (26). The role of galectin-3 in promoting re-epithelialization and modulating inflammation suggest that delivery of this protein to chronic wounds would promote pro-regenerative processes. Therefore, investigation of this protein as a potential therapeutic agent is needed.

Several groups have previously shown that growth factors, bioactive peptides, matricellular proteins, and combinations thereof can be incorporated into scaffolds, while exhibiting biological activity either *in vitro* or *in vivo* (28-31). Electrospinning is a versatile technique for scaffold fabrication that can be fine-tuned to produce highly porous fiber mats with large surface area to volume ratios (32, 33). Delivery of human recombinant galectin-3 via an electrospun scaffold in wound healing is of interest, as the scaffold would provide a large surface area, enabling effective delivery and distribution of the protein in the wound bed to ensure that signals are provided continuously throughout healing (20). In addition, the scaffold would act as an artificial extracellular matrix, guiding regeneration by providing a site for cell adhesion and supporting the proliferation and migration of cells into the wound bed (34-37).

The aim of this study was to fabricate a gelatin scaffold for the delivery of recombinant human galectin-3 using the blend electrospinning method, to test its biocompatibility *in vitro* and to test its efficacy in dermal wound healing *in vivo*. The adhesion, proliferation and secretion of extracellular matrix proteins by human dermal fibroblasts on gelatin/galectin-3 scaffolds were assessed in comparison to gelatin scaffolds. The influence of the gelatin/galectin-3 scaffold in wound healing was then evaluated. Evaluation was based on its effect on wound closure kinetics, re-epithelialization and macrophage populations *in vivo* relative to treatment with topical galectin-3 and gelatin scaffolds.

2.2 Materials and Methods

2.2.1 Electrospinning

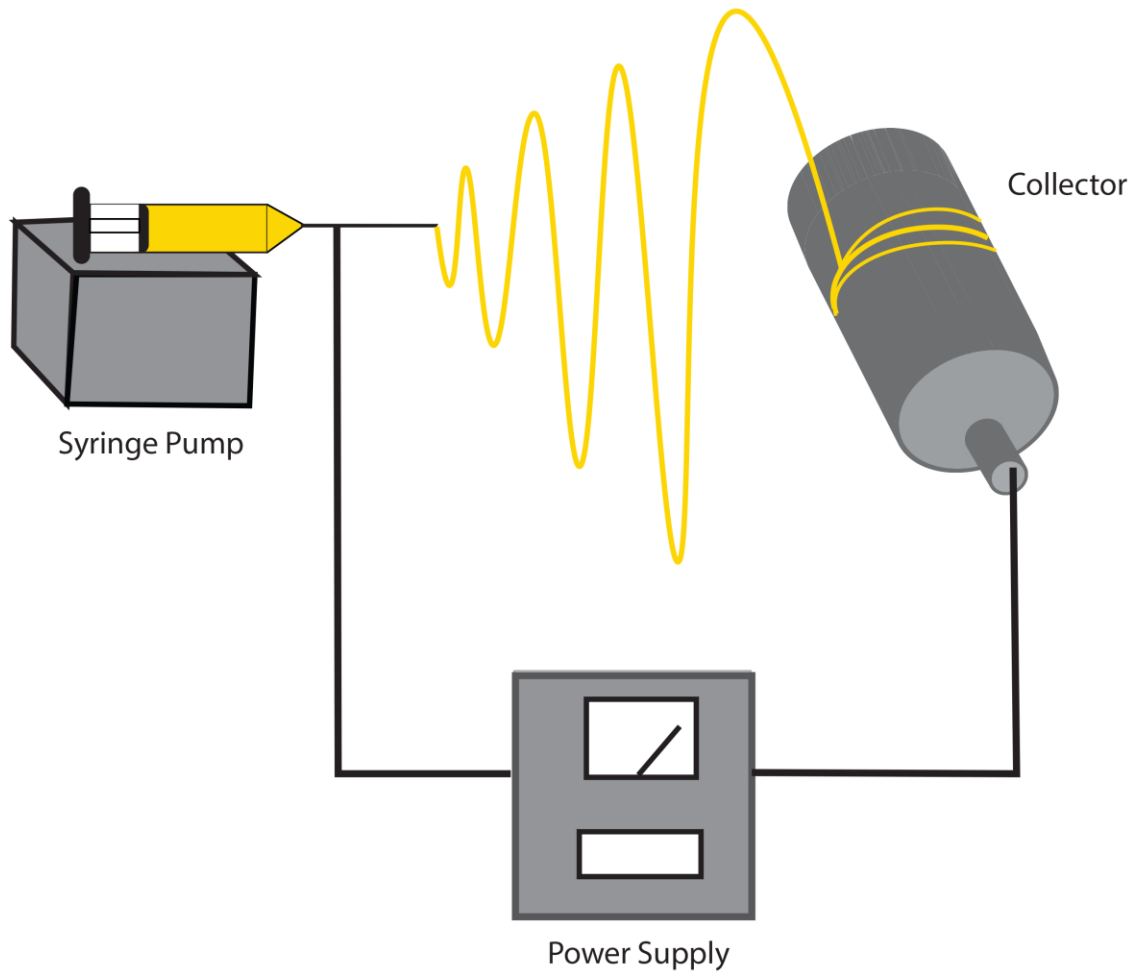
As shown in Figure 2.1, a polymer solution consisting of Type B Bovine gelatin (Sigma-Aldrich, St. Louis, MO, USA) dissolved in 40% v/v acetic acid (Thermo Fisher Scientific, Waltham, MA, USA) was passed through a plastic 1cc syringe (Terumo, Shibuya, Tokyo, Japan) and 20 gauge blunt-tip stainless steel needle using a syringe pump (VWR International, Radnor, PA, USA). The needle was connected to a high voltage DC power supply (Gamma High Voltage Research, Ormond Beach, FL, USA) and a grounded stainless steel rotating mandrel. The mandrel speed was held constant at 100 revolutions per minute (RPM). The gelatin concentration, flowrate and collector distance were varied as outlined in Table 1.

Table 1: A summary of parameter combinations used during electrospinning to compare the effects of the flowrate and collector distance on the resulting fiber diameter

Concentration of Gelatin (% Weight)	Flowrate (mL/h)	Collector Distance (cm)
20	0.1	6
20	0.1	10
20	0.1	14
20	0.3	6
20	0.3	10
20	0.3	14
20	0.5	6
20	0.5	10
20	0.5	14
25	0.5	10
30	0.5	10

To fabricate each gelatin/galectin-3 scaffold, 5 μL of a 1 mg/mL solution of recombinant human galectin-3 (R&D Systems, Minneapolis, MN, USA) in phosphate buffered saline (PBS) was added to 0.75 mL of the polymer solution (gelatin and acetic acid) for a final concentration of 6.7 $\mu\text{g}/\text{mL}$. Low concentration gelatin/galectin-3 scaffolds were fabricated using a 0.5 mg/mL solution of galectin-3 in PBS, resulting in a final concentration of 3.3 $\mu\text{g}/\text{mL}$. In gelatin scaffolds, 5 μL of PBS was added to the electrospinning solution. Scaffolds were produced by electrospinning for 1.5 hours using a total volume of 0.75 mL of each solution. Scaffolds were then crosslinked in a glass desiccator (VWR International) containing drierite (W.A. Hammond Drierite Co. Ltd, Xenia, OH, USA) using the vapour from a 5 mL solution consisting of 1.5% v/v glutaraldehyde (GTA) (Sigma-Aldrich, St. Louis, MO, USA) in anhydrous ethyl alcohol (Commercial Alcohols, Brampton, ON), similar to the methods of Zha et al. (37). The desiccator was held under vacuum for 20 minutes and scaffolds were left in the sealed desiccator for 48h to ensure sufficient crosslinking had taken place. Following crosslinking, scaffolds were stored in separate sealed plastic containers with desiccant at 2-8°C.

Figure 2.1 – Schematic representation of the electrospinning process: A syringe pump is used to feed the polymer solution through a 1cc syringe and 20 gauge needle at the desired flowrate (0.1-0.5 mL/h). The needle is connected to a power supply and grounded collector, creating an electric potential of 15 kV. Fibers are collected on a rotating mandrel collector positioned 6-10 cm away from the tip of the needle.



2.2.2 Assessment of Fiber Morphology

Three separate scaffolds (N=3) were electrospun at each set of conditions listed in Table 1. One circular sample (8 mm diameter) of as-spun fibers was collected per scaffold using a biopsy punch (Integra Miltek, York, PA, USA). Samples were mounted on aluminum stubs and sputter coated with osmium. Images were taken for each sample using a scanning electron microscope (LEO 1530; Carl Zeiss, Oberkochen, Germany) at 2 kV and one of three magnifications: 1000X, 3000X, or 5000X. Using ImageJ software (National Institutes of Health, Bethesda, MD, USA), the diameter of 250 fibers (N=3), were measured from 5 separate images taken at the same magnification.

2.2.3 Mercury Porosimetry

Mercury porosimetry was used to assess the porosity of the refined gelatin scaffolds. For each test, two scaffolds were electrospun from the same polymer solution for 1.5 hours using the parameters outlined in Table 1. The scaffolds were subsequently crosslinked for 48 hours in 1.5% GTA vapour as previously described. Both scaffolds, measuring approximately 4 x 10 cm were then removed from the aluminum foil, folded and placed together in a 5cc stem which was loaded into the AutoPore IV 9500 mercury porosimeter (Micrometrics Instrument Corp., Norcross, GA, U.S.A). The porosimeter generated a pore size distribution, calculated the scaffold porosity and calculated the average pore diameter (pore size) of the scaffolds.

2.2.4 Mass Spectrometry

Mass spectrometry was used to validate the presence of galectin-3 within the scaffold. Prior to conducting mass spectrometry, three gelatin/galectin-3 scaffolds (6.7 µg/mL) were blend electrospun and crosslinked as described in section 2.2.1. One piece of each scaffold measuring approximately 9 cm² was cut from each scaffold for mass spectrometry. Each sample was then processed and mass spectrometry was conducted according to the methods described by Moffe et al. (38). Processing of samples and mass spectrometry were conducted by the Siqueira Laboratory.

2.2.5 Scaffold Preparation for Cell Culture and Animal Studies

Prior to cell culture studies, scaffolds were removed from the sealed plastic containers and each scaffold was quenched in 50 mL of 0.1 M glycine (Sigma-Aldrich) for 1 hour to remove residual glutaraldehyde. Following quenching, three, 15 minute PBS rinses were conducted and the scaffolds were left in PBS at 4°C overnight. For sterilization, scaffolds were placed under ultra violet (UV) light for 60 minutes.

2.2.6 Adhesion Assay

Scaffolds were punched into circular samples using a 6 mm diameter biopsy punch and placed into a 96-well cell culture plate (BD Falcon™, Franklin Lakes, NJ). Cells were suspended in serum free Dulbecco's Modified Eagle Medium (DMEM) (Gibco, Carlsbad, CA, USA) supplemented with 1% antibiotic-antimicotic (AA) (100 U/mL penicillin, 100 µg/mL streptomycin and 0.25 µg/mL amphotericin B; Gibco) and seeded at a concentration of 2.5×10^4 cells/mL. One hour following seeding, the media was removed and wells were rinsed three times with PBS (Gibco) to remove non-adherent cells and residual media. Scaffolds were transferred to a 500 µL microcentrifuge tube (Port City Diagnostics, Wilmington, NC, USA) and both scaffolds and 96-well plates were stored at -80°C until assayed. A cell pellet containing 2×10^5 cells was also frozen at -80°C to generate the standard curve.

Adhesion, measured as cell number attached to the scaffolds, was quantified using the CyQUANT® Proliferation Assay Kit (Molecular Probes, Carlsbad, CA, USA). Briefly, samples were thawed at room temperature, and 200 µL of CyQUANT® GR dye/cell lysis buffer was added to each microcentrifuge tube or well of the 96-well plate for 5 minutes at room temperature while subjected to vortexing. Samples were covered in aluminum foil during incubation. The supernatant from each sample was collected and transferred to a flat-bottom, black 96-well microplate. Serial dilutions of the cell pellet in CyQUANT® GR dye/cell lysis buffer were also transferred to the 96-well microplate to create a standard curve (Appendix A). Fluorescence of each sample was measured using a Safire² microplate reader (Tecan, Männedorf, Switzerland) at an excitation wavelength of 480 nm and an emission wavelength of 520 nm.

2.2.7 Proliferation Assay

Scaffolds were punched into circular samples using a 6 mm diameter biopsy punch and placed into a 96-well cell culture plate (BD Falcon™). Human dermal fibroblasts were seeded into wells at a density of 3.3×10^3 cells/mL and were cultured for 1, 7, 10 or 14 days in DMEM (Gibco) supplemented with 10% fetal bovine serum (FBS) (Gibco) and 1% AA. Split media changes were performed (75 μ L) every 2 days. At each experimental time point, the media was removed and wells were rinsed three times with PBS to remove non-adherent cells and residual media. Scaffolds were transferred to 500 μ L microcentrifuge tubes and both scaffolds and 96-well plates were stored at -80°C until assayed. A cell pellet containing 2×10^5 cells was also frozen at -80°C . The cell number at each timepoint was determined using the CyQUANT® proliferation assay kit as described in section 2.2.6 and the standard curve is shown in Appendix A.

2.2.8 Extracellular Matrix Deposition Studies

Scaffolds were punched into circular samples using a 6 mm diameter biopsy punch and placed into a 96-well cell culture plate (BD Falcon™). Human dermal fibroblasts were seeded into wells at a density of 3.3×10^4 cells/mL and were cultured for 3 and 7 days in DMEM supplemented with 10% FBS (Gibco), 1 % AA and 50 $\mu\text{g/mL}$ ascorbic acid. Media was changed every 2 days. At each experimental timepoint, cells were fixed in 4% paraformaldehyde (PFA) in PBS for 5 minutes. Three rinses with PBS were conducted followed by treatment with 0.1% Triton X-100 in PBS for 5 minutes to permeabilize the cell membranes. Cells were rinsed again in PBS three times, followed by blocking with 1% bovine serum albumin (BSA) in PBS at 4°C overnight. Scaffolds were incubated with primary antibodies against fibronectin (sc-8422; Santa Cruz Biotechnology, Dallas, TX, USA) diluted at 1:100 in 1% BSA in PBS for one hour at room temperature and were rinsed three times with PBS for 5 minutes. Scaffolds were incubated for 90 minutes at room temperature with Indodicarbocyanine (Cy5) Goat Anti-Mouse IgG antibody (Jackson Immuno Research Laboratories, West Grove, PA, USA) at a 1:200 dilution and rhodamine-conjugated phalloidin (Molecular Probes) at a 1:100 dilution. Negative controls were prepared without the addition of the primary antibody. Following incubation, scaffolds were washed three times for 5 minutes in PBS and mounted on

glass coverslips using Vectashield Mounting Medium (Vector Laboratories) containing 4', 6-diamidino-2-phenylindole (DAPI). Coverslips were sealed with clear nail enamel. Samples were analyzed with an Axio Observer Z1 fluorescence microscope (Carl Zeiss) using the appropriate filters. Negative controls were imaged to set the threshold values for the detection of fluorescence (Appendix B).

2.2.9 Wound Closure Kinetics Study

All animal procedures were in compliance with protocols approved by the University Council on Animal Care at Western University. Six diabetic (db/db) (B6.BK(D) Leprdb/J; 000697) and six wild type (WT) (C57BL/6J; 000664) mice (The Jackson Laboratory; Sacramento, CA) were used for experiments. All mice were age and sex-matched and were 11 weeks of age at the time of surgery. Prior to surgery, all mice were given 0.05 mg/kg of buprenorphine as a pre-emptive analgesic. Animals were then anaesthetized using isoflurane, fur was removed from the surgical site and povidone-iodine was used to clean the area. Four full thickness wounds measuring 6 mm in diameter were then created using a sterile biopsy punch.

For wound closure kinetics studies, each wound was assigned one of four treatment conditions: empty (control wound), gelatin scaffold, a gelatin scaffold made using 3.3 $\mu\text{g}/\text{mL}$ galectin-3 or a gelatin scaffold made using 6.7 $\mu\text{g}/\text{mL}$ galectin-3 (N=6 wounds for each treatment group). Treatments were rotated clockwise in each mouse to eliminate positional effects on wound healing. Scaffolds measuring 8 mm in diameter and sterilized under UV light for 60 minutes were then placed into the wounds. Mice were injected with 0.05 mg/kg of buprenorphine again following surgery. On day 17 post-wounding, all mice were euthanized using carbon dioxide exposure. Tissue samples of the wounds were harvested immediately afterwards and were fixed in 10% neutral buffered formalin (Sigma-Aldrich) for 24 hours at 4°C, transferred to 70% ethanol (Commercial Alcohols) and were paraffin embedded. Serial 5 μm sections were taken from the center of the wounds. To calculate wound closure kinetics, all mice were imaged using a digital camera (Canon, Tokyo, Japan) on days 0, 3, 5, 7, 9, 11, 13, 15, and 17. A ruler was included in each image so that the measurements of wound area could be standardized.

Image J software (National Institutes of Health) was used to calculate the wounded area at each time point (39).

2.2.10 Investigation of Re-Epithelialization and Macrophage Polarization

All animal procedures were in compliance with protocols approved by the University Council on Animal Care at Western University. Six db/db (B6.BK(D)Leprdb/J; 000697) and six WT (C57BL/6J; 000664) mice were purchased from The Jackson Laboratory (Sacramento, CA). All mice were age-matched and sex-matched and were 12 weeks of age at the time of surgery. Prior to surgery, all mice were injected with 0.05 mg/kg of buprenorphine. Animals were then anaesthetized using isoflurane, fur was removed from the surgical site and povidone-iodine was used to clean the area. Four full thickness wounds measuring 6 mm in diameter were then created using a sterile biopsy punch.

Each wound was assigned one of four treatment conditions: empty (control wound), topical galectin-3 (6.7 μ L galectin-3 in sterile saline), gelatin scaffold, or a gelatin scaffold containing 6.7 μ g/mL galectin-3 (N=6 wounds for each treatment group). Scaffolds measuring 8 mm in diameter and disinfected under UV light for 60 minutes were then placed into the wounds. Topical galectin-3 was mixed with sterile saline at 6.7 μ g/mL and 10 μ L of this solution was added to the wound following the surgery and each subsequent day until mice were euthanized. Mice were injected with 0.05 mg/kg of buprenorphine following surgery. Mice were euthanized using carbon dioxide exposure on days 5 (N=3 WT mice; N=3 db/db mice) and 7 (N=3 WT mice; N=3 db/db mice) post-wounding. Tissue samples of the wounds were harvested immediately afterwards and were fixed in 10% neutral buffered formalin (Sigma-Aldrich) for 24 hours at 4°C, transferred to 70% ethanol (Commercial Alcohols) and were paraffin embedded. Serial 5 μ m sections were taken from the center of the wounds.

To calculate wound closure kinetics, all mice were imaged on 0, 3, 5, and 7 days. A ruler was included in each image so that the measurements of wound area could be standardized. Image J software (National Institutes of Health) was used to calculate the wounded area at each time point (39).

Masson's Trichrome staining, conducted by the Pathology department within the London Health Sciences Centre, was used to visualize collagen deposition and re-epithelialization. Sections were imaged with a Leica DM100 light microscope (Leica, Wetzlar, Germany). Analysis was conducted on Masson's Trichrome stained sections using ImageJ software (National Institutes of Health) to measure the length of the epithelial tongue and the thickness of the epithelium (26, 39).

Immunohistochemical staining for inducible nitric oxide synthase (iNOS) and arginase I was performed to visualize M1 and M2 macrophage populations. Sections were rehydrated, rinsed with PBS for 5 minutes and subjected to enzymatic antigen retrieval for 15 minutes at 37°C. Samples were rinsed again in PBS for 5 minutes at room temperature and blocked using 10% horse serum in PBS for 30 minutes at room temperature in a humidified chamber. Sections were then incubated in primary goat antibodies against arginase I (sc-18354; Santa Cruz Biotechnology) diluted at 1:100 in 10% horse serum and rabbit antibodies against iNOS (ab3523; Abcam, Cambridge, UK) diluted at 1:25 in 10% horse serum overnight at 4°C. Sections were rinsed in PBS and incubated with secondary antibodies at a dilution of 1:500 in horse serum for one hour at room temperature, while protected from light. Antibodies included an Alexa Fluor 647 anti-rabbit antibody (Abcam) and an Alexa Fluor 488 anti-goat antibody (Abcam). Hoechst 33342 (Trihydrochloride Trihydrate; Thermo Fisher Scientific) was also added at a dilution of 1:1000. Sections were rinsed in PBS to remove unbound antibodies and were mounted using Immuno-Mount (Thermo Fisher Scientific) mounting medium. Coverslips were sealed with clear nail enamel. Sections were imaged using an Axio Observer Z1 fluorescence microscope (Carl Zeiss) using the appropriate filters. Negative controls were sectioned and stained without the addition of primary antibodies. These negative control slides were imaged to set the threshold values for the detection of fluorescence (Appendix C). ImageJ software was used to quantify the number of arginase I-positive macrophages in the wound bed in WT mice at day 7 (N=3, n=3) (National Institutes of Health).

2.3 Results

2.3.1 Influence of Electrospinning Parameters on Fiber Diameter and Scaffold Morphology

To determine the influence of electrospinning parameters on the resulting fiber diameter, 12 different parameters were assessed. The influence of three different concentrations of gelatin, three solution flowrates, and three collector distances on fiber diameter were investigated. In order to determine the influence of the flowrate and needle to collector distances, these parameters were varied while the concentration of gelatin was held constant at 20% weight. Statistical analysis revealed, at each flowrate assessed, there were no significant differences in the fiber diameter when the collector distance was increased (Figure 2.2; $p>0.05$). Additionally, at each collector distance, there were no significant differences in the fiber diameter when the flowrate was increased (Figure 2.2; $p>0.05$). To determine the influence of gelatin concentration on the resulting fiber diameter, both the solution flowrate and the collector distance were held constant while the gelatin concentration was increased. As the concentration of gelatin was increased, the resulting fiber diameter increased. Scaffolds electrospun using a concentration of 30% weight gelatin had a significantly larger mean fiber diameter than fibers electrospun using 20% weight and 25% weight gelatin (Figure 2.3; $p<0.05$). Differences in the mean fiber diameter between 20% weight and 25% weight gelatin were not statistically significant. Increases of fiber diameter corresponding to increases in gelatin concentration were also apparent upon observation of the fiber diameter distributions (Figure 2.4G, H, I).

When 30% weight gelatin was used (Figure 2.4I), the majority of fibers were 500-1500 nm in diameter. There was a large variation in fiber size, with fibers measuring up to 4000 nm in diameter. At 25% weight, the majority of the fibers were within range of 300-500 nm (Figure 2.4H). The distribution of fiber size was even smaller at 20% weight gelatin, with the majority of fibers measuring between 100-200 nm (Figure 2.4I).

To determine whether the differences in fiber diameter were associated with morphological changes in the fibers, fiber morphology was assessed in scanning electron microscopy (SEM) images taken at each concentration of gelatin. At the 20% weight

concentration of gelatin, SEM analysis revealed the presence of beaded fibers in the electrospun fiber mat (Figure 2.4A, D). In the fibrous mats electrospun using a 25% weight solution of gelatin, SEM showed that the mats contained various web-like and ribbon-like fibers (Figure 2.4B and E). Scaffolds electrospun using 30% weight gelatin consisted mainly of the ribbon-like fibers, although the relative abundance of cylindrical and ribbon-like fibrils was not quantified (Figure 2.4C and F).

To determine whether increasing the gelatin concentration above 20% weight could eliminate beaded fibers, while maintaining fiber diameters within the 100-200 nm range, the gelatin concentration was increased to 21% weight and SEM was conducted to determine the morphological characteristics as well as measure the resulting mean fiber diameter. The resulting mean fiber diameter was 224.6 ± 13.39 nm and SEM revealed that there were no beads within the fiber mat (Figure 2.5A). The frequency distribution obtained from this sample revealed that fiber diameters ranged from roughly 100-300 nm and fibers in the range of 230-250 nm were most frequently measured (Figure 2.5B).

Figure 2.2 – Effect of increasing collector distance and flowrate on mean fiber diameter: Fiber diameters measured at 9 combinations of flowrate and collector distances. The flowrate was varied between 0.1, 0.3 and 0.5 mL/h and the collector distance was varied between 6, 10 and 14 cm. The concentration of gelatin was held constant at 20% weight. No significant differences in fiber diameter were observed at any of the conditions assessed. N=3, n=250, two-way ANOVA, $p>0.05$. All data is represented as mean \pm SEM.

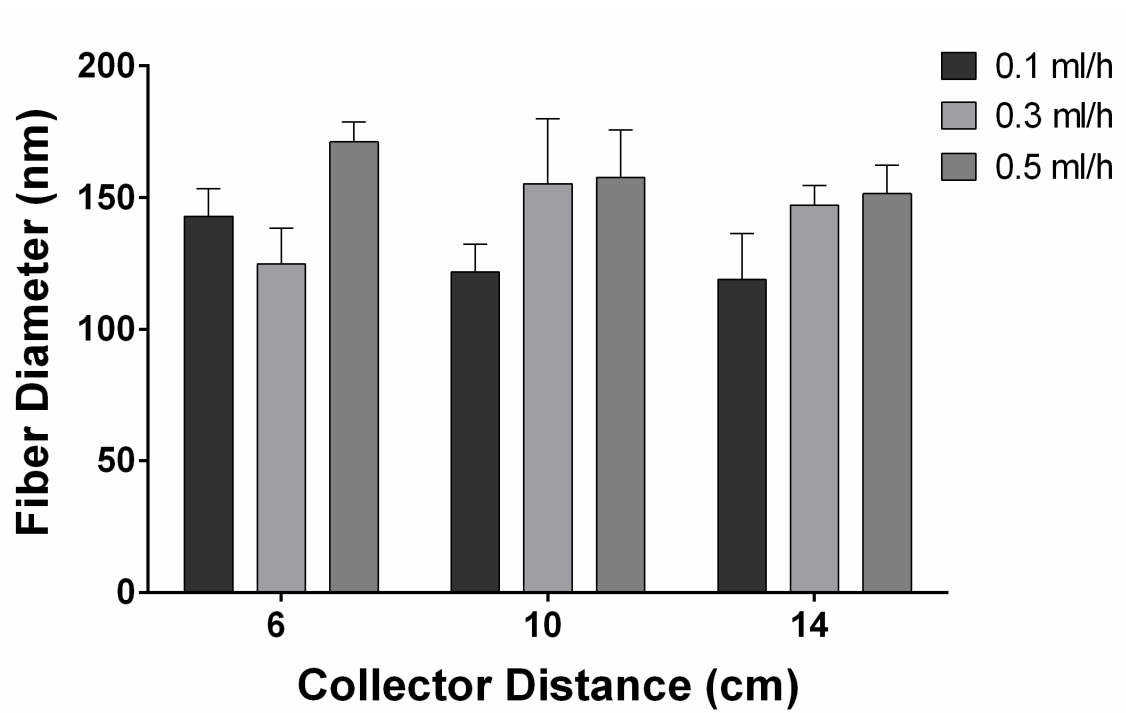


Figure 2.3 – Effect of increasing concentration on mean fiber diameter: Mean fiber diameters measured at 20%, 25% and 30% weight gelatin. The flowrate and collector distance were held constant at 0.5 mL/h and 10 cm, respectively. Fibers electrospun at a concentration of 30% weight gelatin had significantly higher fiber diameters than those electrospun at 25% weight and 20% weight gelatin. N=3, n=250, one-way ANOVA, Tukey post-test for multiple comparisons, *p <0.05. All data is represented as mean \pm SEM.

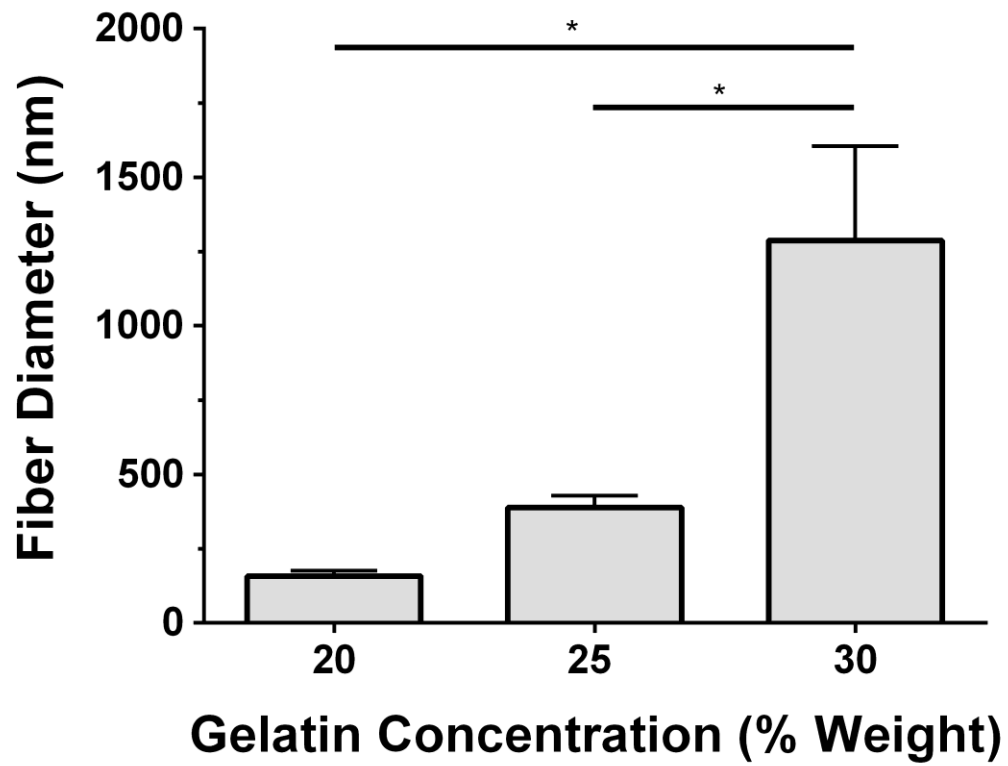


Figure 2.4 – The effect of increasing concentration on fiber morphology and fiber size distribution: A-F: Images of electrospun gelatin nanofibers collected by SEM. Fiber mats were electrospun using a flowrate of 0.5 mL/h, collector distance of 10 cm and varying gelatin concentrations. A-C: Images were taken at 1000x magnification. Scale Bar: 25 μm . D-F: Images were taken at 5000x magnification. Scale Bar: 5 μm . G-I: Frequency distribution graph showing the percentage of fiber diameters (from 750 measurements across N=3 experiments) within each bin range for scaffolds electrospun using a flowrate of 0.5 mL/h, a collector distance of 10 cm, and a gelatin concentration of 20%, 25%, and 30% weight. N=3, n=250. G: Bin size: 20 nm. H: Bin size: 50 nm. I: Bin size: 500 nm. At a concentration of 20% weight gelatin, beaded fibers are shown within the fiber mat and the majority of fibers measured between 100-200 nm in diameter. At 25% weight gelatin, both ribbon-like and web-like fibers were detected in the fiber mat. The majority of fibers measured between 200-500nm in diameter. At 30% weight gelatin, the mat consisted mainly of ribbon-like fibers, the majority of which measured between 500-1500 nm.

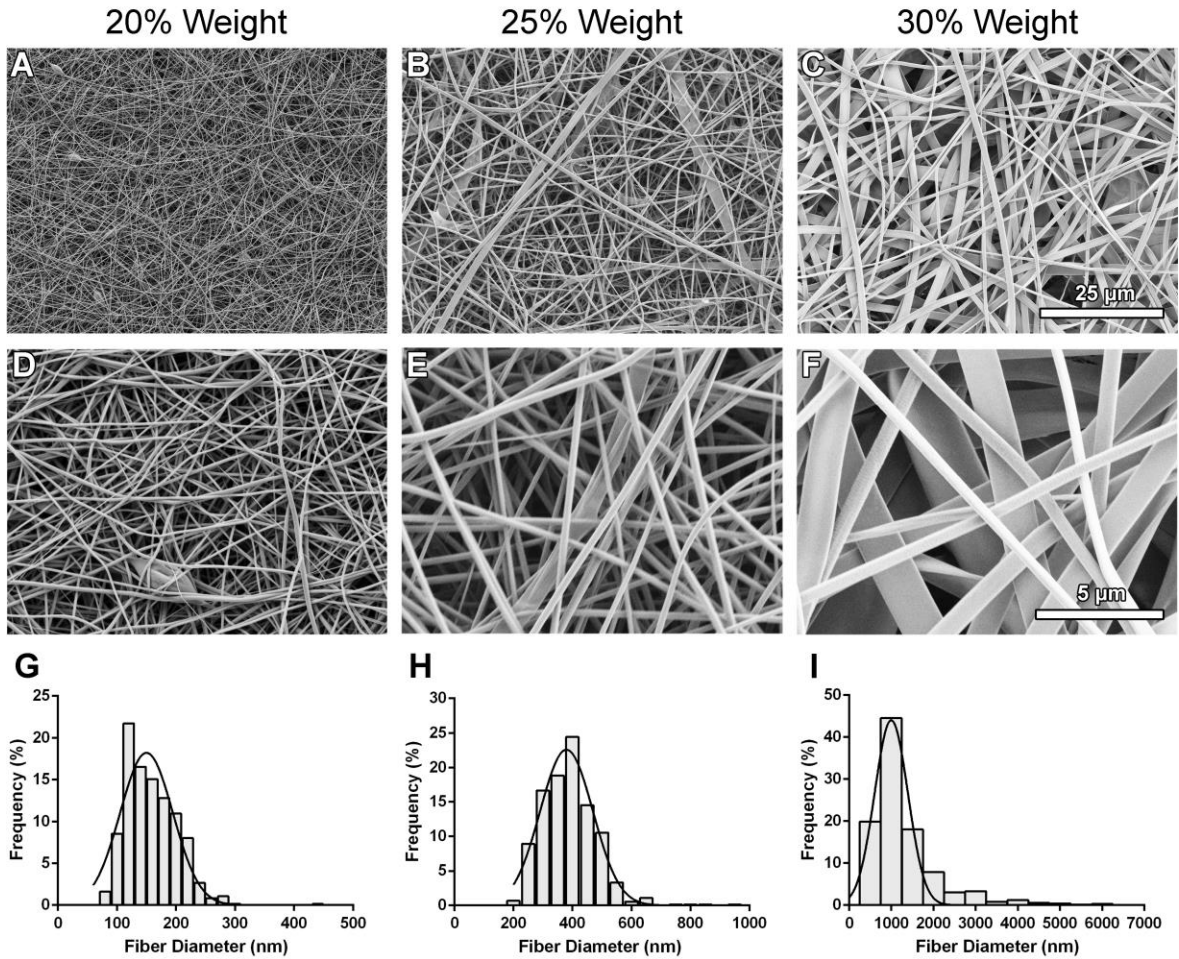
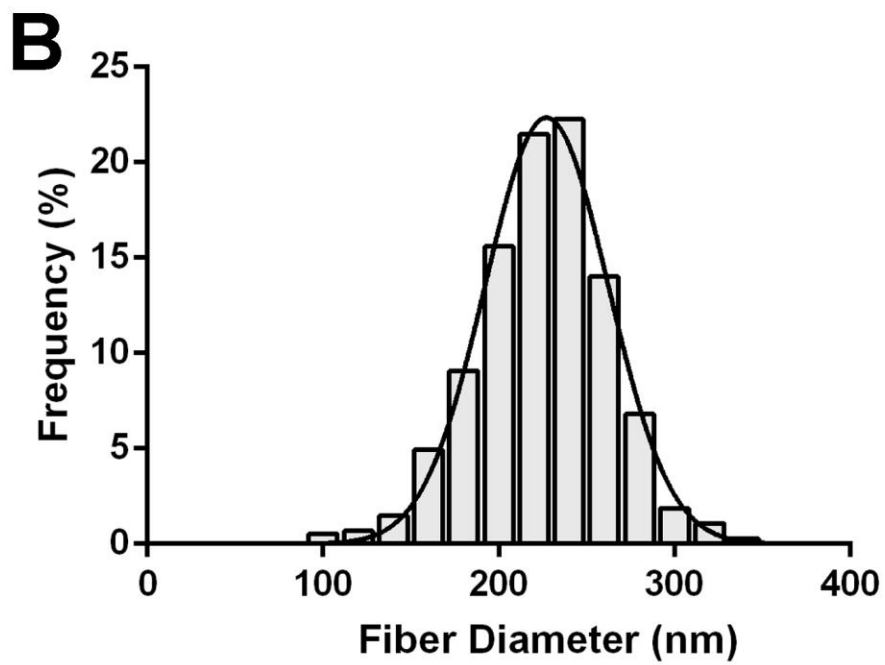
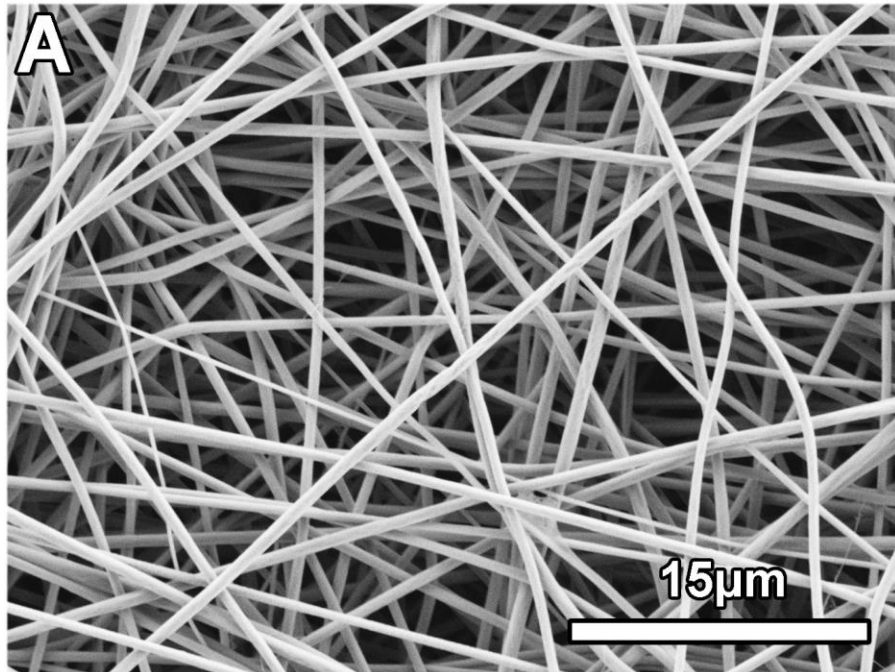


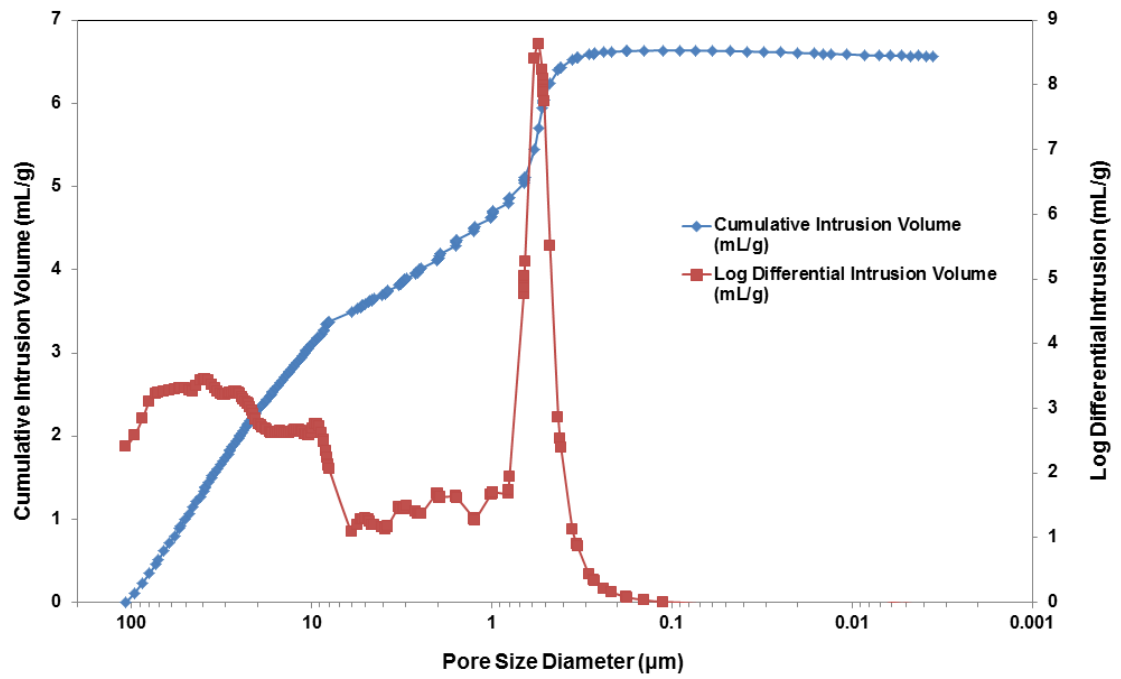
Figure 2.5 – Refined scaffold morphology and fiber size distribution: (A) SEM image of a scaffold electrospun using a flowrate of 0.5 mL/h, a collector distance of 10 cm, and a gelatin concentration of 21% weight. Scale Bar: 15 μm . (B) Frequency distribution graph showing the percentage of fiber diameters within each bin range for scaffolds electrospun using a flowrate of 0.5 mL/h, a collector distance of 10 cm, and a gelatin concentration of 21% weight. N=3, n=250. Bin size: 20 nm.



2.3.2 Scaffold Porosity is Sufficient for Cell Growth

Mercury porosimetry was conducted to evaluate scaffold porosity and to determine whether scaffold pore sizes would be sufficient to allow cell infiltration. Analysis revealed that scaffolds are 83.08 ± 4.06 % porous and have an average pore diameter of 1.15 ± 0.77 μm (N=3). A representative graph showing the pore size distribution is shown in Figure 2.6. The scaffolds contain pores ranging from 0.1 to 100 μm in size, with the majority of the pore diameters are observed within the range of 0.3-0.8 μm and 30-50 μm .

Figure 2.6 – Mercury porosimetry pore size distribution plot: Representative graph of pore diameter distribution measured as a function of differential and cumulative intrusion volumes. The cumulative pore volume curve shows steeper slopes between 10-100 μm and 0.1-1 μm , coinciding with peaks in the log differential intrusion volume. Each log differential intrusion value represents the relative quantity of mercury entering pores of a specific diameter. Mercury porosimetry was repeated three times (N=3) on different batches of scaffolds.



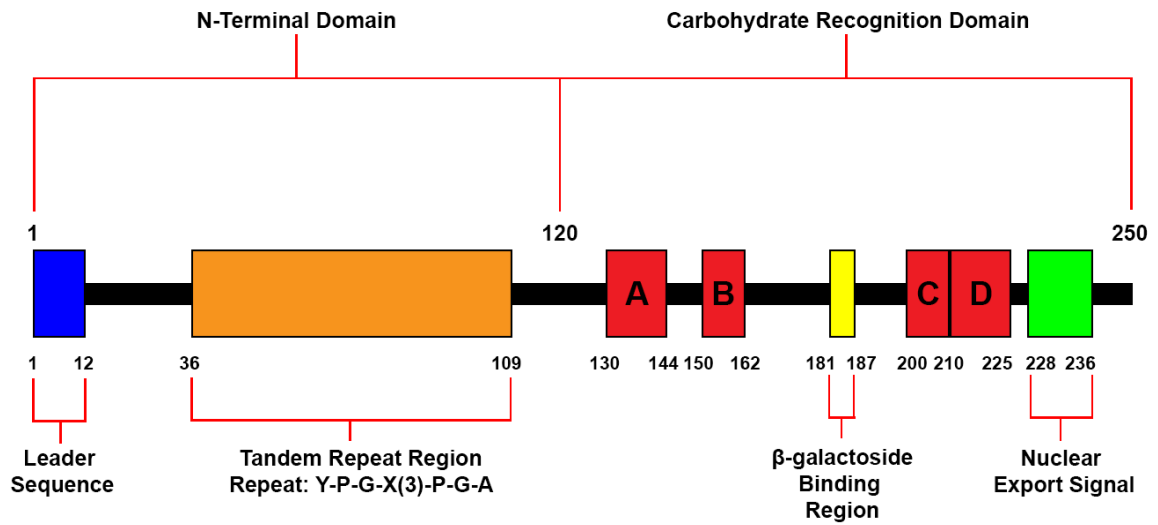
2.3.3 Detection of Galectin-3 in Scaffolds

To ensure the blend electrospinning method resulted in scaffolds containing recombinant human galectin-3, mass spectrometry was conducted on crosslinked samples of scaffolds electrospun with galectin-3. Table 2 summarizes the findings from the mass spectrometry analysis. Four sequences from recombinant human galectin-3 were identified, verifying its presence within the scaffolds. Identified sequences were run using the Basic Local Alignment Search Tool (BLAST) in the Universal Protein Resource (UniProt) database which showed that each detected sequence aligned to a specific sequence contained within the CRD of human recombinant galectin-3 and matched with 100% sequence identity (Figure 2.7).

Table 2: Human recombinant galectin-3 amino acid sequences detected by mass spectrometry

Accession Number	Description	Sequences Detected	Sequence Identity (%)
P17931	LEG3 HUMAN – Galectin-3 Homo Sapiens (Human)	MLITILGTVKPNANR	100
P17931	LEG3 HUMAN – Galectin-3 Homo Sapiens (Human)	GNDVAFHFNPR	100
P17931	LEG3 HUMAN – Galectin-3 Homo Sapiens (Human)	IQVLVEPDHFK	100
P17931	LEG3 HUMAN – Galectin-3 Homo Sapiens (Human)	VAVNDAHLLQYNHR	100

Figure 2.7 – Visualization of detected sequences on recombinant human galectin-3: Mass spectrometry was conducted three times for detection of galectin-3. Four peptide sequences having 100% alignment with the human recombinant galectin-3 protein structure in the carbohydrate recognition domain were detected. (A) 15 amino acid sequence of MLITILGTVKPNANR aligns with the protein at amino acid locations 130-144. (B) 11 amino acid sequence of GNDVAFHFNPR aligns with the protein at amino acid locations 152-162. (C) 11 amino acid sequence of IQVLVEPDHFK aligns with the protein at amino acid locations 200-210. (D) 14 amino acid sequence of VAVNDAHLLQYNHR aligns with the protein at amino acid locations 211-225.



2.3.4 Scaffolds Increase the Initial Adhesion of Human Dermal Fibroblasts

Human dermal fibroblasts were seeded onto tissue culture plastic, gelatin scaffolds and gelatin/galectin-3 scaffolds (6.7 μ g/mL). Cells adhered to all surfaces within one hour (Figure 2.8). Significantly more cells were detected on gelatin scaffolds relative to the tissue culture plastic (N=3, n=3, $p < 0.01$). Similarly, significantly more cells attached to gelatin/galectin-3 scaffolds than tissue culture plastic (N=3, n=3, $p < 0.001$). However, no significant differences in cell number were detected between the gelatin and gelatin/galectin-3 scaffolds at one hour following seeding (N=3, n=3, $p > 0.05$).

2.3.5 Scaffolds Support the Proliferation of Human Dermal Fibroblasts

To assess increases in human dermal fibroblast numbers, cell numbers were quantified at days 1, 7, 10, and 14 post-seeding. Cell numbers increased over a 14 day period when cultured on tissue culture plastic, the gelatin scaffold and the gelatin/galectin-3 scaffold (Figure 2.9). There were no significant differences in cell numbers between the three conditions at each time point assessed (N=3, n=4, $p > 0.05$).

2.3.6 Scaffolds Support the Production of Fibronectin by Human Dermal Fibroblasts

Human dermal fibroblasts were cultured on both gelatin scaffolds and gelatin/galectin-3 scaffolds for up to 7 days to observe whether the scaffolds were able to support secretion of fibronectin. Staining of the filamentous actin (red) demonstrated that the cells were attached and well spread at days 3 and 7 post-seeding (Figure 2.10). Staining for extracellular fibronectin revealed its deposition by fibroblasts on both gelatin and gelatin/galectin-3 scaffolds at days 3 and 7 post-seeding (Figure 2.11). Increased deposition was seen qualitatively on the scaffolds by day 7 although no observable differences in the immunoreactivity for fibronectin was evident between the scaffolds at both of the time points examined.

Figure 2.8 – Adhesion of human dermal fibroblasts on scaffolds: Human dermal fibroblasts were seeded onto tissue culture plastic, gelatin scaffolds and gelatin/galectin-3 scaffolds (6.7 $\mu\text{g}/\text{mL}$) and left to attach for one hour. At one hour following seeding, cell numbers were significantly higher in wells containing the gelatin/galectin-3 scaffolds than in tissue culture plastic wells. Cell numbers were also significantly higher in wells containing the gelatin scaffolds than in tissue culture plastic wells. $N=3$, $n=3$, one-way ANOVA, Tukey post-test for multiple comparisons, $**p<0.01$, $***p<0.001$. All data is represented as mean \pm SEM.

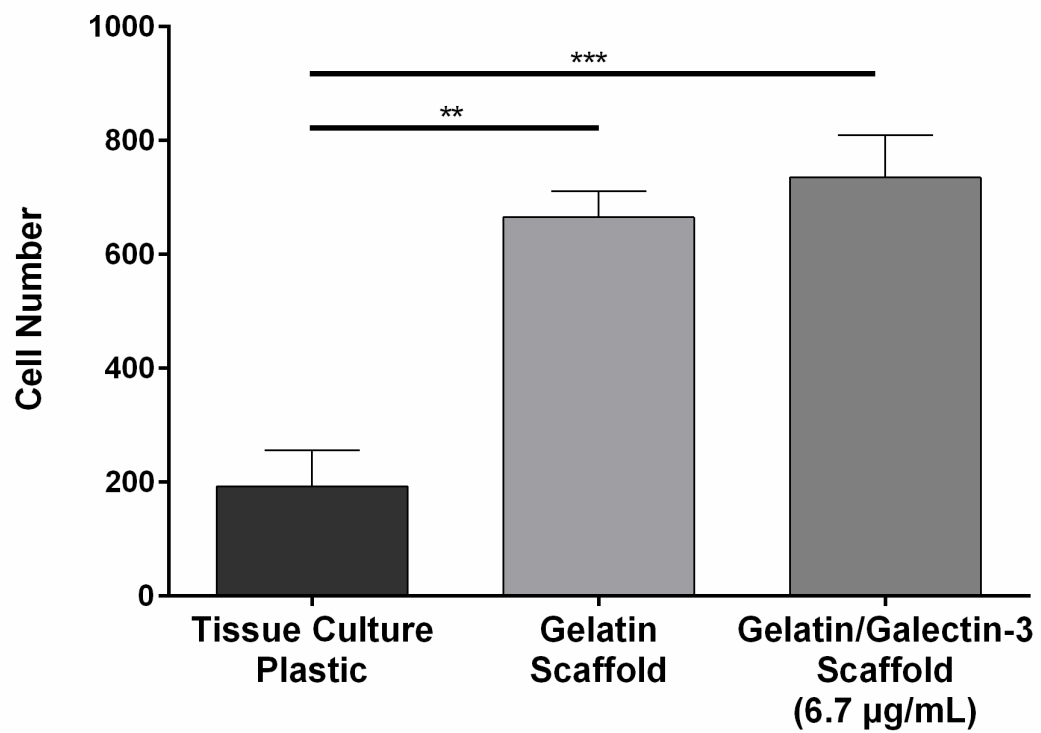


Figure 2.9 – Proliferation of human dermal fibroblasts on scaffolds: Human dermal fibroblasts were cultured on tissue culture plastic, gelatin scaffolds and gelatin/galectin-3 scaffolds (6.7 $\mu\text{g}/\text{mL}$) over 14 days. There were no significant differences in the cell number between the groups at all time points assessed. $N=3$, $n=4$, two-way ANOVA, $p>0.05$. All data is represented as mean \pm SEM.

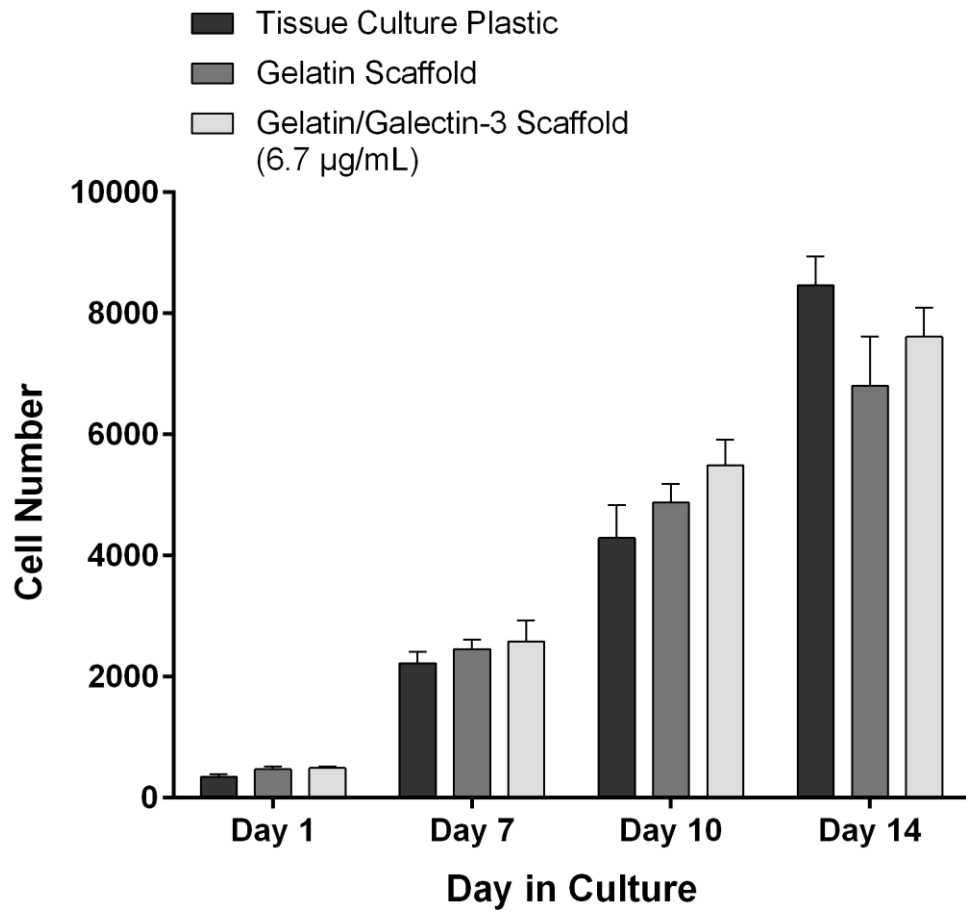


Figure 2.10 – Visualization of human dermal fibroblast cytoskeleton on scaffolds: Human dermal fibroblasts were cultured on tissue culture plastic, gelatin and gelatin/galectin-3 scaffolds (6.7µg/mL) over 7 days. Representative images show the cell cytoskeleton (red) and cell nuclei (blue) using immunocytochemistry. Human dermal fibroblasts cultured on scaffolds show appropriate fibroblast-like morphology and cell spreading after 3 days in culture, consistent with the tissue culture plastic controls. Cells remain spread along the scaffold surface after 7 days in culture. N=3, n=3, scale bar: 50µm.

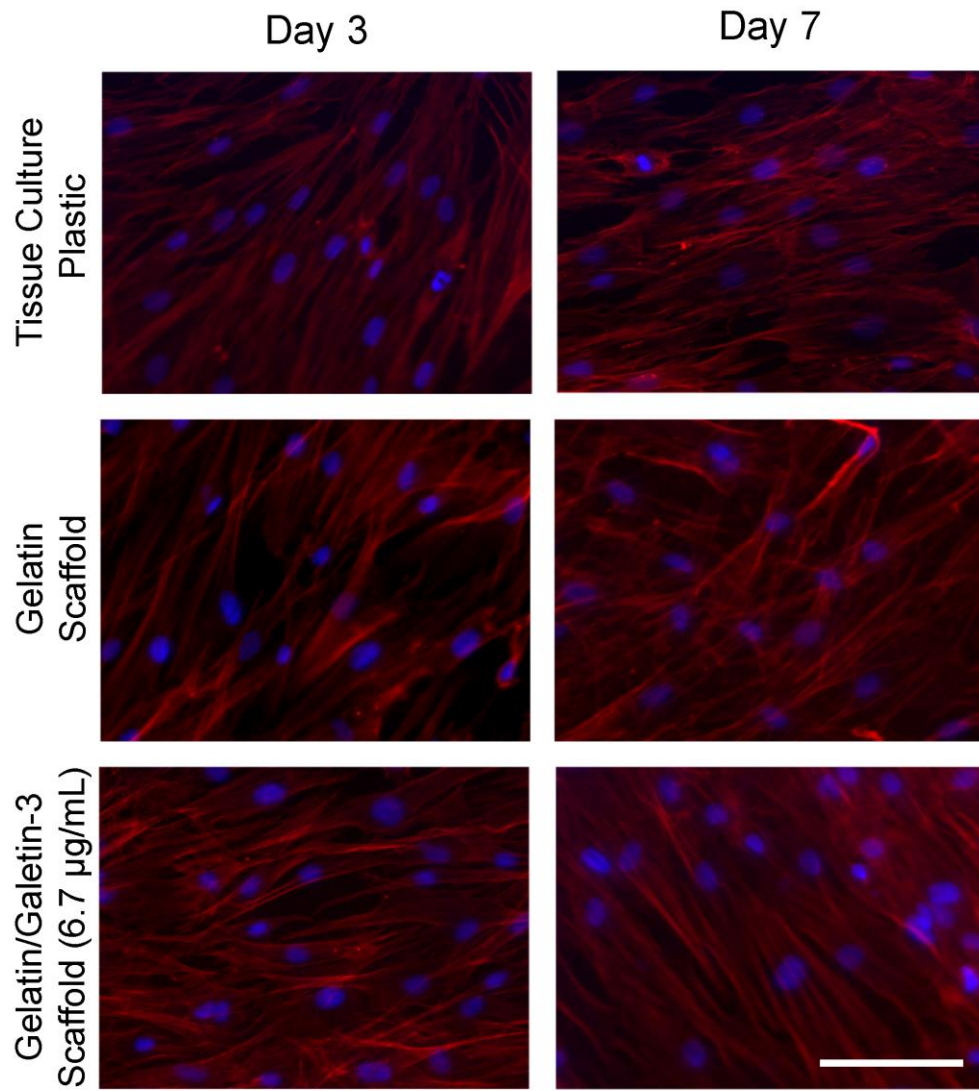
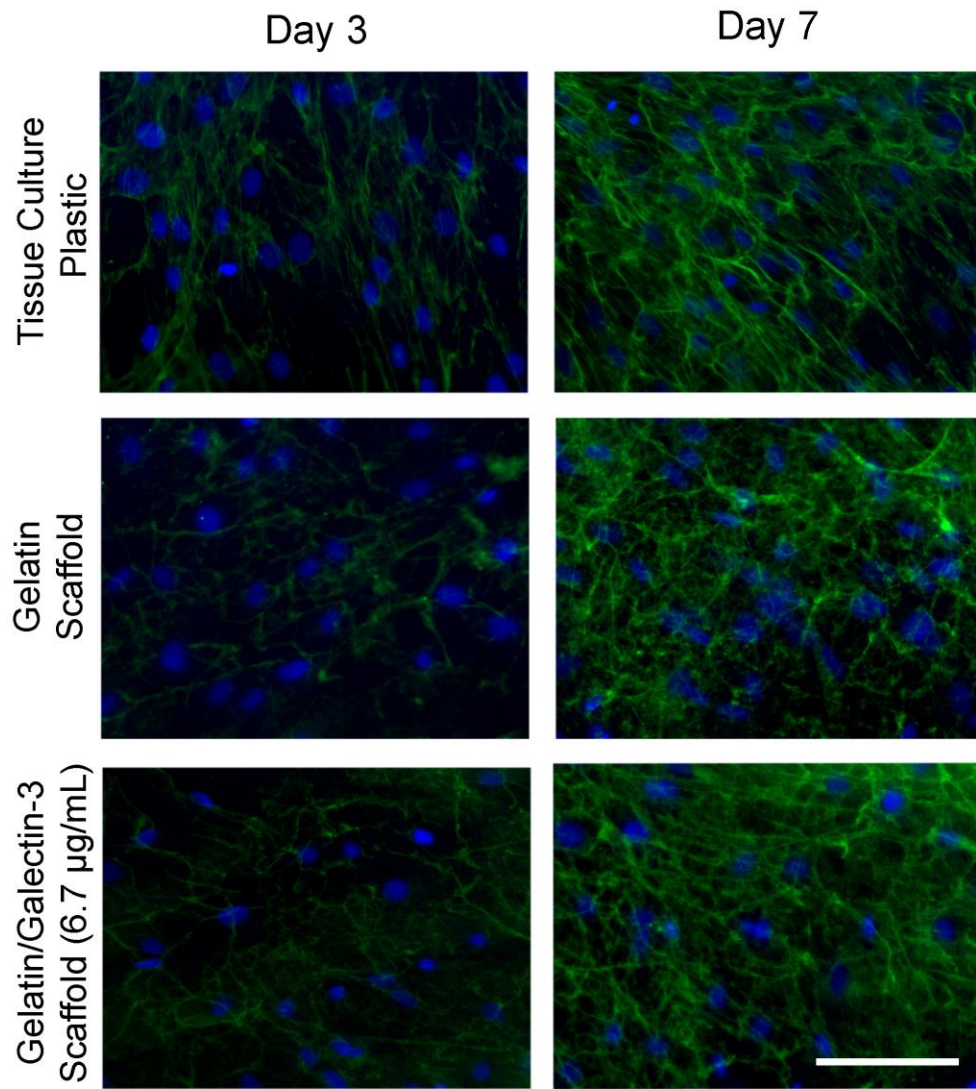


Figure 2.11 – Deposition of fibronectin by human dermal fibroblasts on scaffolds: Human dermal fibroblasts were cultured on tissue culture plastic, gelatin and gelatin/galectin-3 scaffolds (6.7 $\mu\text{g}/\text{mL}$) over 7 days. Representative images show fibronectin (green) and cell nuclei (blue) using immunocytochemistry. Fibronectin was detected after 3 days on the tissue culture plastic, gelatin and gelatin/galectin-3 scaffolds. Fibronectin remained present at 7 days following seeding. There were no observable differences in the amount of fibronectin deposited between the scaffolds. N=3, n=3, scale bar: 50 μm .



2.3.7 Gelatin/Galectin-3 Scaffolds Do Not Alter Skin Closure Kinetics in Wild Type and Diabetic Mice

To determine whether gelatin/galectin-3 scaffolds influence wound closure kinetics in WT mice, each of the four experimentally created wounds were given a different treatment: a gelatin scaffold, a gelatin scaffold loaded with 3.3 $\mu\text{g/mL}$ galectin-3, a gelatin scaffold loaded with 6.7 $\mu\text{g/mL}$ galectin-3 or no treatment (left empty). Representative images of the wounds for each treatment are shown at day 0, day 9, and day 17 in Figure 2.12. Wound closure rates were compared between wounds on days 3, 5, 7, 9, 11, 13, 15, and 17 following surgery (Figure 2.13). At day 7, statistical analysis showed that wounds treated with the gelatin scaffolds had significantly higher wound closure than wounds treated with gelatin/galectin-3 scaffolds (6.7 $\mu\text{g/mL}$) ($p < 0.05$, $N=6$). No statistical differences in wound closure were observed between the treatment groups at all other time points assessed ($p > 0.05$, $N=6$).

To determine whether gelatin/galectin-3 scaffolds influence wound closure kinetics in an impaired model of wound healing, full thickness excisional wounds in db/db mice were treated with the same four treatment groups as described for WT mice. Representative images of the wounds for each treatment at day 0, day 9, and day 17 are shown in Figure 2.14. Wound closure was compared between wounds on days 3, 5, 7, 9, 11, 13, 15, and 17 following surgery (Figure 2.15). Statistical analysis showed that there were no significant differences in wound closure between the treatment groups at all time points assessed ($p > 0.05$, $N=6$).

Masson's trichrome staining in db/db mice revealed that wounds in each condition were completely re-epithelialized by day 17 post-surgery (Figure 2.16). There were no observable differences in the thickness of the epithelium or in the amount of collagen in each of the conditions assessed. At day 17 in WT mice, the wounds had completely closed and the mice had regained hair at the wound site making it difficult to identify the original location of the wounds. Therefore, sectioning and staining was not conducted on WT mice at day 17.

Figure 2.12 – Representative images of the wound area for evaluation of wound closure kinetics in WT mice: Full thickness excisional wounds measuring 6 mm in diameter were treated with a gelatin scaffold, a gelatin/galectin-3 scaffold (3.3 $\mu\text{g}/\text{mL}$), a gelatin/galectin-3 scaffold (6.7 $\mu\text{g}/\text{mL}$), or left empty (control). Representative images of the four conditions from one WT mouse are shown at day 0, day 9 and day 17. Wounds appear much smaller by day 9 in all treatment conditions and by day 17 wounds achieved closure with hair returning to the wound site. N=6, scale bar = 2.5 mm.

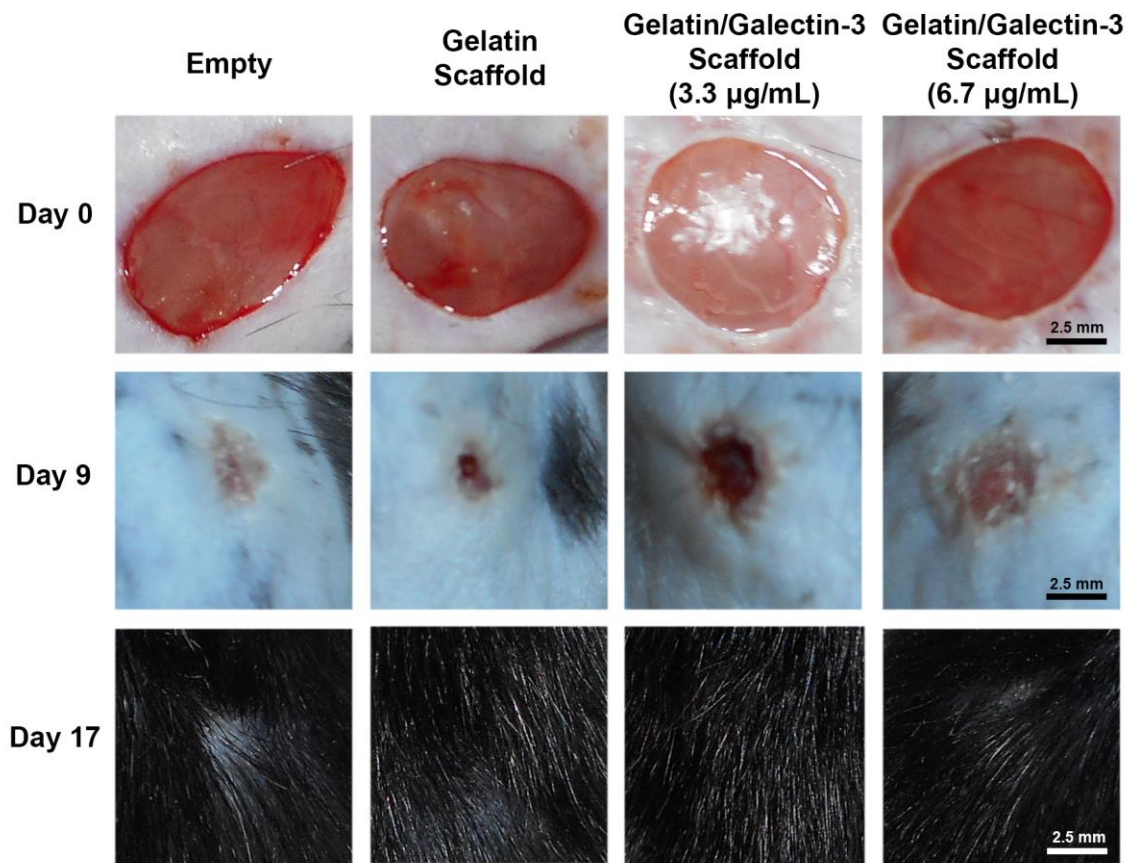


Figure 2.13 – Wound closure kinetics *in vivo* for full thickness wounding in WT mice: Full thickness excisional wounds measuring 6 mm in diameter were treated with a gelatin scaffold, a gelatin/galectin-3 scaffold loaded at 3.3 $\mu\text{g}/\text{mL}$, a gelatin/galectin-3 scaffold loaded at 6.7 $\mu\text{g}/\text{mL}$, or left empty (control). The percentage of closure relative to the original wound was calculated over a 17 day period. There were no significant differences between each of the treatment groups and the experimental control (empty wound) at all time points assessed ($p>0.05$). Wound closure increased steadily over the 17 day period, with all wounds achieving closure by day 17. $N=6$, two-way ANOVA, Tukey post-test for multiple comparisons, $p>0.05$ between each treatment and the control scaffold. Data is represented as mean \pm SEM.

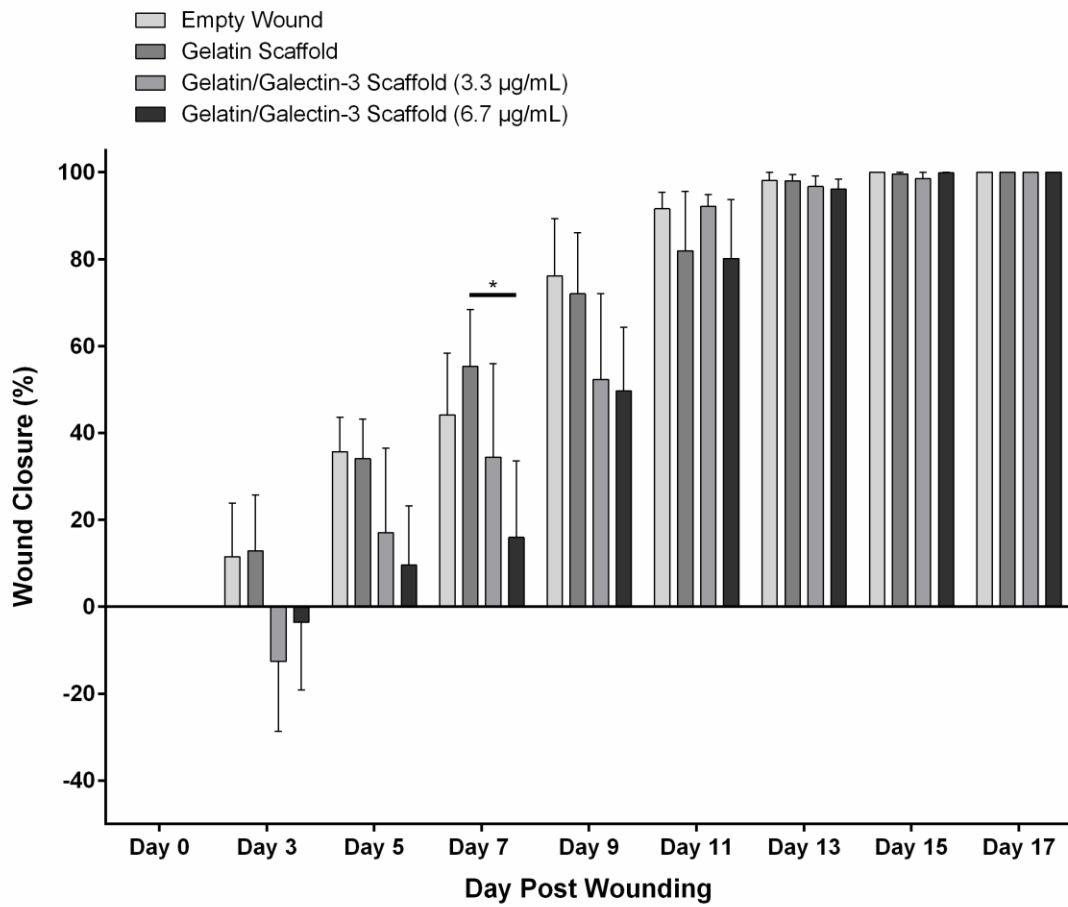


Figure 2.14 – Representative images of the wound area for evaluation of wound closure kinetics in db/db mice: Full thickness excisional wounds measuring 6 mm in diameter were treated with a gelatin scaffold, a gelatin/galectin-3 scaffold (3.3 $\mu\text{g}/\text{mL}$), a gelatin/galectin-3 scaffold (6.7 $\mu\text{g}/\text{mL}$), or left empty (control). Representative images of the four treatment conditions from one db/db mouse are shown at day 0, day 9 and day 17. Wound size was decreased slightly by day 9 in all treatment conditions. At day 17 wounds were still visible. N=6, scale bar = 2.5 mm.

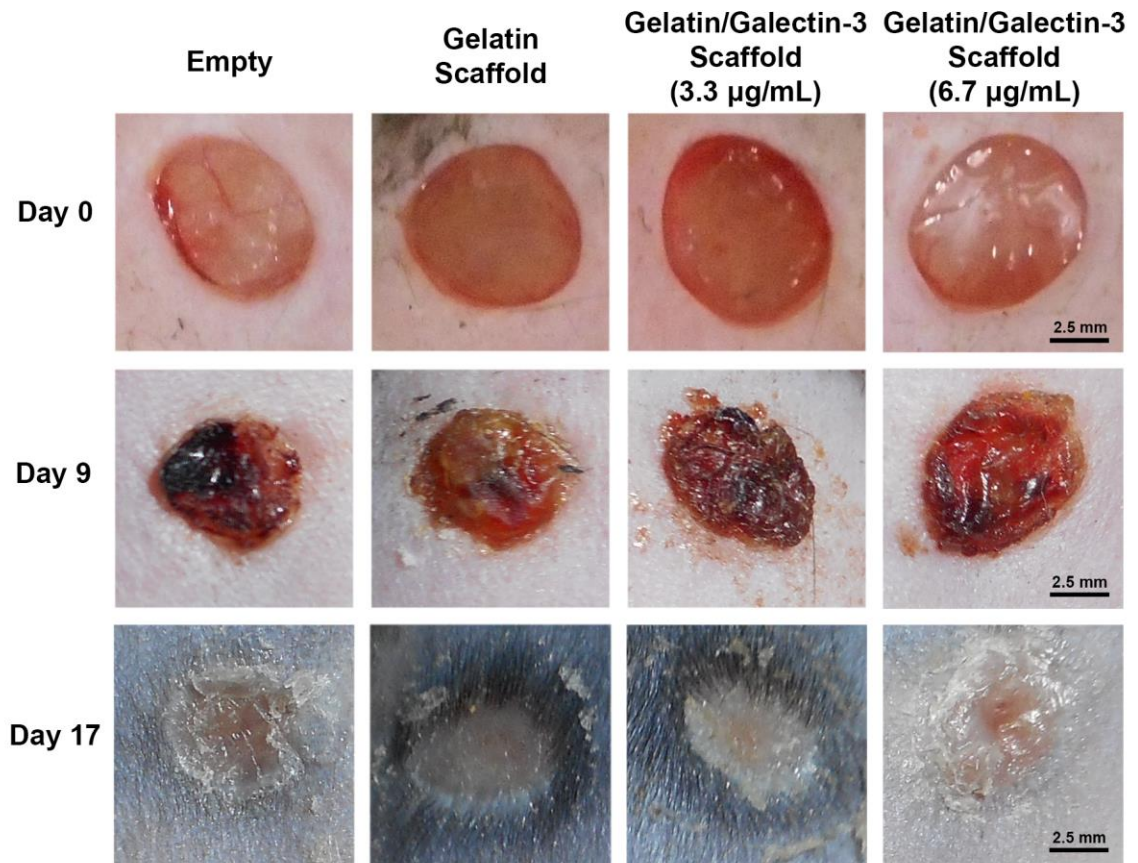


Figure 2.15 – Wound closure kinetics *in vivo* for full thickness wounding in db/db mice: Full thickness excisional wounds measuring 6 mm in diameter were treated with a gelatin scaffold, a gelatin/galectin-3 scaffold loaded at 3.3 $\mu\text{g/mL}$, a gelatin/galectin-3 scaffold loaded at 6.7 $\mu\text{g/mL}$, or left empty (control). The percentage of closure relative to the original wound was calculated over a 17 day period. There were no significant differences between each of the treatment groups and the experimental control (empty wound) at all time points assessed ($p > 0.05$). Wound sizes initially increase in db/db mice, with wound closure steadily increasing after day 9. $N=6$, two-way ANOVA, Tukey post-test for multiple comparisons, $p > 0.05$ between each treatment and the control scaffold. Data is represented as mean \pm SEM.

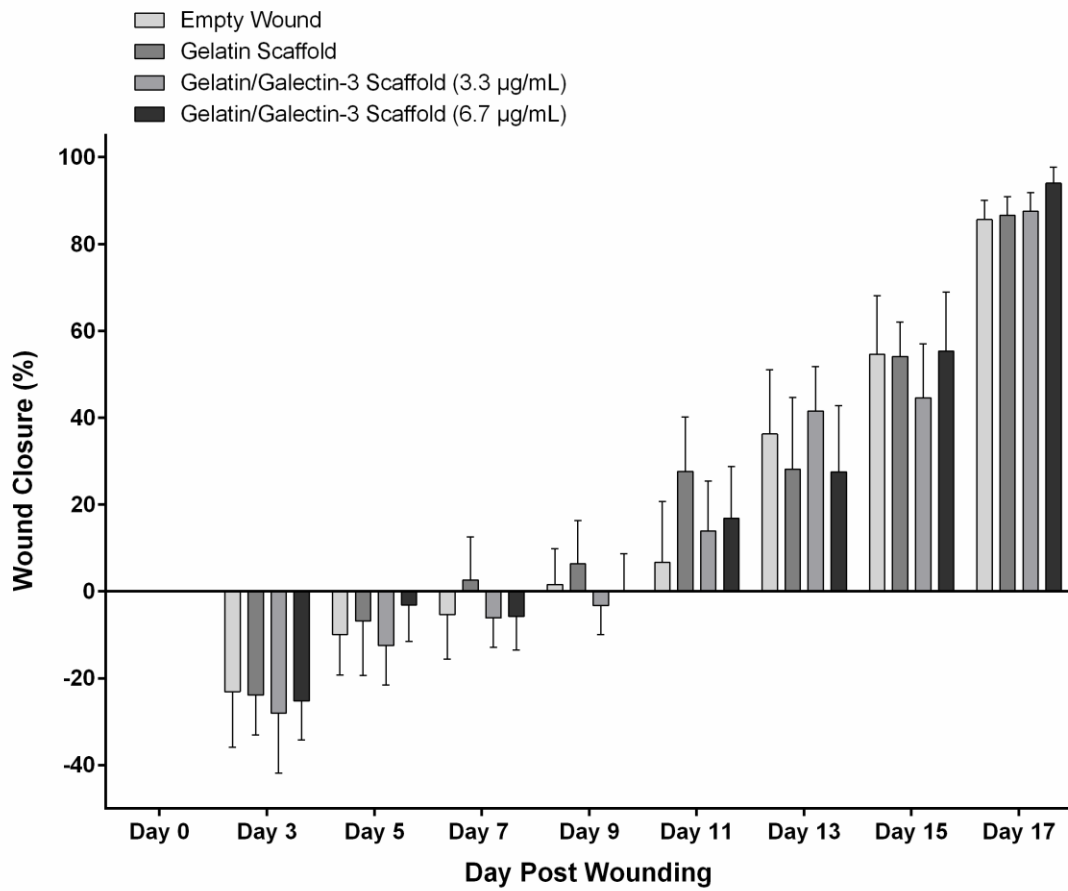
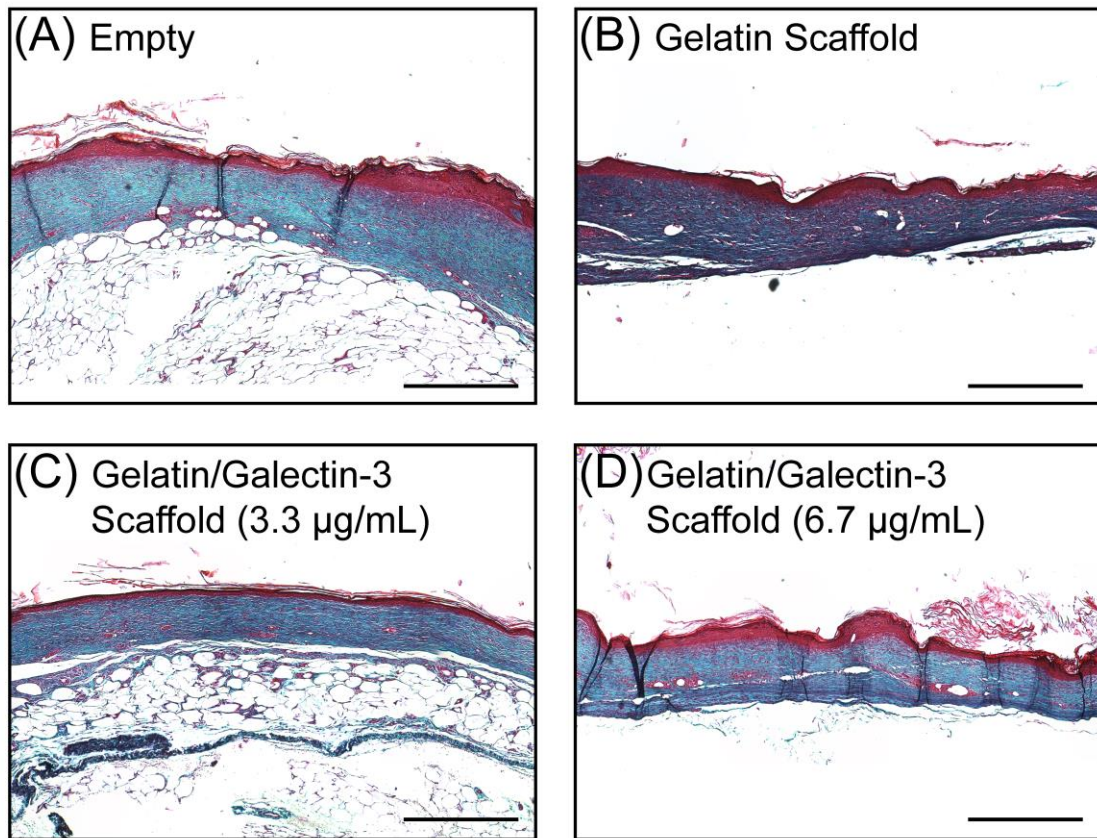


Figure 2.16 – Masson’s Trichrome staining at day 17 following *in vivo* full thickness wounding in db/db mice: Representative images of the center of the wound bed for db/db mice at 17 days post-wounding. Sections from all six mice were stained and analyzed. (A) Empty wound. (B) Wound treated with gelatin scaffold. (C) Wound treated with gelatin/galectin-3 scaffold (3.3 $\mu\text{g}/\text{mL}$). (D) Wound treated with gelatin/galectin-3 scaffold (6.7 $\mu\text{g}/\text{mL}$). Collagen content appeared similar in all conditions assessed at 17 days post-wounding. Wounds subjected to each treatment condition were fully re-epithelialized by 17 days post-wounding. N=6, scale bar: 500 μm .



2.3.8 The Effect of Topical Galectin-3 and Gelatin/Galectin-3 Scaffolds on Re-Epithelialization in Wild-Type and Diabetic Mice

To determine the effect of gelatin/galectin-3 scaffolds on re-epithelialization at earlier time points, full thickness excisional wounds were created in WT and db/db mice and received one of 4 treatments: control (empty), topical galectin-3 (6.7 $\mu\text{g/mL}$), a gelatin scaffold, or a gelatin scaffold containing 6.7 $\mu\text{g/mL}$ galectin-3. In WT mice, analysis revealed that there were no significant differences in the percentage of wound closure across the four treatment groups at 5 and 7 days post-wounding (N=3, $p>0.05$) (Figure 2.17A, B). At both days 5 and 7, there were also no significant differences in the percentage of re-epithelialization (N=3, $p>0.05$) (Figure 2.17C, D) or the thickness of the epithelium (N=3, $p>0.05$) between the treatments (Figure 2.17E, F). Masson's Trichrome staining of sections from each treatment group in WT mice at day 5 and day 7 are shown in Figure 2.18.

In the db/db mice, analysis revealed that there were no significant differences in the percentage of wound closure across the four treatment groups at 5 and 7 days post wounding (N=3, $p>0.05$) (Figure 2.19A,B). At both days 5 and 7, there were no significant differences in the percentage of re-epithelialization (N=3, $p>0.05$) (Figure 2.19C, D), or the thickness of the epithelium (N=3, $p>0.05$) (Figure 2.19E, F). Masson's Trichrome staining of sections from each treatment group in db/db mice at day 5 and day 7 are shown in Figure 2.20.

Figure 2.17 – Wound closure, re-epithelialization and epithelial thickness in WT mice: Full thickness excisional wounds measuring 6 mm in diameter were treated with topical galectin-3 (6.7 $\mu\text{g}/\text{mL}$), a gelatin scaffold, a gelatin/galectin-3 scaffold (6.7 $\mu\text{g}/\text{mL}$), or left empty (control). (A, B) The percentage of closure relative to the original wound was calculated at day 5 (N=3) and day 7 (N=3). There were no significant differences in closure between each of the treatment groups at days 5 and 7. N=3, one-way ANOVA, Tukey post-test for multiple comparisons, $p>0.05$. (C, D) The percentage of re-epithelialization was calculated at day 5 (N=3) and day 7 (N=3). There were no significant differences in re-epithelialization between each of the treatment groups at days 5 and 7. N=3, one-way ANOVA, Tukey post-test for multiple comparisons, $p >0.05$. (E, F) The thickness of the epithelium was calculated at days 5 (N=3) and day 7 (N=3). There were no significant differences in the epithelial thickness between each of the treatment groups at days 5 and 7 following wounding. N=3, one-way ANOVA, Tukey post-test for multiple comparisons, $p>0.05$. All data is represented as mean \pm SEM.

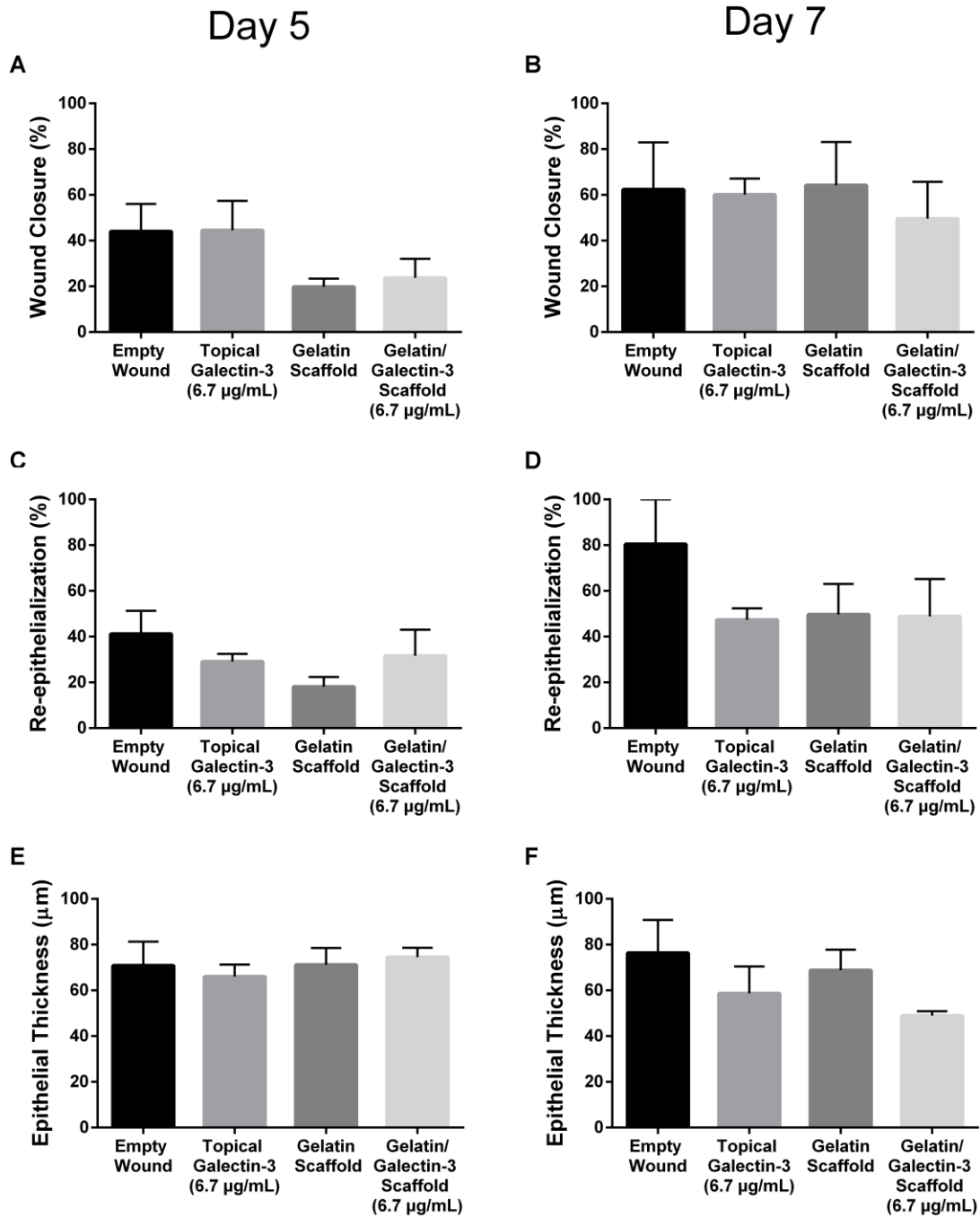


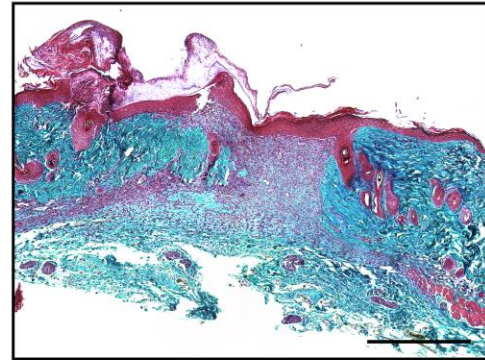
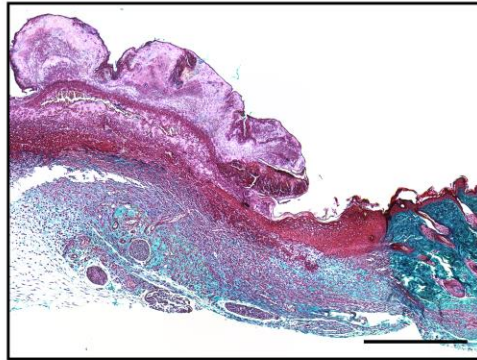
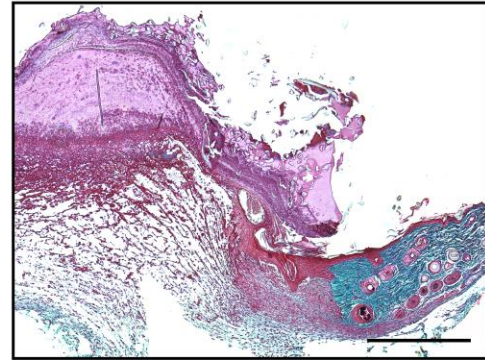
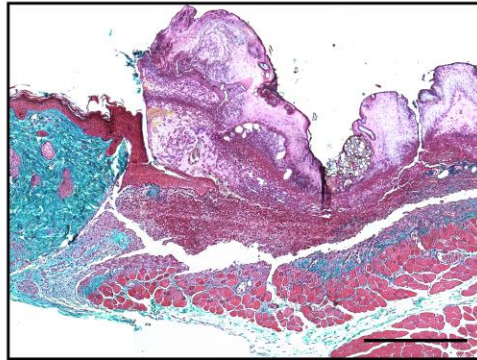
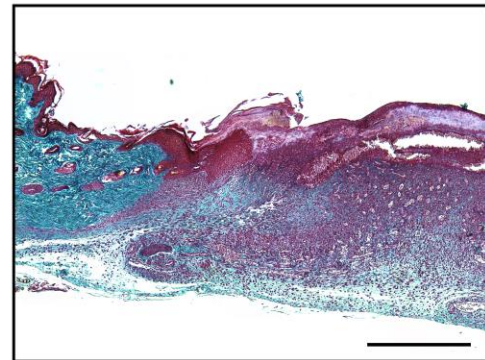
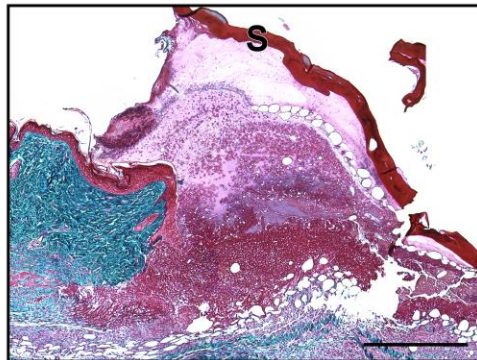
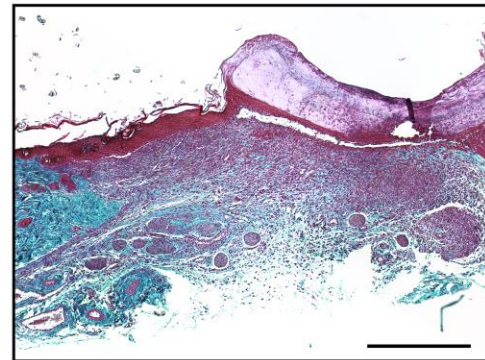
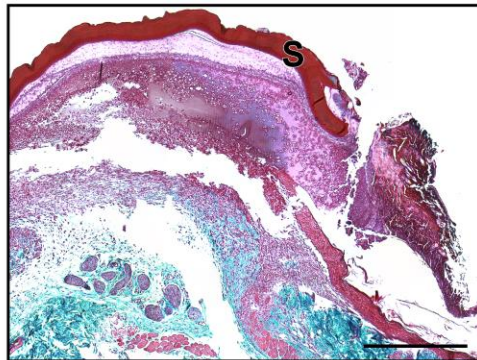
Figure 2.18 – Masson’s Trichrome staining following *in vivo* full thickness wounding in WT mice: Full thickness excisional wounds measuring 6 mm in diameter were treated with topical galectin-3 (6.7 $\mu\text{g}/\text{mL}$), a gelatin scaffold, a gelatin/galectin-3 scaffold (6.7 $\mu\text{g}/\text{mL}$), or left empty (control). Sections show the wound edge for each condition and the epithelial tongue. (A) Images shown of the four treatment conditions are from one mouse at day 5 and one mouse at day 7. (B) Images shown of the four treatment conditions are from a different mouse at day 5 and a different mouse at day 7 to show the variability between mice. S=scaffold, N=3, scale bar: 500 μm .

(A)

Day 5

Day 7

Empty

Topical Galectin-3
(6.7 $\mu\text{g/mL}$)Gelatin
ScaffoldGelatin/Galectin-3
Scaffold (6.7 $\mu\text{g/mL}$)

(B)

Day 5

Day 7

Empty

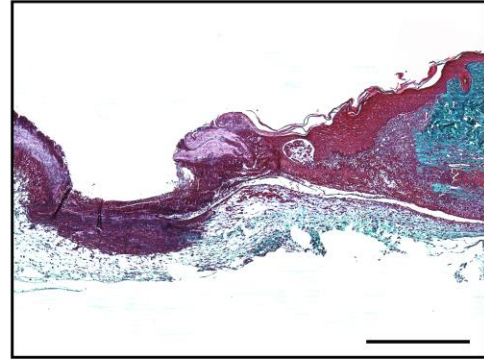
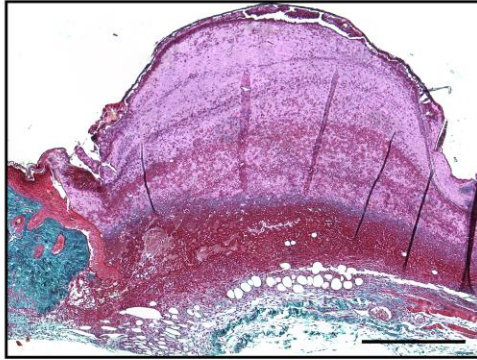
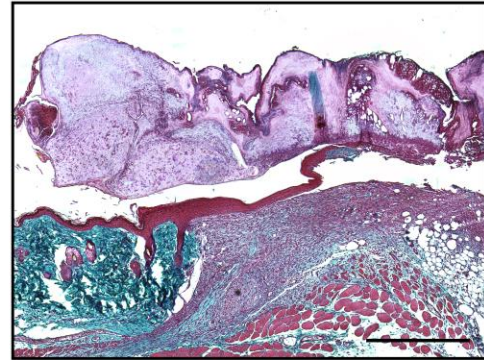
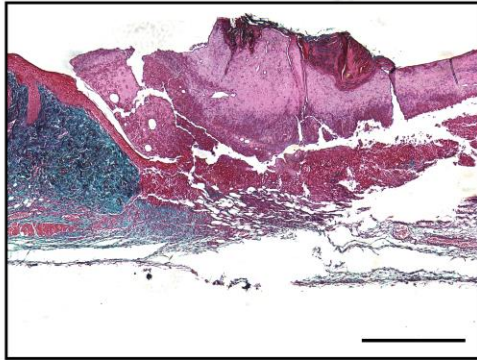
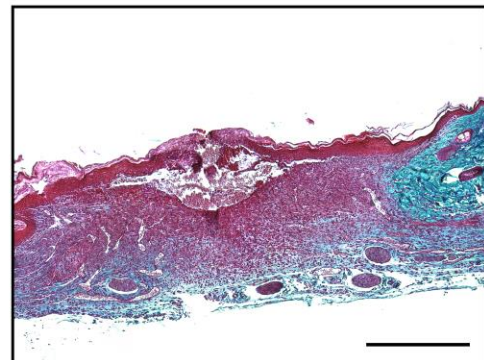
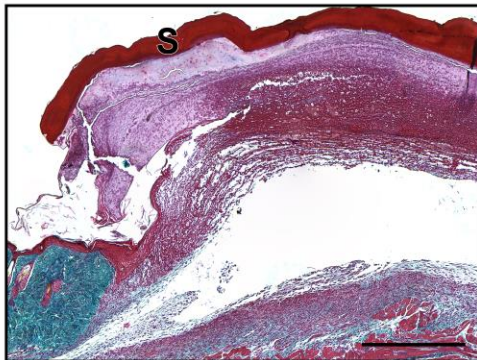
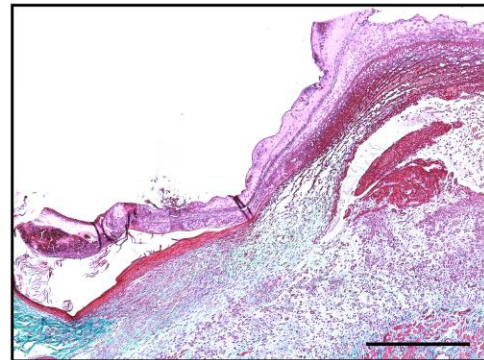
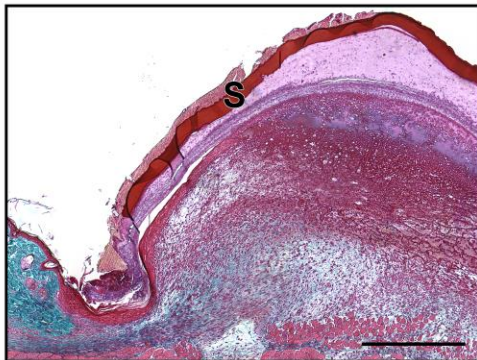
Topical Galectin-3
(6.7 $\mu\text{g/mL}$)Gelatin
ScaffoldGelatin/Galectin-3
Scaffold (6.7 $\mu\text{g/mL}$)

Figure 2.19 – Wound closure, re-epithelialization and epithelial thickness in db/db mice: Full thickness excisional wounds measuring 6 mm in diameter were treated with topical galectin-3 (6.7 $\mu\text{g}/\text{mL}$), a gelatin scaffold, a gelatin/galectin-3 scaffold (6.7 $\mu\text{g}/\text{mL}$), or left empty (control). (A,B) The percentage of closure relative to the original wound was calculated at days 5 (N=3) and day 7 (N=3). There were no significant differences in closure between each of the treatment groups at days 5 and 7. N=3, one-way ANOVA, Tukey post-test for multiple comparisons, $p>0.05$. (C, D) The percentage of re-epithelialization was calculated at days 5 (N=3) and day 7 (N=3). There were no significant differences in re-epithelialization between each of the treatment groups at days 5 and 7. N=3, one-way ANOVA, Tukey post-test for multiple comparisons, $p>0.05$. (E, F) The thickness of the epithelium was calculated at days 5 (N=3) and day 7 (N=3). There were no significant differences in the epithelial thickness between each of the treatment groups at days 5 and 7. N=3, one-way ANOVA, Tukey post-test for multiple comparisons, $p>0.05$. All data is represented as mean \pm SEM.

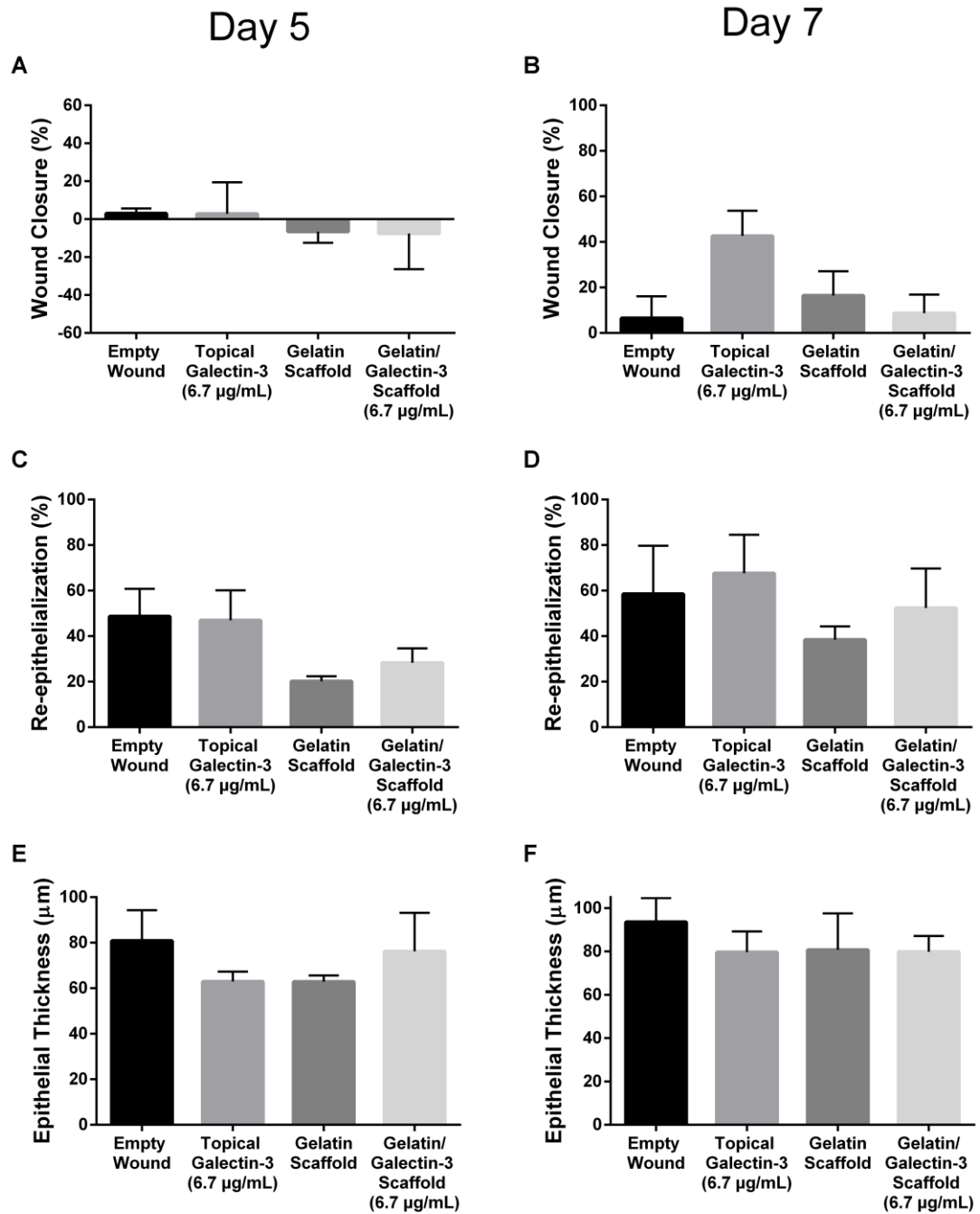


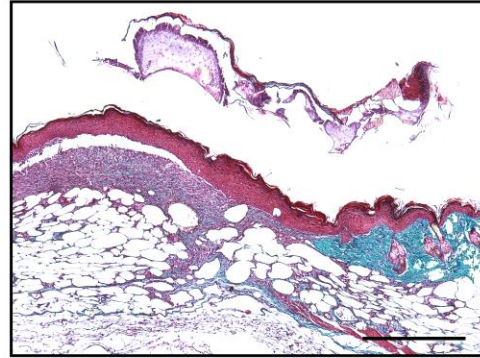
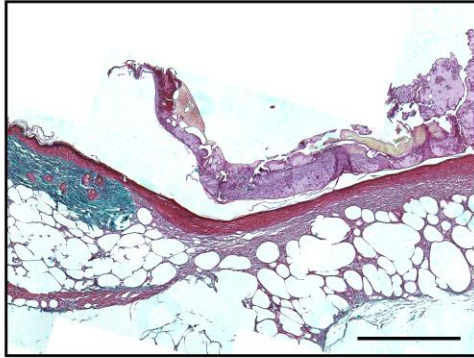
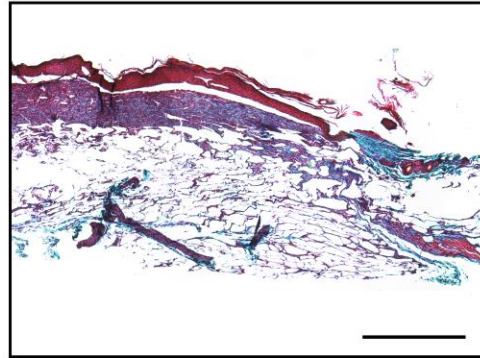
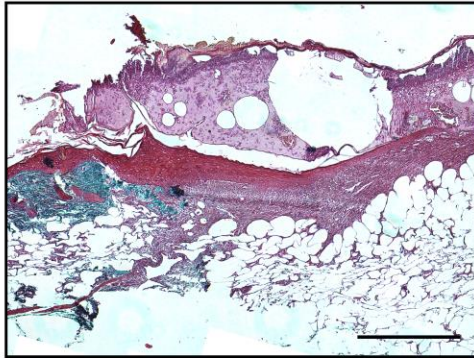
Figure 2.20 – Masson’s Trichrome staining following *in vivo* full thickness wounding in db/db mice: Full thickness excisional wounds measuring 6 mm in diameter were treated with topical galectin-3 (6.7 $\mu\text{g/mL}$), a gelatin scaffold, a gelatin/galectin-3 scaffold (6.7 $\mu\text{g/mL}$), or left empty (control). Sections show the wound edge for each condition and the epithelial tongue. (A) Images shown of the four treatment conditions are from one mouse at day 5 and one mouse at day 7. (B) Images shown of the four treatment conditions are from a different mouse at day 5 and a different mouse at day 7 to show the variability between mice. S=scaffold, N=3, scale bar: 500 μm .

(A)

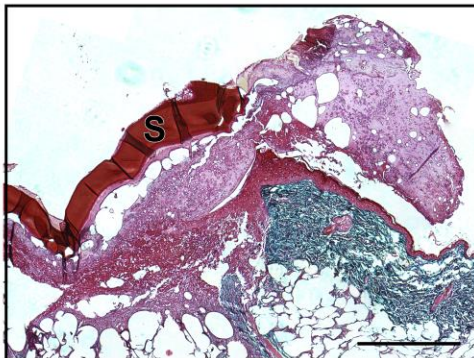
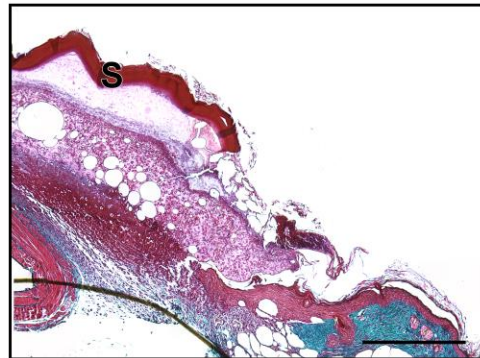
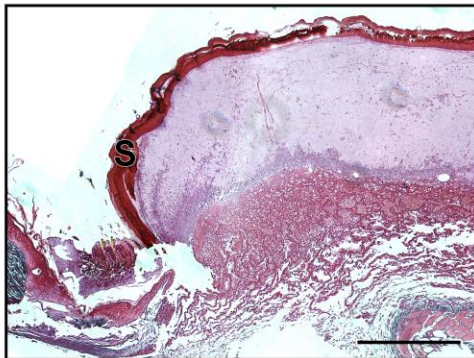
Day 5

Day 7

Empty

Topical Galectin-3
(6.7 $\mu\text{g}/\text{mL}$)

Gelatin Scaffold

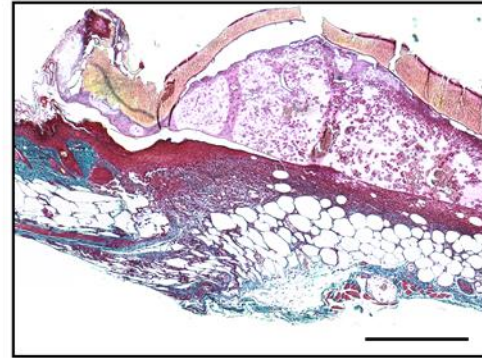
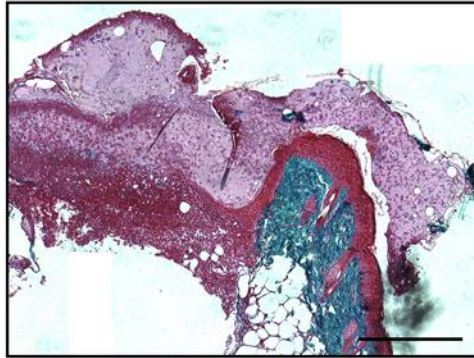
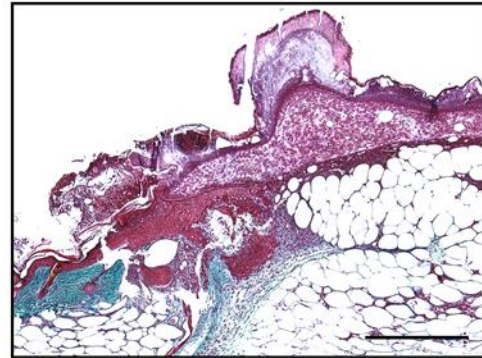
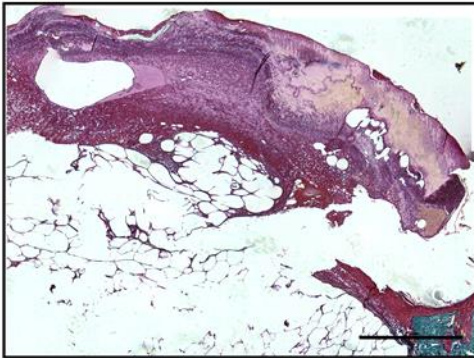
Gelatin/Galectin-3
Scaffold (6.7 $\mu\text{g}/\text{mL}$)

(B)

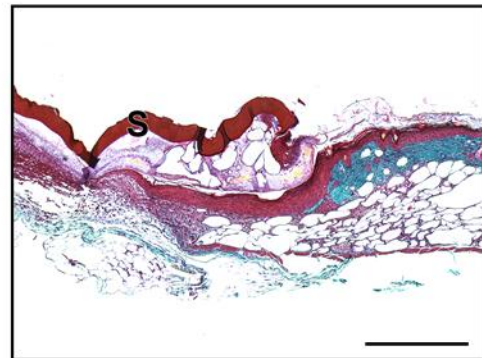
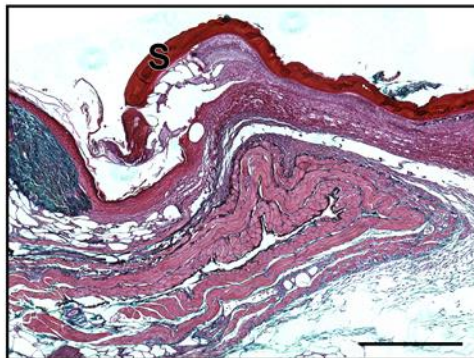
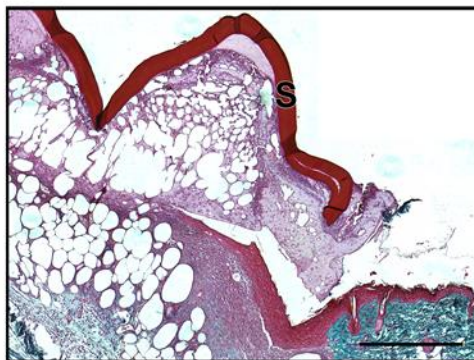
Day 5

Day 7

Empty

Topical Galectin-3
(6.7 $\mu\text{g}/\text{mL}$)

Gelatin Scaffold

Gelatin/Galectin-3
Scaffold (6.7 $\mu\text{g}/\text{mL}$)

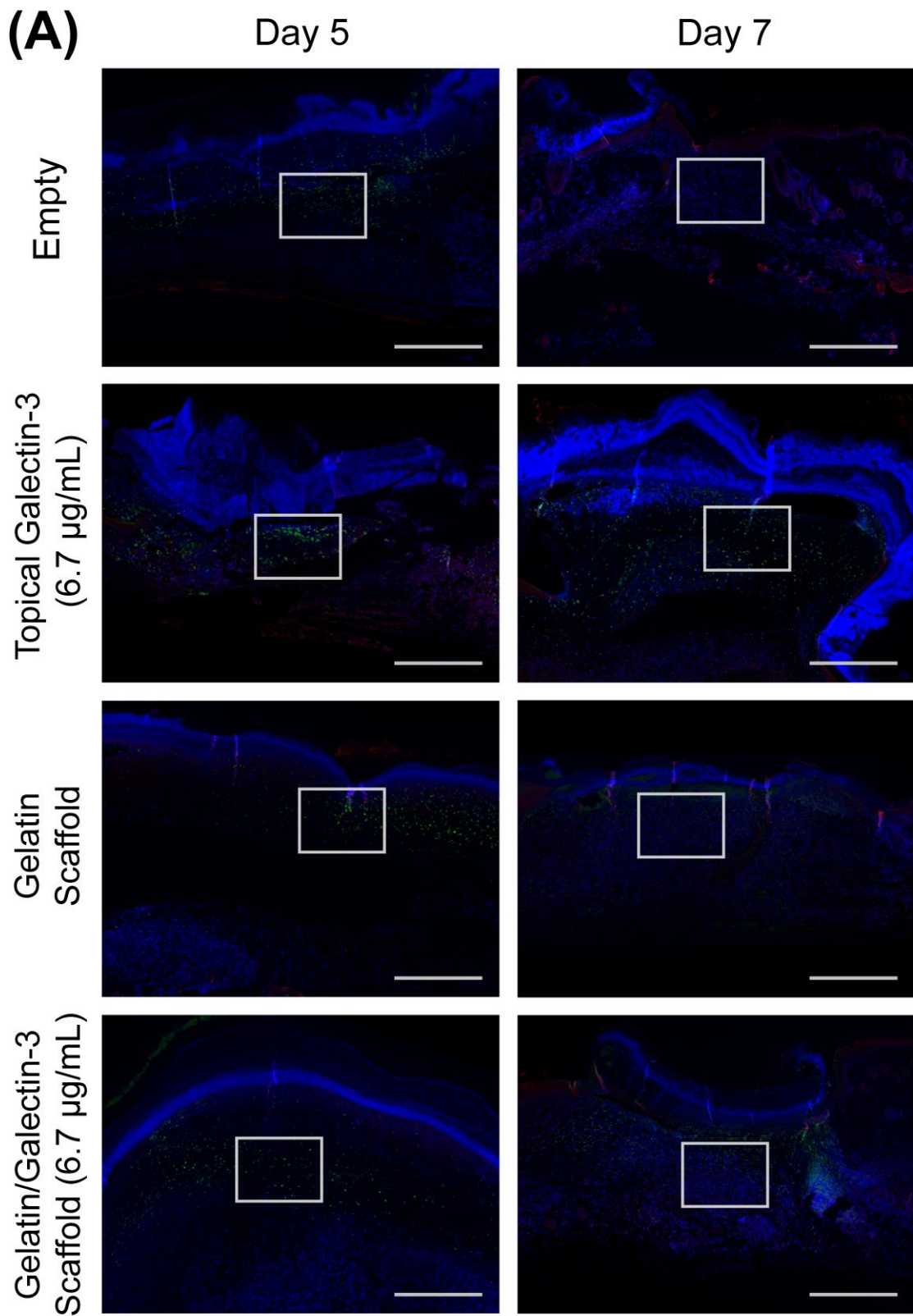
2.3.9 The Influence of Topical Galectin-3 and Gelatin/Galectin-3 Scaffolds on Macrophage Populations in WT and Diabetic Mice During Healing

To determine the effect of gelatin/galectin-3 scaffolds on re-epithelialization at earlier time points, full thickness excisional wounds were created in WT and db/db mice and received one of 4 treatments: empty (control), topical galectin-3 (6.7 $\mu\text{g/mL}$), a gelatin scaffold, or a gelatin scaffold containing 6.7 $\mu\text{g/mL}$ galectin-3.

In the WT mice, there were no observable differences in the amount of arginase I-positive macrophages across the four treatment groups at day 5 (Figure 2.21). At day 7 post-surgery, there qualitatively appeared to be more arginase I-positive macrophages in the wounds treated with topical galectin-3 (Figure 2.21). Quantification revealed that the mean density of arginase I-positive macrophages in the wounds was not statistically significant between treatment conditions at day 7 ($N=3$, $n=3$, $p>0.05$) and is shown in Figure 2.22. Differences in the number of iNOS-positive macrophages were not observed across the four treatment groups at days 5 or 7 (Figure 2.21).

In the db/db mice, there were no observable differences in the amount of arginase I-positive macrophages at days 5 and 7 following wounding (Figure 2.23). There were also no discernable differences in the amount of iNOS-positive macrophages at day 5 and day 7 post-wounding (Figure 2.23).

Figure 2.21 – Macrophage populations during *in vivo* full thickness wounding in WT mice: Full thickness excisional wounds measuring 6 mm in diameter were treated with topical galectin-3 (6.7 $\mu\text{g}/\text{mL}$), a gelatin scaffold, a gelatin/galectin-3 scaffold (6.7 $\mu\text{g}/\text{mL}$), or left empty (control). Sections show the relative amounts of arginase I-positive macrophages (green) and iNOS-positive macrophages (red) in the wound bed for each treatment condition. Cell nuclei are shown in blue. Images shown are representative of sections collected from three separate mice (N=3). (A) At day 5, there are no qualitative differences in the amount or localization of arginase I-positive macrophages and iNOS-positive macrophages. At day 7 there qualitatively appeared to be more arginase I-positive macrophages in wounds treated with topical galectin-3. At day 7 there are no discernable differences in the amount of iNOS-positive macrophages across the four treatment conditions. Scale bar: 500 μm . (B) Higher magnification images of the areas in (A) indicated by grey boxes. Scale bar: 110 μm .



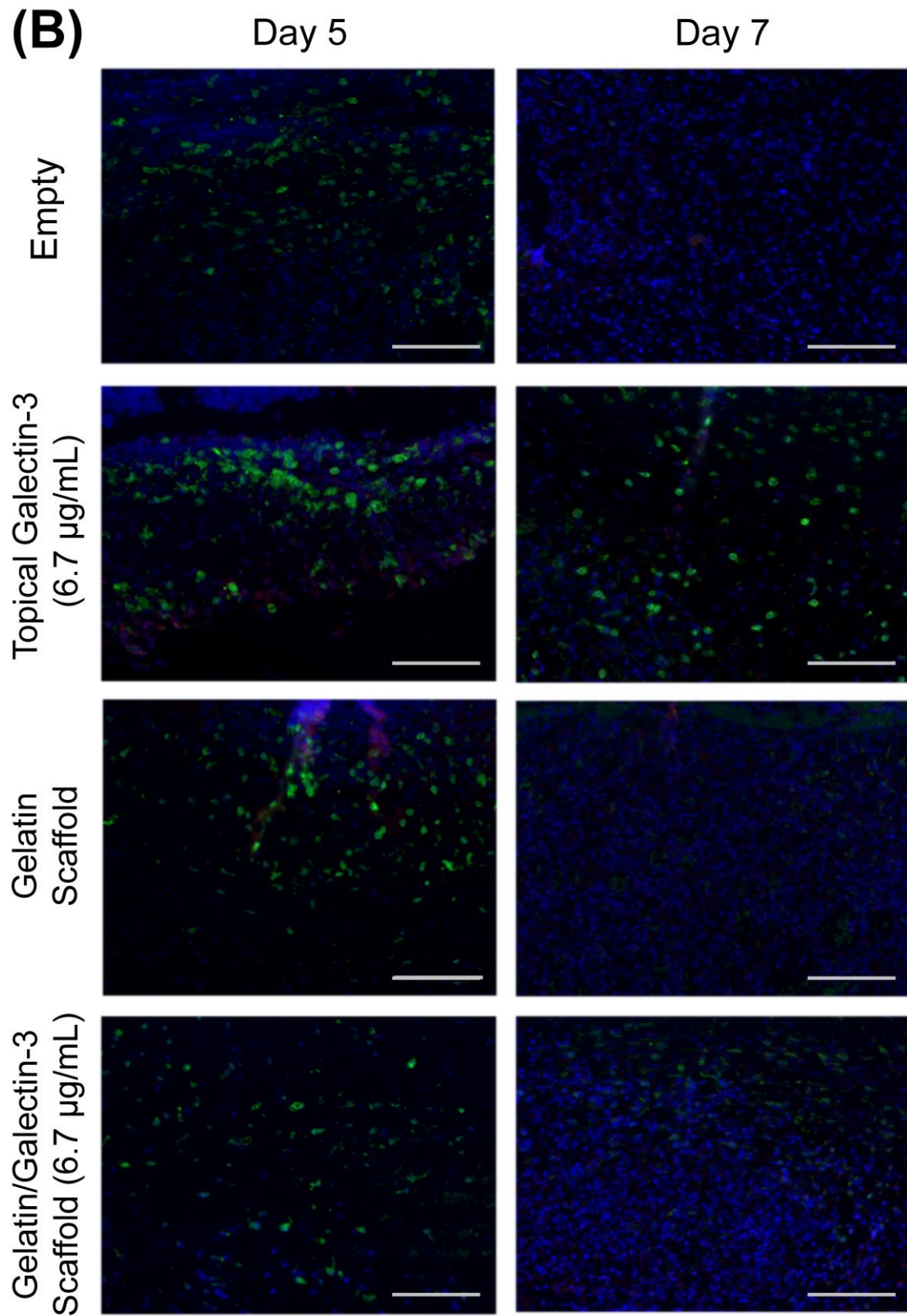


Figure 2.22 – Quantification of arginase I-positive macrophages within the wound bed of WT mice at day 7: Full thickness excisional wounds measuring 6 mm in diameter were treated with topical galectin-3 (6.7 µg/mL), a gelatin scaffold, a gelatin/galectin-3 scaffold (6.7 µg/mL), or left empty (control). The density of arginase I-positive macrophages within the wound was determined in WT mice at day 7 following wounding using three sections from each of the three mice (N=3, n=3). Although the overall density of arginase I-positive macrophages in the wounds was higher in wounds treated with topical galectin-3, the differences were not statistically significant. N=3, n=3, one-way ANOVA, Tukey post-test for multiple comparisons, $p>0.05$. All data is represented as mean \pm SD.

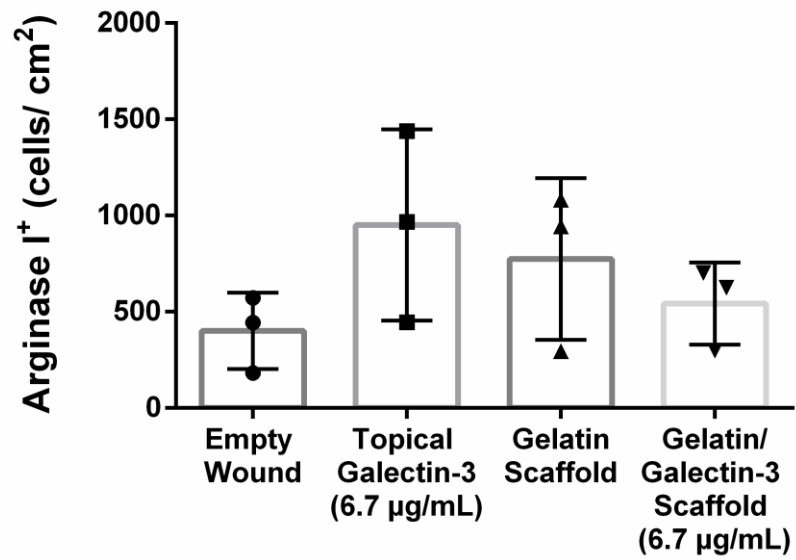
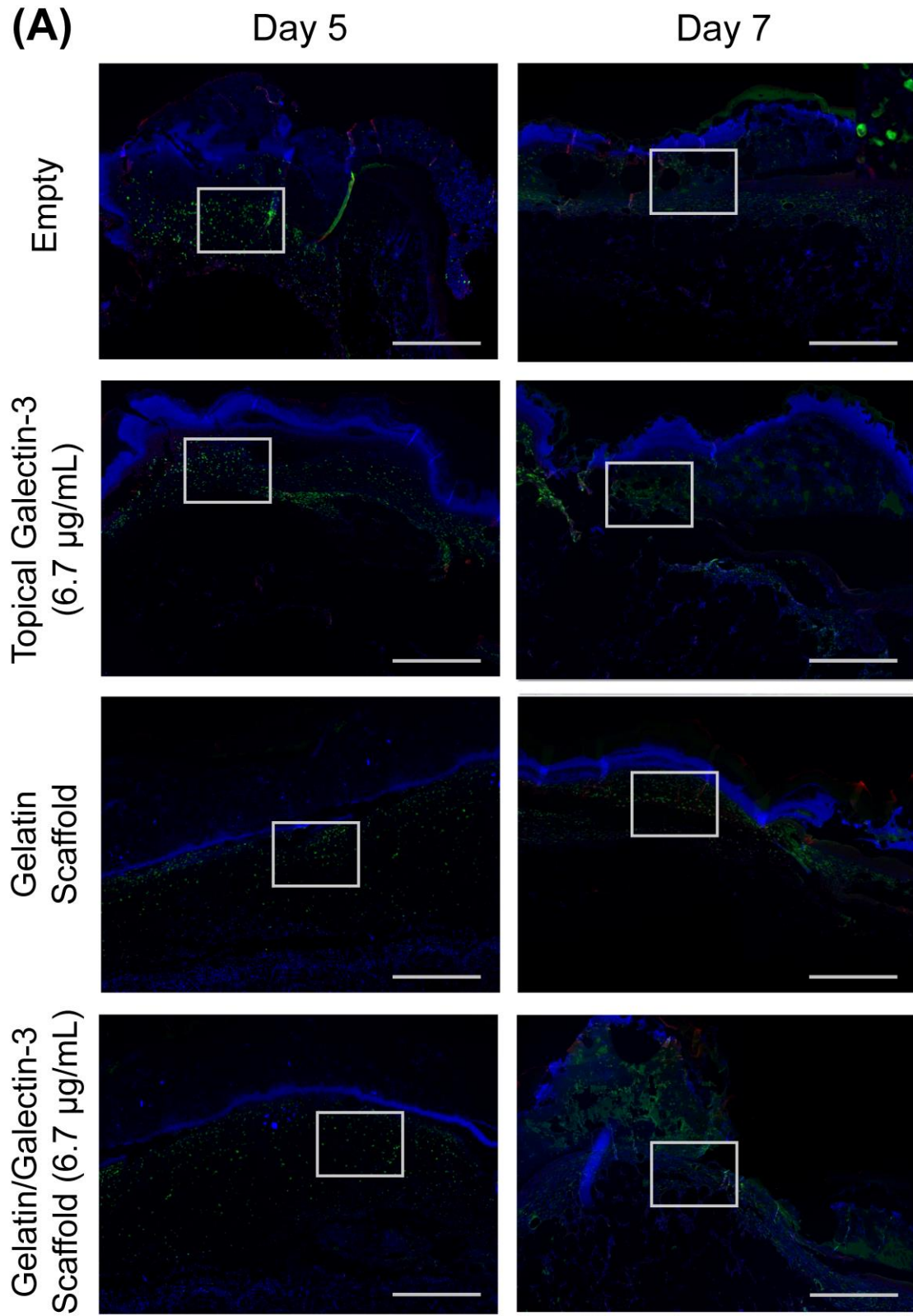
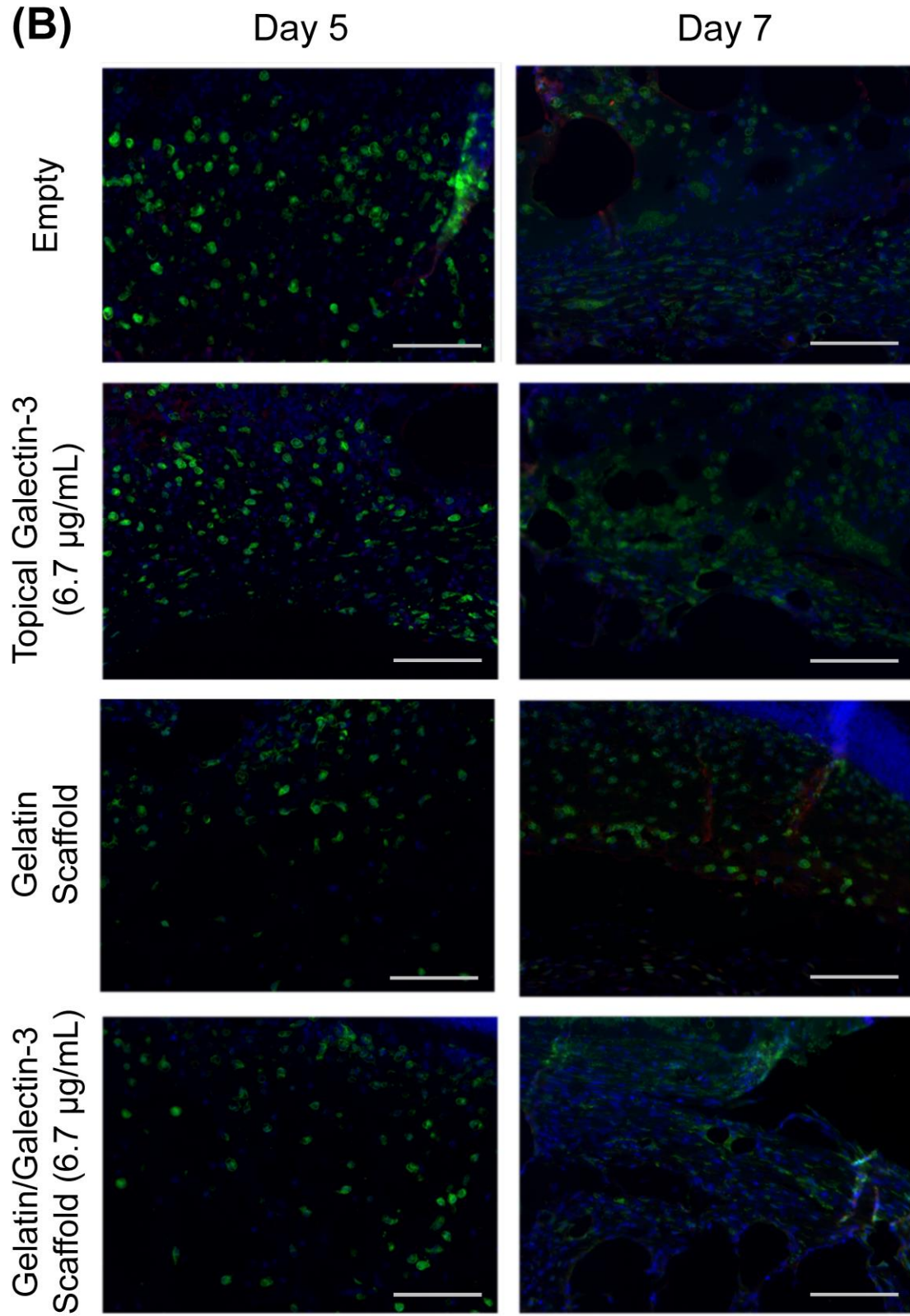


Figure 2.23 – Macrophage populations during *in vivo* full thickness wounding in db/db mice: Full thickness excisional wounds measuring 6 mm in diameter were treated with topical galectin-3 (6.7 $\mu\text{g}/\text{mL}$), a gelatin scaffold, a gelatin/galectin-3 scaffold (6.7 $\mu\text{g}/\text{mL}$), or left empty (control). Sections show the relative amounts of arginase I-positive macrophages (green) and iNOS-positive macrophages (red) in the wound bed for each treatment condition. Cell nuclei are shown in blue. Images shown are representative of sections collected from three separate mice (N=3). (A) At days 5 and 7, there are no qualitative differences in the amount or localization of arginase I-positive macrophages and iNOS-positive macrophages in the wound bed. Scale bar: 500 μm . (B) Higher magnification images of the areas in (A) indicated by grey boxes. Scale bar: 110 μm





2.4 Discussion

Chronic skin wounds are problematic as they persist in a pro-inflammatory state, unable to progress to the proliferative phase and restore the barrier function of the epithelium (13). Galectin-3 is a protein that has previously been implicated in monocyte migration (22), alternative macrophage activation (24), and increased re-epithelialization in corneal wounds (25, 40). The use of exogenous galectin-3 in treating full thickness skin wounds has yet to be explored. We hypothesized that local delivery of galectin-3 could regulate inflammation and increase re-epithelialization in skin healing, ultimately leading to wound closure. An electrospun scaffold structure was used to deliver galectin-3 as it provides a large surface area for distribution of the protein, for cell adhesion and migration, and to protect it from biodegradation (28, 41). The aim of this study was to assess the efficacy of an electrospun gelatin scaffold loaded with the matricellular protein human galectin-3 for applications in skin healing.

Type B Bovine gelatin was used as the main structural component of the scaffold. We selected gelatin as it is derived from collagen (42), which represents the primary structural protein of the dermal extracellular matrix (43). Thus, gelatin provides some chemical similarity to the extracellular matrix while reducing cost of scaffold fabrication (44). In this thesis, electrospinning was used as the fiber fabrication method. While many studies have used collagen as the structural unit in electrospinning, its use is controversial as previous reports have demonstrated that collagen loses its tertiary structure following electrospinning and fibers generated are typically similar to gelatin in structure (45). Gelatin has previously been electrospun by several groups, with results showing good biocompatibility of the generated scaffolds, including a study demonstrating increased wound closure in a full thickness wound healing model in rats (34-37). Electrospun gelatin scaffolds, both alone and in combination with other polymers, have also been used with success for the delivery of growth factors and bioactive compounds (46-48). Furthermore, the biodegradability of gelatin can be tuned to facilitate protein delivery using glutaraldehyde crosslinking, in which aldehyde groups from glutaraldehyde react with lysine or hydroxylysine residues to form aldimine linkages (-C=N-) (49, 50). Subsequent quenching of the scaffolds in 0.1M glycine is used to block unreacted

aldehyde groups (51). Electrospinning of Type B Bovine gelatin was performed using 40% v/v acetic acid as a solvent. Use of 40% v/v acetic acid has previously been used for the electrospinning of collagen, demonstrating bead free fibers in the 100-200 nm range along with several other concentrations of this solvent (52, 53). Electrospinning with acetic acid is advantageous as it avoids the use of fluoroalcohols, which are highly cytotoxic and can cause the loss of tertiary structure and changes in the secondary structure of proteins (54).

The first objective of the thesis was to refine scaffold manufacturing protocols, specifically to determine electrospinning parameters that would provide bead-free and ribbon-free fibers with diameters measuring within the range of the native extracellular matrix (ECM). The polymer solution flowrate, distance between the needle tip and collector (collector distance), and the concentration of the polymer have all previously been reported to influence the resulting electrospun fiber diameter and morphology (43, 55, 56). Therefore, to identify an appropriate combination of these parameters, three concentrations of gelatin, three flowrates, and three collector distances were tested by electrospinning at each set of parameters listed in Table 1.

Changing the flowrate was not found to significantly influence the resulting mean fiber diameter. As a result, a flowrate of 0.5 mL/h was selected for subsequent electrospinning as using a higher flowrate decreases the amount of time required for electrospinning and decreasing time over which the protein is exposed to the solvent. Similarly, changing the collector distance did not influence the resulting mean fiber diameter. A collector distance of 10 cm was selected for subsequent electrospinning as this resulted in a wider distribution of fibers on the rotating mandrel, creating a larger scaffold surface area, without depositing fibers outside of the mandrel.

Consistent with other studies, increasing the concentration of gelatin resulted in an increase in the fiber diameter (37, 51, 57). Although differences in fiber diameter resulting from 20% weight and 25% weight gelatin were not considered significant, the frequency distribution plot highlighted that when 20% weight gelatin is used, more fibers fall within the 100-200 nm range, and there is a narrower distribution of fiber diameters

at this concentration, making it more reflective of the native tissue ECM which has fiber diameters within the range of 30-130 nm (44). However, use of 20% weight gelatin produced detectable amounts of beaded fibers, which are thought to negatively impact cellular interactions with scaffolds (58). Additionally, ribbon-like fibers, which do not reflect the morphology of collagen fibrils in the native tissue, were detected at both 25% weight and 30% weight gelatin. Therefore, additional experiments were conducted to determine whether increasing the gelatin concentration to 21% weight would eliminate the fibrous beads, while retaining a small fiber diameter. As expected, the resulting scaffolds were free of beaded fibers and did not exhibit ribbon-like fibers. Although the fiber diameter was increased, the frequency distribution of the fibers showed that the fiber sizes remained within range of collagen fibril sizes found in human tissues (33).

In the fabrication of electrospun scaffolds, a high porosity is preferable to support cell ingrowth and to facilitate the diffusion of waste and nutrients (59). The porosity obtained in the refined scaffolds fell within the range of porosities shown in scaffolds electrospun using a variety of polymers and electrospinning parameters, ranging from approximately 60-90% (34, 60, 61). The pore size distribution was also comparable to those seen for electrospun gelatin (34, 60). Although the obtained porosity is reasonable, obtaining a porosity of 90% has been suggested to be ideal (59). The electrospun scaffolds in this study had a low average pore diameter (pore size) of 1.15 μm . Having more pores in the 50-100 μm range would have also been preferable to coincide with the size of the cells on the scaffold and support their infiltration. In fact, scaffolds having pore sizes of approximately 100 μm and porosity in the 90% range have been shown to support the infiltration of cells from the surface of the scaffold (62). However, it is difficult to obtain scaffolds having both pore sizes in this range and fiber sizes in the 100 nm range as decreasing fiber size is associated with decreasing pore sizes (63). To overcome this problem, several groups have employed strategies whereby substances including salt, or simultaneously-electrospun secondary polymers (sacrificial fibers) are deposited within the mat during the electrospinning process and are later removed. This process has resulted in increased scaffold infiltration by cells (64, 65).

Recombinant human galectin-3 was added to the electrospinning solution during scaffold fabrication to achieve a final concentration of 6.7 $\mu\text{g/mL}$. This concentration was chosen as it fell within the range used by other groups to achieve effects *in vitro*. For example, in studies in skin, concentrations as low as 1 $\mu\text{g/mL}$ have been used to increase keratinocyte migration speed (27) and galectin-3 has previously been shown to have a concentration dependent effect on monocyte recruitment from 0.001-0.01 μM (66). Additionally, the use of 6.3 $\mu\text{g/mL}$ promotes human keratinocyte migration, while use of higher concentrations (50 $\mu\text{g/mL}$) can inhibit migration *in vitro* (67). Detection of galectin-3 protein sequences from scaffold samples confirmed that the blend electrospinning method could generate scaffolds with galectin-3 dispersed throughout the fibers. The sequences identified are located within the protein's CRD, which is important as this domain is required for many of the proteins functions (23-25, 68). Identification of galectin-3 was expected, as several groups have previously used the blend electrospinning method for the delivery of matricellular proteins and growth factors (31, 46-48).

During healing, the granulation tissue is essential in guiding cells into the wound by supporting their adhesion and migration (1). Therefore, in order to appropriately mimic the extracellular matrix, it is imperative that the scaffolds support the adhesion and proliferation of cells (43). The ability of cells to adhere and proliferate on the scaffolds was therefore used as a measure of biocompatibility. Dermal fibroblasts were used for the study as they interact with and remodel the granulation tissue during healing (1, 14). The initial adhesion of human dermal fibroblasts was improved relative to the tissue culture plastic in both gelatin and gelatin/galectin-3 scaffolds. This improved adhesion in both the gelatin and gelatin/galectin-3 scaffolds likely results from the arginine-glycine-aspartate (RGD) sequences contained within gelatin, which promote cell adhesion through integrin binding (69, 70). The improved adhesion in both scaffolds can also be attributed in part to the increased surface area that the scaffolds offer for attachment, further promoting cell matrix interactions (32). Over a two-week period, the proliferation profile of human dermal fibroblasts on the gelatin and gelatin/galectin-3 scaffolds was consistent with that of the tissue culture plastic controls. This finding confirms that both the gelatin and gelatin/galectin-3 scaffolds are non-toxic and can support cell growth, eliminating concern regarding the use of glutaraldehyde as a crosslinking agent. Our

findings are consistent with other groups who have shown consistent proliferation of human dermal fibroblasts between gelatin scaffolds and tissue culture plastic controls (35, 37). Proliferation on scaffolds that is consistent with culture on tissue culture plastic is an important finding, as scaffolds made from other materials, including chitosan and polycaprolactone, have demonstrated reduced rates of proliferation (35, 71).

Surface topography can influence cell responses including adhesion, migration and differentiation (72). When cultured on gelatin and gelatin/galectin-3 scaffolds, human dermal fibroblasts exhibited a spindle-like morphology and showed alignment of their actin filaments. This positive interaction between dermal fibroblasts and gelatin scaffolds has also been noted by other groups, who have shown cell spreading and alignment on gelatin scaffolds (34, 35, 37). Ensuring that fibroblasts portray a spindle-like morphology is significant, as cell spreading is important for cell viability in adherent cell types (73). A rounded morphology in fibroblasts is associated with cell detachment (74), which would have implied cytotoxicity of the scaffolds (75). Both gelatin and gelatin/galectin-3 scaffolds also supported the deposition of fibronectin by fibroblasts, indicating dermal fibroblasts are able to synthesize extracellular matrix while cultured on the scaffolds. Fibronectin deposition by fibroblasts is important during wound healing, as it mediates cell adhesion and migration, stimulates collagen deposition, and contributes to wound contraction (76).

Based on the evidence suggesting that the scaffolds were biocompatible *in vitro*, the influence of the scaffolds on wound closure kinetics in mouse models of normal and impaired wound healing were investigated. The use of gelatin scaffolds with and without the addition of a low and high concentration of galectin-3 did not significantly alter the wound closure kinetics in both WT and db/db mice over the 17-day period. At day 17 the appearance of cells were consistent with fibroblasts and collagen production in the wounds suggest that use of scaffolds did not result in a foreign body response (77). The addition of topical galectin-3 also did not increase closure at day 5 or 7, but this does not eliminate the possibility of changes early in the inflammatory phase which do not manifest in measurable closure changes. Although treating wounds with topical galectin-3 and scaffolds containing galectin-3 did not significantly increase wound closure

kinetics, this is supported by the finding that wound closure kinetics are not impaired in galectin-3 knockout mice, which also show no differences in immune cell infiltration, angiogenesis, or fibrotic response (26). Interestingly, use of gelatin scaffolds alone has previously been reported to increase wound closure in a full thickness skin model in rats, which is in contrast to our findings (34). However, several factors could have contributed to the differences in the results obtained by Dubsky et al., including their use of rats as an animal model rather than mice, the difference in size of the initial wounds, and their use of Tegaderm™ to cover the wounds throughout the study. Dubsky et al. also covered control wounds with wetted gauze and the scaffolds were placed over the wound rather than being tucked under the surrounding tissue (34).

During wound healing, keratinocyte proliferation and migration is stimulated by growth factors including epidermal growth factor (EGF) (14), resulting in their migration over the dermis to restore the epithelial barrier (1). Studies of dermal healing have demonstrated that galectin-3 knockout mice exhibit impaired re-epithelialization, which manifests in decreased length of the epithelial tongue, and therefore decreased re-epithelialization at days 2 (27) and 7 (26) post-wounding. This deficient re-epithelialization was attributed to a migratory defect in keratinocytes caused by aberrant EGFR endocytosis and recycling, which cytosolic galectin-3 was shown to mediate through binding to ALIX (27). When recombinant human galectin-3 was added to wounds of WT mice topically or using a gelatin scaffold, differences in epithelial thickness were not quantified at days 5 or 7 post wounding. Similarly, differences were not observed in db/db mice at these time points. This result was consistent with previous reports showing no defect in epithelial thickness in galectin-3 knockout mice (26, 27). Differences in re-epithelialization were also not observed in both WT and db/db mice at day 5 and 7 following wounding which was consistent with the finding that exogenous galectin-3 was not effective in correcting the defective EGFR endocytosis and recycling in galectin-3 knockout mice (27, 50). In contrast, studies of corneal healing have shown that exogenous human recombinant galectin-3 can increase re-epithelialization in WT mice (25) and in monkey corneal explants (40). However, this increase was suggested to be attributed to the modulation of galectin-7 by exogenous galectin-3, as galectin-7 was found to accelerate re-epithelialization in galectin-3 knockout mice and mouse embryonic

fibroblasts from galectin-3 knockout mice showed reduced levels of galectin-7 (25). Studies in skin, which show that gene expression of galectin-7 is not altered at day 7 following wounding in WT mice, imply that the mechanism suggested to account for increased re-epithelialization in the cornea might not apply to the skin (26). This discrepancy highlights the issue of the context-specific roles of matricellular proteins (78).

In wound healing, inflammation follows hemostasis, a process during which monocytes are recruited to the wound by chemoattractants and differentiate into macrophages (2). Macrophages are vital constituents of the wound healing process, mediating wound healing through the release of regulatory molecules which is based on their phenotype (79). Classically activated (M1) macrophages produce nitric oxide and secrete pro-inflammatory cytokines including TNF- α , IL-1, IL-6, and IL-12, while alternatively activated macrophages (M2) are implicated in tissue remodeling and secrete TGF- β (80). Galectin-3 has previously been implicated in macrophage function (23, 24, 66); therefore macrophage populations in WT and db/db mice were investigated after treatment with topical galectin-3 and gelatin/galectin-3 scaffolds in order to discern whether exogenous human recombinant galectin-3 could increase the number of M2 polarized macrophages. Macrophage populations appeared unchanged following treatments in db/db mice at both time points. In WT mice, differences were not observed at day 5. At day 7, there qualitatively appeared to be more M2 macrophages in wounds treated with topical galectin-3, although quantification showed no significant differences in M2 macrophage density across the four treatment groups. This result was unexpected as Mackinnon et al. reported that bone marrow derived macrophages (BMDMs) from galectin-3 knockout mice show a defect in IL-4 and IL-13 M2 macrophage polarization *in vivo* and *in vitro* (24). In addition they showed that IL-4 and IL-13 can stimulate galectin-3 upregulation and release in BMDMs (24). Of note, this study did not test the addition of exogenous galectin-3, therefore there is currently no indication as to whether its use would be sufficient in rescuing the deficient M2 polarization of BMDMs in galectin-3 knockout mice. It is also possible that the effect of exogenously added human recombinant galectin-3 occurs at earlier time points as the number of galectin-3-positive cells peak at one day following wounding in WT mice (78). Or perhaps, exogenous galectin-3 alone is

not sufficient in upregulating the expression of surface bound galectin-3, the secretion of galectin-3 or upregulating CD98 which are each implicated in the suggested autocrine loop that controls M2 activation (24). As human and murine galectin-3 share only 80% homology (81), another possibility is that the differences in homology of these species contribute to the lack of functionality of exogenous galectin-3 in this feedback loop.

2.5 Conclusion

In summary, blend electrospun gelatin/galectin-3 scaffolds have been developed which show biocompatibility when tested both *in vitro* and *in vivo*. Using human dermal fibroblasts, scaffolds increased initial cell adhesion, supported their proliferation over a 14 day period and supported their production of the extracellular matrix protein fibronectin. *In vivo*, use of the scaffolds in excisional wounds in WT and db/db mice did not delay healing or result in a foreign body response at day 17. Use of topical galectin-3 and gelatin/galectin-3 scaffolds did not affect wound closure, epithelial thickness, or re-epithelialization in WT and db/db mice, or influence the amount of M1 or M2 macrophages in WT and db/db mice. Future work should explore the exact pathological contexts in which galectin-3 can modulate inflammation.

2.6 References

1. Gurtner GC, Werner S, Barrandon Y, Longaker MT. Wound repair and regeneration. *Nature*. 2008;453(7193):314-21.
2. Singer AJ, Clark RA. Cutaneous wound healing. *The New England journal of medicine*. 1999;341(10):738-46.
3. Morton LM, Phillips TJ. Wound healing and treating wounds: Differential diagnosis and evaluation of chronic wounds. *Journal of the American Academy of Dermatology*. 2016;74(4):589-605; quiz -6.
4. Fonder MA, Lazarus GS, Cowan DA, Aronson-Cook B, Kohli AR, Mamelak AJ. Treating the chronic wound: A practical approach to the care of nonhealing wounds and wound care dressings. *Journal of the American Academy of Dermatology*. 2008;58(2):185-206.
5. Zhao R, Liang H, Clarke E, Jackson C, Xue M. Inflammation in Chronic Wounds. *International journal of molecular sciences*. 2016;17(12).
6. Canadian Association of Wound Care. Statistics 2017 [Available from: <http://cawc.net/index.php/public/facts-stats-and-tools/statistics/>].
7. Skorkowska-Telichowska K, Czemplik M, Kulma A, Szopa J. The local treatment and available dressings designed for chronic wounds. *Journal of the American Academy of Dermatology*. 2013;68(4):e117-26.
8. Powers JG, Higham C, Broussard K, Phillips TJ. Wound healing and treating wounds: Chronic wound care and management. *Journal of the American Academy of Dermatology*. 2016;74(4):607-25; quiz 25-6.
9. Greaves NS, Iqbal SA, Baguneid M, Bayat A. The role of skin substitutes in the management of chronic cutaneous wounds. *Wound repair and regeneration : official publication of the Wound Healing Society [and] the European Tissue Repair Society*. 2013;21(2):194-210.
10. Snyder DL, Sullivan N, Schoelles KM. AHRQ Technology Assessments. *Skin Substitutes for Treating Chronic Wounds*. Rockville (MD): Agency for Healthcare Research and Quality (US); 2012.
11. Alavi A, Sibbald RG, Mayer D, Goodman L, Botros M, Armstrong DG, et al. Diabetic foot ulcers: Part II. Management. *Journal of the American Academy of Dermatology*. 2014;70(1):21.e1-.e4.
12. Marston W, Tang J, Kirsner RS, Ennis W. Wound Healing Society 2015 update on guidelines for venous ulcers. *Wound repair and regeneration : official publication of the Wound Healing Society [and] the European Tissue Repair Society*. 2016;24(1):136-44.

13. Brem H, Tomic-Canic M. Cellular and molecular basis of wound healing in diabetes. *The Journal of clinical investigation*. 2007;117(5):1219-22.
14. Barrientos S, Stojadinovic O, Golinko MS, Brem H, Tomic-Canic M. Growth factors and cytokines in wound healing. *Wound repair and regeneration : official publication of the Wound Healing Society [and] the European Tissue Repair Society*. 2008;16(5):585-601.
15. Blakytyn R, Jude E. The molecular biology of chronic wounds and delayed healing in diabetes. *Diabetic medicine : a journal of the British Diabetic Association*. 2006;23(6):594-608.
16. Wlaschek M, Scharffetter-Kochanek K. Oxidative stress in chronic venous leg ulcers. *Wound repair and regeneration : official publication of the Wound Healing Society [and] the European Tissue Repair Society*. 2005;13(5):452-61.
17. Peppas M, Stavroulakis P, Raptis SA. Advanced glycoxidation products and impaired diabetic wound healing. *Wound repair and regeneration : official publication of the Wound Healing Society [and] the European Tissue Repair Society*. 2009;17(4):461-72.
18. Singh VP, Bali A, Singh N, Jaggi AS. Advanced glycation end products and diabetic complications. *Korean J Physiol Pharmacol*. 2014;18(1):1-14.
19. Domic J, Dabelic S, Flogel M. Galectin-3: an open-ended story. *Biochimica et biophysica acta*. 2006;1760(4):616-35.
20. Barondes SH. Galectins: A family of b-Galactoside-Binding Lectins. *Cell*. 1994;76:597-8.
21. Cherayil BJ, Chaitovitz S, Wong C, Pillai S. Molecular cloning of a human macrophage lectin specific for galactose. *Proceedings of the National Academy of Sciences of the United States of America*. 1990;87(18):7324-8.
22. Sano H, Hsu DK, Yu L, Apgar JR, Kuwabara I, Yamanaka T, et al. Human galectin-3 is a novel chemoattractant for monocytes and macrophages. *Journal of immunology*. 2000;165(4):2156-64.
23. Karlsson A, Christenson K, Matlak M, Bjorstad A, Brown KL, Telemo E, et al. Galectin-3 functions as an opsonin and enhances the macrophage clearance of apoptotic neutrophils. *Glycobiology*. 2009;19(1):16-20.
24. MacKinnon AC, Farnworth SL, Hodkinson PS, Henderson NC, Atkinson KM, Leffler H, et al. Regulation of alternative macrophage activation by galectin-3. *Journal of immunology*. 2008;180(4):2650-8.

25. Cao Z, Said N, Amin S, Wu HK, Bruce A, Garate M, et al. Galectins-3 and -7, but not galectin-1, play a role in re-epithelialization of wounds. *The Journal of biological chemistry*. 2002;277(44):42299-305.
26. Walker JT, Elliott CG, Forbes TL, Hamilton DW. Genetic Deletion of Galectin-3 Does Not Impair Full-Thickness Excisional Skin Healing. *J Invest Dermatol*. 2016.
27. Liu W, Hsu DK, Chen HY, Yang RY, Carraway KL, 3rd, Isseroff RR, et al. Galectin-3 regulates intracellular trafficking of EGFR through Alix and promotes keratinocyte migration. *J Invest Dermatol*. 2012;132(12):2828-37.
28. Moura LI, Dias AM, Suesca E, Casadiegos S, Leal EC, Fontanilla MR, et al. Neurotensin-loaded collagen dressings reduce inflammation and improve wound healing in diabetic mice. *Biochimica et biophysica acta*. 2014;1842(1):32-43.
29. Bertonecelj V, Pelipenko J, Kristl J, Jeras M, Cukjati M, Kocbek P. Development and bioevaluation of nanofibers with blood-derived growth factors for dermal wound healing. *European journal of pharmaceutics and biopharmaceutics : official journal of Arbeitsgemeinschaft fur Pharmazeutische Verfahrenstechnik eV*. 2014;88(1):64-74.
30. Peh P, Lim NS, Blocki A, Chee SM, Park HC, Liao S, et al. Simultaneous Delivery of Highly Diverse Bioactive Compounds from Blend Electrospun Fibers for Skin Wound Healing. *Bioconjugate chemistry*. 2015;26(7):1348-58.
31. Elliott CG, Wang J, Guo X, Xu SW, Eastwood M, Guan J, et al. Periostin modulates myofibroblast differentiation during full-thickness cutaneous wound repair. *Journal of cell science*. 2012;125(Pt 1):121-32.
32. Zhong SP, Zhang YZ, Lim CT. Tissue scaffolds for skin wound healing and dermal reconstruction. *Wiley Interdiscip Rev Nanomed Nanobiotechnol*. 2010;2(5):510-25.
33. Xie J, Li X, Xia Y. Putting Electrospun Nanofibers to Work for Biomedical Research. *Macromolecular rapid communications*. 2008;29(22):1775-92.
34. Dubsky M, Kubinova S, Sirc J, Voska L, Zajicek R, Zajicova A, et al. Nanofibers prepared by needleless electrospinning technology as scaffolds for wound healing. *Journal of materials science Materials in medicine*. 2012;23(4):931-41.
35. Gomes SR, Rodrigues G, Martins GG, Roberto MA, Mafra M, Henriques CM, et al. In vitro and in vivo evaluation of electrospun nanofibers of PCL, chitosan and gelatin: a comparative study. *Materials science & engineering C, Materials for biological applications*. 2015;46:348-58.
36. Powell HM, Boyce ST. Fiber density of electrospun gelatin scaffolds regulates morphogenesis of dermal-epidermal skin substitutes. *Journal of biomedical materials research Part A*. 2008;84(4):1078-86.

37. Zha Z, Teng W, Markle V, Dai Z, Wu X. Fabrication of gelatin nanofibrous scaffolds using ethanol/phosphate buffer saline as a benign solvent. *Biopolymers*. 2012;97(12):1026-36.
38. Moffa EB, Machado MA, Mussi MC, Xiao Y, Garrido SS, Giampaolo ET, et al. In Vitro Identification of Histatin 5 Salivary Complexes. *PloS one*. 2015;10(11):e0142517.
39. Schneider CA, Rasband WS, Eliceiri KW. NIH Image to ImageJ: 25 years of image analysis. *Nature Methods*. 2012;9(7):671-5.
40. Fujii A, Shearer TR, Azuma M. Galectin-3 enhances extracellular matrix associations and wound healing in monkey corneal epithelium. *Exp Eye Res*. 2015;137:71-8.
41. Ji W, Sun Y, Yang F, van den Beucken JJ, Fan M, Chen Z, et al. Bioactive electrospun scaffolds delivering growth factors and genes for tissue engineering applications. *Pharmaceutical research*. 2011;28(6):1259-72.
42. Malafaya PB, Silva GA, Reis RL. Natural-origin polymers as carriers and scaffolds for biomolecules and cell delivery in tissue engineering applications. *Adv Drug Deliv Rev*. 2007;59(4-5):207-33.
43. Murugan R, Ramakrishna S. Design strategies of tissue engineering scaffolds with controlled fiber orientation. *Tissue engineering*. 2007;13(8):1845-66.
44. Kim HN, Jiao A, Hwang NS, Kim MS, Kang do H, Kim DH, et al. Nanotopography-guided tissue engineering and regenerative medicine. *Adv Drug Deliv Rev*. 2013;65(4):536-58.
45. Zeugolis DI, Khew ST, Yew ES, Ekaputra AK, Tong YW, Yung LY, et al. Electro-spinning of pure collagen nano-fibres - just an expensive way to make gelatin? *Biomaterials*. 2008;29(15):2293-305.
46. Montero RB, Vazquez-Padron RI, Pham SM, D'Ippolito G, Andreopoulos FM. Electrospun Gelatin Constructs with Tunable Fiber Orientation Promote Directed Angiogenesis. *Open Journal of Regenerative Medicine*. 2014;03(01):1-12.
47. Han F, Jia X, Dai D, Yang X, Zhao J, Zhao Y, et al. Performance of a multilayered small-diameter vascular scaffold dual-loaded with VEGF and PDGF. *Biomaterials*. 2013;34(30):7302-13.
48. Shan YH, Peng LH, Liu X, Chen X, Xiong J, Gao JQ. Silk fibroin/gelatin electrospun nanofibrous dressing functionalized with astragaloside IV induces healing and anti-scar effects on burn wound. *International journal of pharmaceutics*. 2015;479(2):291-301.

49. Damink LO, Dijkstra P, Van Luyn M, Van Wachem P, Nieuwenhuis P, Feijen J. Glutaraldehyde as a crosslinking agent for collagen-based biomaterials. *Journal of materials science: materials in medicine*. 1995;6(8):460-72.
50. Akin H, Hasirci N. Preparation and characterization of crosslinked gelatin microspheres. *Journal of Applied Polymer Science*. 1995;58(1):95-100.
51. Montero RB, Vial X, Nguyen DT, Farhand S, Reardon M, Pham SM, et al. bFGF-containing electrospun gelatin scaffolds with controlled nano-architectural features for directed angiogenesis. *Acta biomaterialia*. 2012;8(5):1778-91.
52. Liu T, Teng WK, Chan BP, Chew SY. Photochemical crosslinked electrospun collagen nanofibers: synthesis, characterization and neural stem cell interactions. *Journal of biomedical materials research Part A*. 2010;95(1):276-82.
53. Erencia M, Cano F, Tornero JA, Macanas J, Carrillo F. Resolving the electrospinnability zones and diameter prediction for the electrospinning of the gelatin/water/acetic acid system. *Langmuir : the ACS journal of surfaces and colloids*. 2014;30(24):7198-205.
54. Gast K, Siemer A, Zirwer D, Damaschun G. Fluoroalcohol-induced structural changes of proteins: some aspects of cosolvent-protein interactions. *Eur Biophys J*. 2001;30(4):273-83.
55. Pezeshki-Modaress M, Mirzadeh H, Zandi M. Gelatin-GAG electrospun nanofibrous scaffold for skin tissue engineering: Fabrication and modeling of process parameters. *Materials science & engineering C, Materials for biological applications*. 2015;48:704-12.
56. Subbiah T, Bhat GS, Tock RW, Parameswaran S, Ramkumar SS. Electrospinning of nanofibers. *Journal of Applied Polymer Science*. 2005;96(2):557-69.
57. Song JH, Kim HE, Kim HW. Production of electrospun gelatin nanofiber by water-based co-solvent approach. *Journal of materials science Materials in medicine*. 2008;19(1):95-102.
58. Tsing P. *Electrospinning natural polymers for tissue engineering applications*: University of Pennsylvania; 2007.
59. Karande TS, Ong JL, Agrawal CM. Diffusion in musculoskeletal tissue engineering scaffolds: design issues related to porosity, permeability, architecture, and nutrient mixing. *Ann Biomed Eng*. 2004;32(12):1728-43.
60. Rho KS, Jeong L, Lee G, Seo BM, Park YJ, Hong SD, et al. Electrospinning of collagen nanofibers: effects on the behavior of normal human keratinocytes and early-stage wound healing. *Biomaterials*. 2006;27(8):1452-61.

61. Li WJ, Laurencin CT, Caterson EJ, Tuan RS, Ko FK. Electrospun nanofibrous structure: a novel scaffold for tissue engineering. *J Biomed Mater Res.* 2002;60(4):613-21.
62. Zhu XL, Cui WG, Li XH, Jin Y. Electrospun fibrous mats with high porosity as potential scaffolds for skin tissue engineering. *Biomacromolecules.* 2008;9(7):1795-801.
63. Eichhorn SJ, Sampson WW. Statistical geometry of pores and statistics of porous nanofibrous assemblies. *J R Soc Interface.* 2005;2(4):309-18.
64. Nam J, Huang Y, Agarwal S, Lannutti J. Improved cellular infiltration in electrospun fiber via engineered porosity. *Tissue engineering.* 2007;13(9):2249-57.
65. Skotak M, Ragusa J, Gonzalez D, Subramanian A. Improved cellular infiltration into nanofibrous electrospun cross-linked gelatin scaffolds templated with micrometer-sized polyethylene glycol fibers. *Biomed Mater.* 2011;6(5):055012.
66. Danella Polli C, Alves Toledo K, Franco LH, Sammartino Mariano V, de Oliveira LL, Soares Bernardes E, et al. Monocyte Migration Driven by Galectin-3 Occurs through Distinct Mechanisms Involving Selective Interactions with the Extracellular Matrix. *ISRN Inflamm.* 2013;2013:259256.
67. Kariya Y, Kawamura C, Tabei T, Gu J. Bisecting GlcNAc residues on laminin-332 down-regulate galectin-3-dependent keratinocyte motility. *The Journal of biological chemistry.* 2010;285(5):3330-40.
68. Saravanan C, Liu FT, Gipson IK, Panjwani N. Galectin-3 promotes lamellipodia formation in epithelial cells by interacting with complex N-glycans on alpha3beta1 integrin. *Journal of cell science.* 2009;122(Pt 20):3684-93.
69. Ruoslahti E. RGD and other recognition sequences for integrins. *Annu Rev Cell Dev Biol.* 1996;12:697-715.
70. Grover CN, Gwynne JH, Pugh N, Hamaia S, Farndale RW, Best SM, et al. Crosslinking and composition influence the surface properties, mechanical stiffness and cell reactivity of collagen-based films. *Acta biomaterialia.* 2012;8(8):3080-90.
71. Gautam S, Dinda AK, Mishra NC. Fabrication and characterization of PCL/gelatin composite nanofibrous scaffold for tissue engineering applications by electrospinning method. *Materials science & engineering C, Materials for biological applications.* 2013;33(3):1228-35.
72. Kim D-H, Provenzano PP, Smith CL, Levchenko A. Matrix nanotopography as a regulator of cell function. *The Journal of Cell Biology.* 2012;197(3):351-60.
73. Bashur CA, Dahlgren LA, Goldstein AS. Effect of fiber diameter and orientation on fibroblast morphology and proliferation on electrospun poly(D,L-lactic-co-glycolic acid) meshes. *Biomaterials.* 2006;27(33):5681-8.

74. Rosen JJ, Culp LA. Morphology and cellular origins of substrate-attached material from mouse fibroblasts. *Experimental cell research*. 1977;107(1):139-49.
75. Wang MO, Etheridge JM, Thompson JA, Vorwald CE, Dean D, Fisher JP. Evaluation of the in vitro cytotoxicity of cross-linked biomaterials. *Biomacromolecules*. 2013;14(5):1321-9.
76. Lensenlink EA. Role of fibronectin in normal wound healing. *Int Wound J*. 2015;12(3):313-6.
77. Anderson JM, Rodriguez A, Chang DT. Foreign body reaction to biomaterials. *Semin Immunol*. 2008;20(2):86-100.
78. Hamilton D, Walker J, Kim S, Michelsons S, Creber K, Elliott C, et al. Cell-matrix interactions governing skin repair: matricellular proteins as diverse modulators of cell function. *Research and Reports in Biochemistry*. 2015:73.
79. Brancato SK, Albina JE. Wound macrophages as key regulators of repair: origin, phenotype, and function. *The American journal of pathology*. 2011;178(1):19-25.
80. Rodero MP, Khosrotehrani K. Skin wound healing modulation by macrophages. *International journal of clinical and experimental pathology*. 2010;3(7):643-53.
81. Haudek KC, Spronk KJ, Voss PG, Patterson RJ, Wang JL, Arnoys EJ. Dynamics of galectin-3 in the nucleus and cytoplasm. *Biochimica et biophysica acta*. 2010;1800(2):181-9.

Chapter 3

3 General Discussion

3.1 Summary and Final Conclusions

Objective 1: To develop a scaffold for the delivery of exogenous galectin-3

Electrospinning parameters that influence fiber formation were investigated, demonstrating that altering the flowrate and collector distance did not significantly change the resulting electrospun fiber diameters. The largest variable identified was the concentration of gelatin in the polymer solution used for electrospinning: at 20% weight gelatin, the fiber diameters were smaller, with some fibers showing beads; while at higher concentrations, fiber diameters increased significantly and displayed a ribbon-like structure. By electrospinning using a polymer solution with 21% weight gelatin, a flowrate of 0.5 ml/h and a collector distance of 10 cm, the resulting fibers had diameters within the range of extracellular matrix fibers found in dermis. Scaffolds exhibited a high porosity, but the average pore diameter was approximately 1 μ m, which is not conducive to cell infiltration. Detection of four sequences from the human galectin-3 carbohydrate recognition domain were identified using mass spectroscopy from within a crosslinked gelatin/galectin-3 scaffold validating that galectin-3 was incorporated into the gelatin scaffolds using the blend electrospinning method.

Objective 2: To evaluate the biocompatibility of the gelatin/galectin-3 scaffolds *in vitro* using human dermal fibroblasts

Gelatin and gelatin/galectin-3 scaffolds were shown to increase the adhesion of human dermal fibroblasts 1 hour after seeding compared to tissue culture plastic, as well as supporting their proliferation over a two-week period. Human dermal fibroblasts also spread and elongated on the scaffold fibers, and secreted fibronectin while cultured on both the gelatin and gelatin/galectin-3 scaffolds. These findings demonstrated that the scaffolds were biocompatible *in vitro*, with no cytotoxic response evident in the cells.

Objective 3: To evaluate the effect of the gelatin/galectin-3 scaffold on wound healing in murine models

- a. Assess the influence of the scaffold on wound closure kinetics

Treatment of wounds with gelatin and gelatin/galectin-3 scaffolds did not alter wound closure kinetics in either wild type (WT) or diabetic (db/db) mice. Collagen production and the appearance of cells consistent with fibroblasts in the tissue of db/db mice showed that use of the scaffolds did not result in a foreign body response at 17 days.

- b. Compare and contrast the efficacy of local delivery of topical galectin-3 versus gelatin/galectin-3 electrospun scaffolds on re-epithelialization and macrophage polarization during skin healing.

Treatment of wounds with either topical galectin-3 or gelatin/galectin-3 scaffolds caused no measureable effect on processes associated with re-epithelialization in WT and db/db mice at the time points assessed. No significant differences were observed qualitatively in the numbers of M1 or M2 macrophages in db/db mice at either time point, or in WT mice at day 5 following wounding. At day 7, qualitative assessment suggested that more arginase I-positive macrophages were present in wounds treated with topical galectin-3. Although quantification revealed that the density of arginase I-positive macrophages was higher in these wounds, the results were not significant. Taken together, these findings suggest that exogenous galectin-3 is not sufficient for stimulating re-epithelialization in skin. However, the role of topical galectin-3 as a therapeutic for M2 macrophage polarization requires future investigation.

3.2 Contributions to the Current State of Knowledge

3.2.1 Galectin-3 as a Modulator of Re-epithelialization

Galectin-3 is a matricellular protein that has been implicated in processes associated with both the inflammatory and proliferative phases of healing. Studies using experimentally-created defects in the cornea and skin of knockout mice have identified defects in re-epithelialization in the absence of galectin-3, in comparison with the same process in WT

mice (1-3). Re-epithelialization is an essential process during skin healing, restoring barrier function (4). Cao et al. have shown that when applied to knockout mice, human recombinant galectin-3 was able to increase re-epithelialization in WT but not knockout mice, which was attributed to its effect on the upregulation of galectin-7, a protein shown to increase re-epithelialization in both phenotypes (1). In contrast to this research, we report here that local delivery of galectin-3 to both WT and db/db mice, does not increase re-epithelialization. Although the concentration used in our study (6.7 μ g/mL) was lower than the concentration used in the cornea (10 and 20 μ g/mL), it was consistent with the concentration of 6.3 μ g/mL previously used to stimulate keratinocyte migration *in vitro* through laminin 322 binding (5) and with Liu et al., who also showed a pro-migratory effect when human recombinant galectin-3 was added at 1 μ g/mL to keratinocytes from WT mice *in vitro* (2). Our findings, together with the finding that defective epidermal growth factor receptor endocytosis (which is controlled via cytosolic galectin-3 rather than secreted galectin-3) is the mechanism responsible for impaired re-epithelialization in galectin-3 knockout mice in skin (2), suggest that galectin-3 may not be effective in promoting re-epithelialization in a recombinant form or when delivered into the extracellular microenvironment.

3.2.2 Galectin-3 as a Modulator of Inflammatory Processes

With respect to inflammation, galectin-3 typically shows a higher gene and protein expression in M2 polarized macrophages (6). It has also been shown to be a chemoattractant for monocytes and macrophages (7), and increases the infiltration of tumors by M2 macrophages in mice (8). These findings, together with its reported role in regulating M2 macrophage polarization (9), suggested that it could represent a legitimate therapeutic for mediating inflammation during skin healing *in vivo*. The findings of this thesis do not support a definite connection between the use of exogenous recombinant human galectin-3 in dermal wounds *in vivo* with an associated change in the amount of M2 macrophages at days 5 and 7 following wounding. Similar infiltration of M2 macrophages in the dermal wounds left empty, treated with topical galectin-3, or treated with gelatin/galectin-3 scaffolds during healing is consistent with previous studies from our laboratory showing that compared to WT mice, galectin-3 knockout mice do not

exhibit differences in the abundance of M1 or M2 macrophages during the inflammatory phase of healing (3). This is not the first discrepancy in the literature pertaining to the role of galectin-3 during inflammation as the finding by Mackinnon et.al that exposure of bone marrow derived macrophages to 100 ng/mL lipopolysaccharides (LPS) suppressed the expression and secretion of galectin-3 (9) was in contrast to the finding by Novak et al. who reported that treatment of human blood-monocyte derived macrophages exposed to 100 ng/mL LPS and 20 ng/mL interferon gamma showed a significant increase in galectin-3 expression (6). This discrepancy demonstrates the issue of the context-specific roles of the protein (10). Another key issue, in elucidating the role of galectin-3 on macrophage polarization, is that its characterization *in vitro* may not necessarily translate *in vivo* as factors contributing to polarization *in vivo*, including cell maturation, matrix composition and chemoattractants, are often overlooked (11).

The results of this thesis suggest that in a recombinant form delivered extracellularly, there is a lack of evidence to support galectin-3 in increasing re-epithelialization or modulating inflammation and that galectin-3 in a recombinant form may not be an effective therapeutic for treating chronic skin wounds. However, in order to completely dismiss the protein as a therapeutic for this application, further work needs to be performed to elucidate the exact pathological contexts in which galectin-3 can modulate inflammation.

3.2.3 Models of Impaired Healing and Galectin-3

Some groups have suggested that galectin-3 signaling can be either pro-inflammatory or anti-inflammatory and depends on the pathophysiological state of the microenvironment (12). Considering this hypothesis, it is conceivable that in a chronic wound environment in humans, where bacterial colonization can easily occur (13) and where levels of pro-inflammatory cytokines and reactive oxygen species are exacerbated (14), that the delivery of the exogenous galectin-3 would exhibit a modulatory effect on the state of inflammation. However, no animal model can accurately mimic the microenvironment within a human chronic skin wound, such that the complexity and heterogeneity of these wounds can be fully recapitulated (15). This issue is due in part to the multiple factors that can contribute to the development of a chronic wound, including infection,

malnutrition, hyperglycemia, and vascular insufficiencies, which are not reflected together in animal models (13). Rather, most animal models in mice are monogenic models of obesity and diabetes, limiting their clinical translation to humans (16). The variability between patients in the cell populations and proteins that are present in the wound bed also make translation from animal models difficult (17). As a result, many therapeutic targets, including several growth factors, have shown promise for improving healing in animal models, but lack efficacy or fail completely in clinical trials (18, 19). One such growth factor is vascular endothelial growth factor (VEGF). Pre-clinical studies showed that when applied topically, VEGF can accelerate healing in db/db mice (20), yet a phase I trial in chronic neuropathic diabetic foot ulcers found no significant differences between the reduction in total ulcer surface area in wounds treated with topical VEGF relative to placebo-treated wounds after 29, 43, and 84 days (21). The study also failed to meet its primary exploratory endpoint of reduced total ulcer surface area at 43 days (21). Furthermore, recent clinical studies on platelet derived growth factor, which is the only growth factor currently approved by the Food and Drug Administration (22), show that it does not significantly improve healing in diabetic foot ulcers relative to those treated with an offloading cast, casting doubt on its efficacy (23).

3.2.4 The Efficacy of Matricellular Proteins as Therapeutics

Matricellular proteins are non-structural components of the extracellular matrix that are normally not expressed in adult tissue, but become upregulated during wound healing and pathological processes. Matricellular proteins exhibit tightly regulated expression patterns, acting spatially and temporally to control specific cell behaviours, making them ideal candidates as therapeutics in wound healing (24). The topical application of matricellular proteins has been previously investigated in wound healing in mice *in vivo*. The topical application of exogenous cysteine-rich angiogenic inducer 61 (CCN1) was able to reverse the profibrotic phenotype of CCN1 knockin mice that expressed a senescence-defective CCN1 mutant, increasing expression of matrix metalloproteinases (MMPs) and decreasing expression of transforming growth factor beta (TGF- β) (25). Another matricellular protein, angiopoietin-like 4, significantly accelerated wound closure relative to saline when applied topically to full thickness excisional splint wounds

in ob/ob mice (26). Similarly, the subcutaneous injection of recombinant human galectin-1 in wounds of WT and streptozotocin-induced diabetic mice also led to accelerated closure (27). Our laboratory has shown that scaffolds can also be used to deliver matricellular proteins, resulting in effects beneficial to the wound healing process. Delivery of periostin via an electrospun collagen scaffold was able to recover alpha smooth muscle actin expression in periostin knockout mice (28). Additionally, the delivery of periostin and connective tissue growth factor (CCN2), alone or in combination, using an electrospun collagen scaffold significantly accelerated closure in full thickness excisional wounds in db/db mice relative to empty controls (Hamilton Laboratory, unpublished data). In our study, we show that delivery of exogenous galectin-3 either topically, or using an electrospun gelatin scaffold, has shown the lowest efficacy *in vivo* for improving and accelerating the repair of full thickness excisional skin wounds.

3.2.5 Galectin-3 Bioactivity

An important consideration in assessing the lack of efficacy of both topical and scaffold delivery of galectin-3 is the bioactivity of the protein. Post-translational modifications can have significant impacts on the biological function of a protein (29). Galectin-3 is known to undergo several types of post-translational modifications including cleavage, phosphorylation, and acetylation, each having implications on the protein's function (30). For example, galectin-3 can undergo cleavage at multiple sites, including at alanine⁶²-tyrosine⁶³ by MMPs 2, 7, 9, and, 13, that results in two distinct peptides and inhibits processes requiring N-terminal self-association of the protein (30). The protein can also be phosphorylated at tyrosine⁷⁹, tyrosine¹⁰⁷, and tyrosine¹¹⁸ by c-Abl (31), and by casein kinase I at serine⁶ (32). Phosphorylation can regulate its binding to ligands, its cellular distribution, and its apoptotic activity (30). Additionally, in galectin-3 isolated from rat lung, alanine² can be acetylated (33). Therefore, the activity of galectin-3 is dependent on many extrinsic microenvironmental factors and it is conceivable that although the protein in its recombinant form is able to agglutinate red blood cells (as provided by the manufacturer) (34), it may not contain the post translational modifications required for its function in triggering M2 macrophage polarization. Other matricellular proteins also

exhibit post-translational modification-dependent effects. For example, osteopontin has multiple isoforms with differing degrees of phosphorylation that depend on the cell type from which it is produced. As a result, the effects of the interaction of this protein with cell receptors change depending on its phosphorylation state (35). Therefore, future work should focus on determining the exact contexts in which recombinant human galectin-3 can influence macrophage function.

3.3 Future Directions

3.3.1 Improving Scaffold Pore Size

In addition to a high porosity, large pore sizes are important to ensure the infiltration of the scaffolds by cells (36, 37). Co-electrospinning with sacrificial fibers that can be later removed in solution is one way to increase the pore area within electrospun scaffolds (38). Co-electrospinning of gelatin scaffolds with micrometer sized polyethylene glycol fibers has previously been conducted to increase the pore size of scaffolds from 1 μm to 10-100 μm whereby polyethylene is removed using tert-butanol following crosslinking (39). For our purposes, poly ethylene oxide (PEO) would be a good candidate as it is highly soluble in water, which would allow removal following gelatin crosslinking (38). Klumpp et al. used this method for the electrospinning of a polycaprolactone/collagen blended scaffold with PEO as their sacrificial fiber. Following soaking in water, they were able to create a scaffold with dense pockets and open sites for cell infiltration (40). *In vivo* they were able to show complete infiltration of their scaffolds after 4 weeks in a model of vascularization in rats (40). Using this method to improve porosity in the electrospun scaffolds could promote cell infiltration of our scaffolds *in vivo* during excisional healing.

3.3.2 Establishing Galectin-3 Bioactivity *In Vitro* and *In Vivo*

One of the findings from this thesis relates to the bioactivity of the recombinant human galectin-3 protein used in this study. The bioactivity of the protein was quantified by R&D systems based on its ability to agglutinate red blood cells. A paper by Hadari et al. is referenced, which stated that galectin-3 bioactivity was measured in this manner using rabbit erythrocytes (34). Other groups have reported testing galectin-3 bioactivity by

treating a Jurkat acute T-cell leukemia cell line with 15 μM of the protein for 6 hours and measuring cell viability (6), as the protein has previously been shown to induce apoptosis in these cells (41). Our study showed a lack of efficacy of recombinant human galectin-3 when added to wounds either topically or in combination with a gelatin scaffold. Assessing whether the protein had low bioactivity is further compounded by the findings from our laboratory that show galectin-3 knockout mice do not display an impairment in closure of full thickness excisional wounds (3). Moreover, it is now known that galectin-3 contains several sites through which activity can be modified by post translational modifications, which may be required in order to generate the desired activities associated with the protein (30). Therefore, it appears that a well-developed assay for detection of recombinant human galectin-3 bioactivity is lacking. As a result, future work should be conducted to quantify whether the protein used in the study has bioactivity pertaining to macrophage function. As Mackinnon et al. have shown that bone marrow derived macrophages from galectin-3 knockout mice exhibit reduced arginase I activity from interleukin 4 (IL-4) and IL-13 activation, evaluating the influence of the protein on macrophage polarization *in vitro* using the human monocytic cell line THP-1 might be an appropriate area of investigation (9). It would be valuable to identify whether treatment with exogenous recombinant human galectin-3 can upregulate M2 macrophage markers, including TGF- β and the mannose receptor (MR) (42) in monocytes as well as M1 and M2 macrophages. This study would elucidate whether the protein can induce a switch in phenotype from M1 to M2 macrophages and if the protein can guide monocytic differentiation towards an M2 phenotype. Testing of various concentrations would also be appropriate as galectin-3 exhibits concentration dependent effects *in vitro* and would provide a better measure for translation to *in vivo* studies (7, 43). Once the bioactivity can be reproducibly established *in vitro*, investigation of its role *in vivo* via topical delivery in comparison to untreated wounds could again be explored using a larger number of animals to increase the power of the study. Furthermore, elucidating the role of galectin-3 at earlier time points during healing would be interesting, as the number of galectin-3-positive cells peak at one day following wounding in WT mice (10).

3.4 Limitations

3.4.1 Animal Model

Chronic skin wound development is extremely complex and multifactorial, with infection, aging, malnutrition and systemic conditions including hyperglycemia and vascular insufficiency each contributing to the exacerbation of inflammation (13). In addition, these wounds exhibit heterogeneity across patients (13). As a result, no animal model exists that can fully recapitulate the multifactorial nature and complexity of human chronic wounds (15). The animal model selected in this study was the db/db monogenic mouse model of type 2 diabetes. While this model does show prolonged inflammation during healing (44), bacterial infection was not considered in the study despite playing a contributing role in the delayed healing of human chronic wounds (45). Furthermore, although this model has shown impaired wound contraction, it has been suggested that this is attributed to the stretching of skin in these mice due to their obesity rather than to the disease itself, limiting its translation to chronic wounds in diabetic patients (16).

3.4.2 Calculation of Wound Size and Number of Animals Used in Mouse Studies

In calculating wound closure kinetics, one limitation is the formation of the eschar which covers the underlying healing tissue. Calculations of the wound area included the eschar present on the surface of the skin. The eschars were not manipulated or removed in any of the animals throughout the study and left to fall off naturally as manipulation could have disrupted the underlying tissue. As a result, calculated wound areas could have appeared larger due to the presence of the eschar, despite the underlying tissue being healed. The validity of the mouse studies conducted at earlier time points are also limited by the low number of mice used for each condition and at each time point. Including more mice in the study would have improved the power of the study, providing stronger evidence of the findings.

3.5 Final Summary

This thesis demonstrated that both gelatin and gelatin/galectin-3 scaffolds can be electrospun, creating a scaffold with an overall porosity of approximately 83% and average pore diameter of approximately 1.15 μ m. Both gelatin and gelatin/galectin-3 scaffolds can support the adhesion, deposition of matrix and proliferation of human dermal fibroblasts *in vitro* providing evidence that they are biocompatible. *In vivo*, both gelatin and gelatin/galectin-3 scaffolds did not increase wound closure kinetics, yet did not induce a foreign body response in db/db mice at day 17. Treatment of wounds with topical galectin-3, gelatin and gelatin/galectin-3 scaffolds did not enhance re-epithelialization or influence macrophage phenotypes in the wound, demonstrating a lack of efficacy for use of galectin-3 in modulating these processes in mice. Future work should elucidate the exact pathological instances in which galectin-3 might modulate inflammation.

3.6 References

1. Cao Z, Said N, Amin S, Wu HK, Bruce A, Garate M, et al. Galectins-3 and -7, but not galectin-1, play a role in re-epithelialization of wounds. *The Journal of biological chemistry*. 2002;277(44):42299-305.
2. Liu W, Hsu DK, Chen HY, Yang RY, Carraway KL, 3rd, Isseroff RR, et al. Galectin-3 regulates intracellular trafficking of EGFR through Alix and promotes keratinocyte migration. *J Invest Dermatol*. 2012;132(12):2828-37.
3. Walker JT, Elliott CG, Forbes TL, Hamilton DW. Genetic Deletion of Galectin-3 Does Not Impair Full-Thickness Excisional Skin Healing. *J Invest Dermatol*. 2016.
4. Gurtner GC, Werner S, Barrandon Y, Longaker MT. Wound repair and regeneration. *Nature*. 2008;453(7193):314-21.
5. Kariya Y, Kawamura C, Tabei T, Gu J. Bisecting GlcNAc residues on laminin-332 down-regulate galectin-3-dependent keratinocyte motility. *The Journal of biological chemistry*. 2010;285(5):3330-40.
6. Novak R, Dabelic S, Dumic J. Galectin-1 and galectin-3 expression profiles in classically and alternatively activated human macrophages. *Biochimica et biophysica acta*. 2012;1820(9):1383-90.
7. Sano H, Hsu DK, Yu L, Apgar JR, Kuwabara I, Yamanaka T, et al. Human galectin-3 is a novel chemoattractant for monocytes and macrophages. *Journal of immunology*. 2000;165(4):2156-64.
8. Jia W, Kidoya H, Yamakawa D, Naito H, Takakura N. Galectin-3 accelerates M2 macrophage infiltration and angiogenesis in tumors. *The American journal of pathology*. 2013;182(5):1821-31.
9. MacKinnon AC, Farnworth SL, Hodgkinson PS, Henderson NC, Atkinson KM, Leffler H, et al. Regulation of alternative macrophage activation by galectin-3. *Journal of immunology*. 2008;180(4):2650-8.
10. Hamilton D, Walker J, Kim S, Michelsons S, Creber K, Elliott C, et al. Cell-matrix interactions governing skin repair: matricellular proteins as diverse modulators of cell function. *Research and Reports in Biochemistry*. 2015:73.
11. Martinez FO, Gordon S. The M1 and M2 paradigm of macrophage activation: time for reassessment. *F1000Prime Rep*. 2014;6:13.
12. Rabinovich GA, Rubinstein N, Toscano MA. Role of galectins in inflammatory and immunomodulatory processes. *Biochimica et biophysica acta*. 2002;1572(2-3):274-84.

13. Zhao R, Liang H, Clarke E, Jackson C, Xue M. Inflammation in Chronic Wounds. *International journal of molecular sciences*. 2016;17(12).
14. Brem H, Tomic-Canic M. Cellular and molecular basis of wound healing in diabetes. *The Journal of clinical investigation*. 2007;117(5):1219-22.
15. Nunan R, Harding KG, Martin P. Clinical challenges of chronic wounds: searching for an optimal animal model to recapitulate their complexity. *Dis Model Mech*. 2014;7(11):1205-13.
16. Fang RC, Kryger ZB, Buck DW, 2nd, De la Garza M, Galiano RD, Mustoe TA. Limitations of the db/db mouse in translational wound healing research: Is the NONcNZO10 polygenic mouse model superior? *Wound repair and regeneration : official publication of the Wound Healing Society [and] the European Tissue Repair Society*. 2010;18(6):605-13.
17. Pepe D, Elliott CG, Forbes TL, Hamilton DW. Detection of galectin-3 and localization of advanced glycation end products (AGE) in human chronic skin wounds. *Histology and histopathology*. 2014;29(2):251-8.
18. Hershcovitch MD, Hom DB. Update in wound healing in facial plastic surgery. *Arch Facial Plast Surg*. 2012;14(6):387-93.
19. Lichtman MK, Otero-Vinas M, Falanga V. Transforming growth factor beta (TGF-beta) isoforms in wound healing and fibrosis. *Wound repair and regeneration : official publication of the Wound Healing Society [and] the European Tissue Repair Society*. 2016;24(2):215-22.
20. Galiano RD, Tepper OM, Pelo CR, Bhatt KA, Callaghan M, Bastidas N, et al. Topical Vascular Endothelial Growth Factor Accelerates Diabetic Wound Healing through Increased Angiogenesis and by Mobilizing and Recruiting Bone Marrow-Derived Cells. *The American journal of pathology*. 2004;164(6):1935-47.
21. Hanft JR, Pollak RA, Barbul A, van Gils C, Kwon PS, Gray SM, et al. Phase I trial on the safety of topical rhVEGF on chronic neuropathic diabetic foot ulcers. *J Wound Care*. 2008;17(1):30-2, 4-7.
22. Baltzis D, Eleftheriadou I, Veves A. Pathogenesis and treatment of impaired wound healing in diabetes mellitus: new insights. *Advances in therapy*. 2014;31(8):817-36.
23. Ma C, Hernandez MA, Kirkpatrick VE, Liang LJ, Nouvong AL, Gordon, II. Topical platelet-derived growth factor vs placebo therapy of diabetic foot ulcers offloaded with windowed casts: a randomized, controlled trial. *Wounds*. 2015;27(4):83-91.
24. Midwood KS, Williams LV, Schwarzbauer JE. Tissue repair and the dynamics of the extracellular matrix. *Int J Biochem Cell Biol*. 2004;36(6):1031-7.

25. Jun JI, Lau LF. The matricellular protein CCN1 induces fibroblast senescence and restricts fibrosis in cutaneous wound healing. *Nat Cell Biol.* 2010;12(7):676-85.
26. Chong HC, Chan JS, Goh CQ, Gounko NV, Luo B, Wang X, et al. Angiopoietin-like 4 stimulates STAT3-mediated iNOS expression and enhances angiogenesis to accelerate wound healing in diabetic mice. *Molecular therapy : the journal of the American Society of Gene Therapy.* 2014;22(9):1593-604.
27. Lin YT, Chen JS, Wu MH, Hsieh IS, Liang CH, Hsu CL, et al. Galectin-1 accelerates wound healing by regulating the neuropilin-1/Smad3/NOX4 pathway and ROS production in myofibroblasts. *J Invest Dermatol.* 2015;135(1):258-68.
28. Elliott CG, Wang J, Guo X, Xu SW, Eastwood M, Guan J, et al. Periostin modulates myofibroblast differentiation during full-thickness cutaneous wound repair. *Journal of cell science.* 2012;125(Pt 1):121-32.
29. Jensen ON. Modification-specific proteomics: characterization of post-translational modifications by mass spectrometry. *Curr Opin Chem Biol.* 2004;8(1):33-41.
30. Gao X, Liu J, Liu X, Li L, Zheng J. Cleavage and phosphorylation: important post-translational modifications of galectin-3. *Cancer metastasis reviews.* 2017.
31. Balan V, Nangia-Makker P, Jung YS, Wang Y, Raz A. Galectin-3: A novel substrate for c-Abl kinase. *Biochimica et biophysica acta.* 2010;1803(10):1198-205.
32. Mazurek N, Conklin J, Byrd JC, Raz A, Bresalier RS. Phosphorylation of the beta-galactoside-binding protein galectin-3 modulates binding to its ligands. *The Journal of biological chemistry.* 2000;275(46):36311-5.
33. Herrmann J, Turck CW, Atchison RE, Huflejt ME, Poulter L, Gitt MA, et al. Primary structure of the soluble lactose binding lectin L-29 from rat and dog and interaction of its non-collagenous proline-, glycine-, tyrosine-rich sequence with bacterial and tissue collagenase. *The Journal of biological chemistry.* 1993;268(35):26704-11.
34. Hadari YR, Arbel-Goren R, Levy Y, Amsterdam A, Alon R, Zakut R, et al. Galectin-8 binding to integrins inhibits cell adhesion and induces apoptosis. *Journal of cell science.* 2000;113 (Pt 13):2385-97.
35. Christensen B, Kazanecki CC, Petersen TE, Rittling SR, Denhardt DT, Sorensen ES. Cell type-specific post-translational modifications of mouse osteopontin are associated with different adhesive properties. *The Journal of biological chemistry.* 2007;282(27):19463-72.
36. Karande TS, Ong JL, Agrawal CM. Diffusion in musculoskeletal tissue engineering scaffolds: design issues related to porosity, permeability, architecture, and nutrient mixing. *Ann Biomed Eng.* 2004;32(12):1728-43.

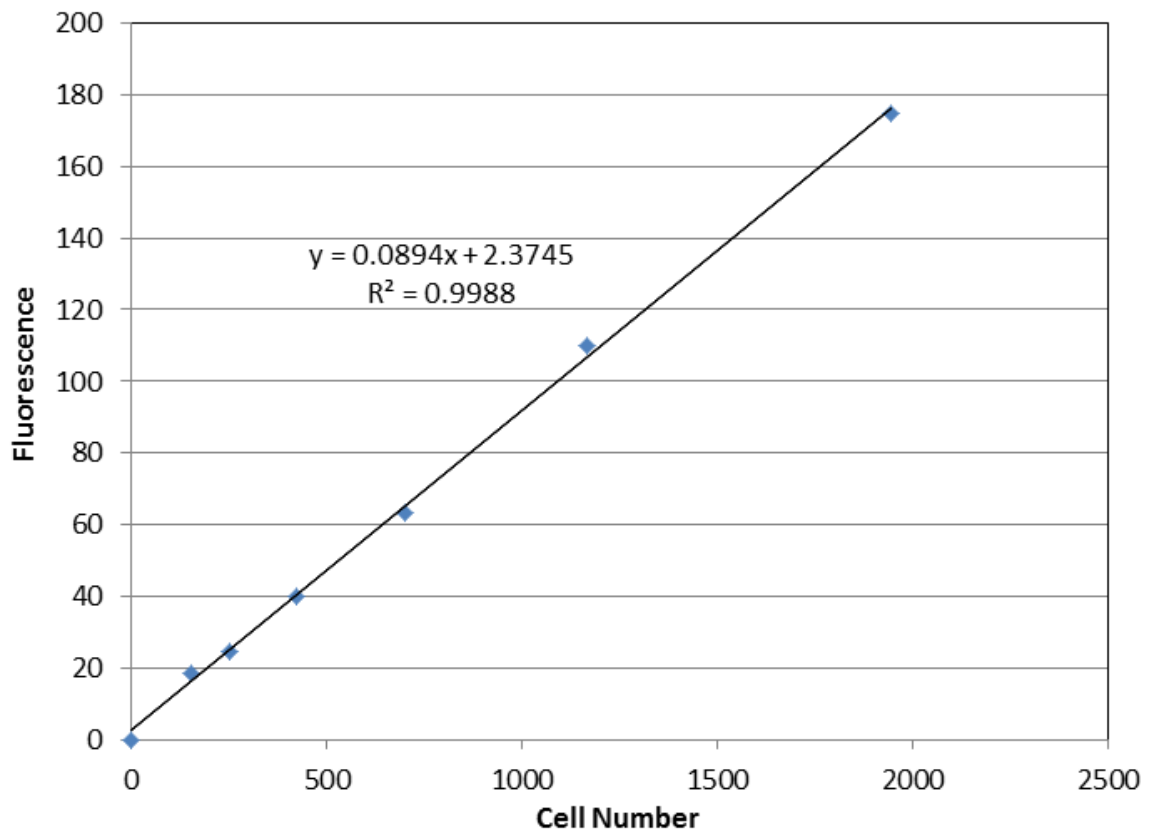
37. Zhu XL, Cui WG, Li XH, Jin Y. Electrospun fibrous mats with high porosity as potential scaffolds for skin tissue engineering. *Biomacromolecules*. 2008;9(7):1795-801.
38. Wu J, Hong Y. Enhancing cell infiltration of electrospun fibrous scaffolds in tissue regeneration. *Bioactive Materials*. 2016;1(1):56-64.
39. Skotak M, Ragusa J, Gonzalez D, Subramanian A. Improved cellular infiltration into nanofibrous electrospun cross-linked gelatin scaffolds templated with micrometer-sized polyethylene glycol fibers. *Biomed Mater*. 2011;6(5):055012.
40. Klumpp D, Rudisile M, Kuhnle RI, Hess A, Bitto FF, Arkudas A, et al. Three-dimensional vascularization of electrospun PCL/collagen-blend nanofibrous scaffolds in vivo. *Journal of biomedical materials research Part A*. 2012;100(9):2302-11.
41. Fukumori T, Takenaka Y, Yoshii T, Kim HR, Hogan V, Inohara H, et al. CD29 and CD7 mediate galectin-3-induced type II T-cell apoptosis. *Cancer research*. 2003;63(23):8302-11.
42. Brancato SK, Albina JE. Wound macrophages as key regulators of repair: origin, phenotype, and function. *The American journal of pathology*. 2011;178(1):19-25.
43. Danella Polli C, Alves Toledo K, Franco LH, Sammartino Mariano V, de Oliveira LL, Soares Bernardes E, et al. Monocyte Migration Driven by Galectin-3 Occurs through Distinct Mechanisms Involving Selective Interactions with the Extracellular Matrix. *ISRN Inflamm*. 2013;2013:259256.
44. Bannon P, Wood S, Restivo T, Campbell L, Hardman MJ, Mace KA. Diabetes induces stable intrinsic changes to myeloid cells that contribute to chronic inflammation during wound healing in mice. *Dis Model Mech*. 2013;6(6):1434-47.
45. Schultz GS, Davidson JM, Kirsner RS, Bornstein P, Herman IM. Dynamic reciprocity in the wound microenvironment. *Wound repair and regeneration : official publication of the Wound Healing Society [and] the European Tissue Repair Society*. 2011;19(2):134-48.

Appendices

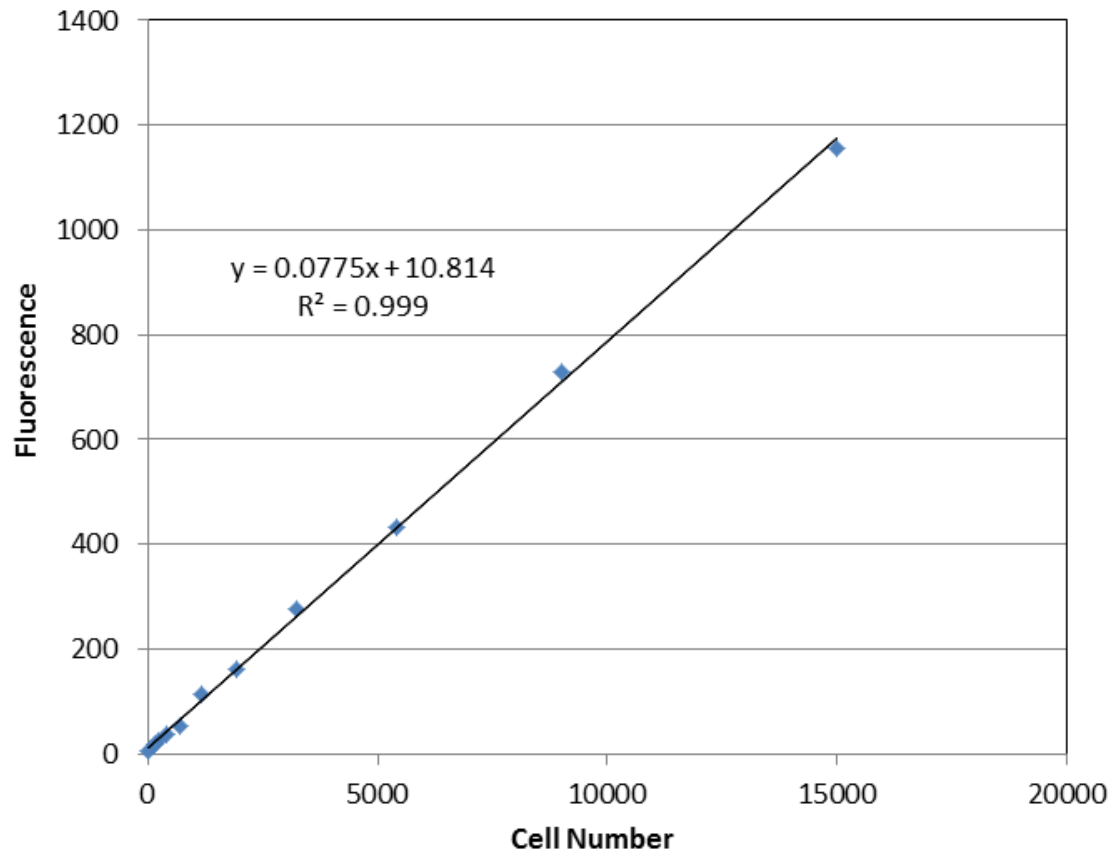
Appendix A: Standard curves for the quantification of cell numbers using the CyQUANT® Cell Proliferation Assay Kit.

The fluorescence values were converted into cell numbers using a standard curve generated using human dermal fibroblasts. A) Sample standard curve used for cell number quantification in adhesion assay. B) Sample standard curve used for cell number quantification in proliferation assay.

(A)

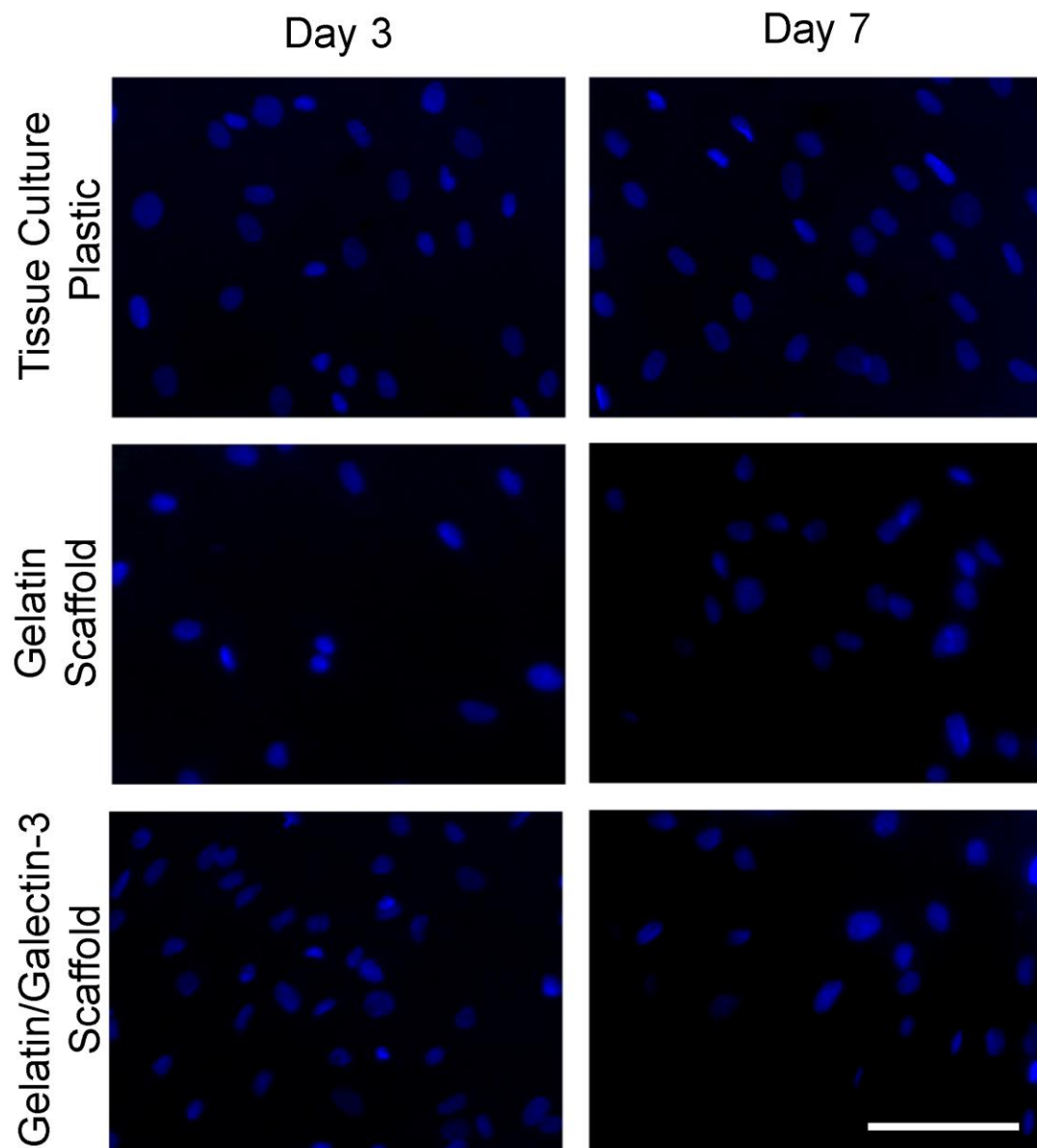


(B)



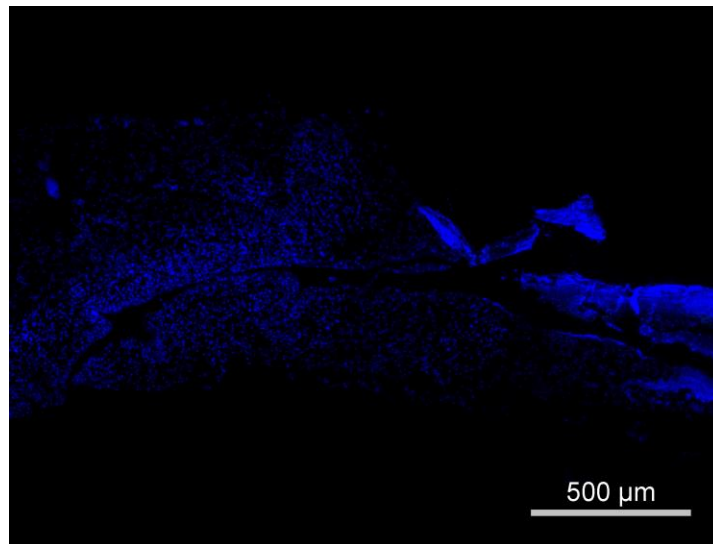
Appendix B: No primary antibody negative control for fibronectin immunofluorescence.

The deposition of the extracellular matrix protein fibronectin was visualized using immunocytochemistry. Fibronectin is shown in green and cell nuclei are shown in blue. Negative control images were taken of sections that were stained without the use of the primary antibody. Negative control images were used to set the threshold values for fibronectin fluorescence. Scale bar = 50 μ m.



Appendix C: No primary antibody negative control for arginase I /iNOS immunofluorescence.

The presence of M1 (iNOS⁺) and M2 (arginase I⁺) macrophages was visualized using immunocytochemistry. M1 macrophages (iNOS⁺ cells) are shown in red and M2 macrophages (arginase I⁺ cells) are shown in green. Negative control images were taken of sections that were stained without the use of the primary antibodies. Negative control images were used to set the threshold values for fibronectin fluorescence. Scale bar = 500 μ m.



Appendix D: Copyright permissions

7/10/2017

Copyright Clearance Center



Confirmation Number: 11654000
Order Date: 07/04/2017



This is not an invoice

Order Details

Research and Reports in Biochemistry

Billing Status:
N/A

Order detail ID: 70592672
ISSN: 2230-3154
Publication Type: e-Journal
Volume:
Issue:
Start page:
Publisher: Dove Medical Press Ltd

Permission Status: **Granted**
Permission type: Republish or display content
Type of use: Republish in a thesis/dissertation
Order License Id: 4142080932894
Order ref number: N/A

Requestor type: Academic institution
Format: Electronic
Portion: image/photo
Number of images/photos requested: 1
Title or numeric reference of the portion(s): pg. 84 Figure 4
Title of the article or chapter the portion is from: Cell-matrix interactions governing skin repair: matricellular proteins as diverse modulators of cell function
Editor of portion(s): N/A
 John T Walker, Shawna S Kim, Sarah Michelsons, Kendal Creber, Christopher G Elliott, Andrew Leask, Douglas W Hamilton
Author of portion(s):
Volume of serial or monograph: N/A
Issue, if republishing an article from a serial: N/A
Page range of portion: 84
Publication date of portion: 5 March 2015
Rights for: Main product
Duration of use: Life of current edition
 no

<https://www.copyright.com/printOrder.do?id=11654000>

1/2

Curriculum Vitae

Name: Karrington McLeod

Post-secondary Education and Degrees: The University of Western Ontario
London, Ontario, Canada
2015-2017 M.ESc

Queen's University
Kingston, Ontario, Canada
2009-2013 B.ASc

Honours and Awards: CMHR Transdisciplinary Bone and Joint Training Award
2015-2016

Related Work Experience Intern, Purification Pilot Plant
Genentech, South San Francisco, CA, USA
2016

Publications:

Walker, J. T., McLeod, K., Kim, S., Conway, S. J., & Hamilton, D. W. (2016). Periostin as a multifunctional modulator of the wound healing response. *Cell and Tissue Research*, 1-13.